การวิเคราะห์ปรากฏการณ์เกาะความร้อนเขตเมืองเชิงพื้นที่และ
ความสัมพันธ์กับลักษณะการใช้ประโยชน์ที่ดินและสิ่งปกคลุมดินและ
การบริโภคพลังงานไฟฟ้า: กรณีศึกษาในเขตกรุงเทพมหานครและปริมณฑล

พันเอก ปริญญา ฉายะพงษ์

SPATIAL ANALYSIS OF URBAN HEAT ISLAND

PHENOMENON AND ITS RELATIONSHIP WITH

LAND USE AND LAND COVER AND ELETRICAL

ENERGY CONSUMPTION: A CASE STUDY IN

BANGKOK METROPOLITAN AREA

Col. Parinya Chayapong

A Thesis Submitted in Partial Fulfillment of the Requirements for the

Degree of Doctor of Philosophy in Geoinformatics

Suranaree University of Technology

Academic Year 2010

SPATIAL ANALYSIS OF URBAN HEAT ISLAND PHENOMENON AND ITS RELATIONSHIP WITH LAND USE AND LAND COVER AND ELETRICAL ENERGY CONSUMPTION: A CASE STUDY IN BANGKOK METROPOLITAN AREA

Suranaree University of Technology has approved this thesis submitted in partial fulfillment of the requirements for the Degree of Doctor of Philosophy.

Thesis Examining Committee
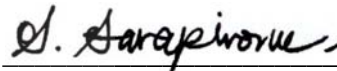
_____
(Asst. Prof. Dr. Sunya Sarapirome)

Chairperson

_____
(Asst. Prof. Dr. Songkot Dasananda)

Member (Thesis Advisor)

_____
(General. Dr. Vichit Satharanond)

Member
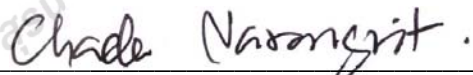
_____
(Assoc. Prof. Dr. Chada Narongrit)

Member
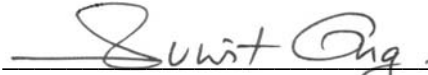
_____
(Asst. Prof. Dr. Suwit Ongsomwang)

Member

_____
(Dr. Dusdi Chanlikit)

Member

_____
(Assoc. Prof. Dr. Prapun Manyum)

_____
(Dr. Wut Dankittikul)

Acting Vice Rector for Academic Affairs

Dean of Institute of Science

พันเอก ปริญญา ฉายะพงษ์ : การวิเคราะห์ปรากฏการณ์เกาะความร้อนเขตเมืองเชิงพื้นที่และ
ความสัมพันธ์กับลักษณะการใช้ประโยชน์ที่ดินและสิ่งปกคลุมดินและการบริโภคพลังงาน
ไฟฟ้า: กรณีศึกษาในเขตกรุงเทพมหานครและปริมณฑล (SPATIAL ANALYSIS OF
URBAN HEAT ISLAND PHENOMENON AND ITS RELATIONSHIP WITH LAND
USE AND LAND COVER AND ELETRICAL ENERGY CONSUMPTION: A CASE
STUDY IN BANGKOK METROPOLITAN AREA) อาจารย์ที่ปรึกษา : ผู้ช่วยศาสตราจารย์
ดร.ทรงกต ทศานนท์, 136 หน้า.

วัตถุประสงค์หลักของงานวิจัยนี้ คือตรวจสอบหาความสัมพันธ์ระหว่างอุณหภูมิที่ระดับผิว
ดินที่สังเกตได้และองค์ประกอบของการใช้ประโยชน์ที่ดินและสิ่งปกคลุมดิน ในเขต
กรุงเทพมหานครและปริมณฑล (BMA) และประเมินอิทธิพลของอุณหภูมิอากาศที่เพิ่มขึ้นต่อความ
ต้องการไฟฟ้า สำหรับในงานส่วนแรกพบว่าพื้นที่เมืองและสิ่งก่อสร้างเพิ่มสูงขึ้นเป็นอย่างมาก
(ประมาณร้อยละ 92.5) ในช่วงเวลา 16 ปี (พ.ศ.2535-2551) โดยส่วนใหญ่เปลี่ยนมาจากเขตพืช
พรรณและพื้นที่ว่างเปล่า โดยอัตราการเพิ่มสูงสุดพบในช่วง พ.ศ. 2539-2543 (ร้อยละ 31.62) และ
ช่วง พ.ศ. 2547-2551 (ร้อยละ 32.38) การขยายตัวของเมืองมักพบเริ่มจากกรุงเทพมหานคร
ตอนกลางออกไปยังเมืองบริวาร และในพื้นที่เขตชานเมืองแทบทุกทิศทาง ข้อมูลซึ่งได้จากแผนที่
อุณหภูมิระดับผิวดินที่ทำขึ้น บ่งชี้ถึงการเกิดปรากฏการณ์เกาะความร้อนเขตเมืองที่รุนแรงเหนือเขต
กรุงเทพมหานครและปริมณฑล โดยในเขตกรุงเทพมหานครตอนกลาง คงมีเฉพาะที่ตำบลบาง
กระเจ้าเท่านั้นที่ไม่ประสบปัญหาดังกล่าวมากนัก โดยทั่วไปพบว่าการเพิ่มขึ้นของพื้นที่เมืองและ
สิ่งก่อสร้าง จะส่งเสริมให้เกิดปรากฏการณ์เกาะความร้อนเขตเมืองเพิ่มขึ้นอย่างเห็นได้ชัด ขณะที่พืช
พรรณสีเขียวจะช่วยบรรเทาความรุนแรงของปรากฏการณ์ดังกล่าว เช่นเดียวกับแหล่งน้ำขนาดใหญ่

ในงานส่วนที่สองพบว่าข้อมูลอุณหภูมิระดับผิวดิน มีความสัมพันธ์ทางลบในระดับปาน
กลาง กับค่าดัชนีพืชพรรณ NDVI ที่สอดคล้องกันในระดับเซลล์ภาพ (R^2 = 0.408) ขณะที่มันมี
ความสัมพันธ์ในทางบวกเป็นอย่างสูงกับค่าเฉลี่ยของดัชนี %ISC และ NDBI (ที่ R^2 = 0.836 และ
0.734 ตามลำดับ) นอกจากนั้น ยังพบว่า %ISC และ NDBI มีระดับของความสัมพันธ์ระหว่างกันใน
ทางบวกที่สูงมากเช่นกัน (R^2 = 0.922) สำหรับในงานส่วนที่สาม พบว่าสวนสาธารณะทั้งสามแห่งที่
เลือกมามีผลกระทบต่ออุณหภูมิแวดล้อมในระดับที่แตกต่างกัน โดยสวนที่มีขนาดใหญ่ที่สุด (กลุ่ม
สวนจตุจักร) ปรากฏผลกระทบชัดเจนที่สุดโดยทำให้อุณหภูมิลดลงประมาณ 4°C ในช่วงระยะ
ประมาณ 1.6 กิโลเมตรออกไปจากศูนย์กลางสวน ขณะที่สวนอื่นอีกสองสวนปรากฏผลที่ใกล้เคียง
กันคือทำให้อุณหภูมิลดลงประมาณ 0.5-1.0°C ในช่วงระยะทางประมาณ 0.5-0.7 กิโลเมตร งานใน

ส่วนที่ 4 พบว่าปริมาณการใช้ไฟฟ้ารายเดือนและค่าเฉลี่ยอุณหภูมิอากาศของกรุงเทพมหานครและ
ปริมณฑล มีความสัมพันธ์ต่อกันทางบวกในระดับสูง โดยเฉพาะในส่วนของผู้ใช้ครัวเรือนและ
ผู้ประกอบการทั่วไประดับเล็ก (ที่ค่า R^2 = 0.937 และ 0.843 ตามลำดับ)

สาขาวิชาการรับรู้จากระยะไกล ลายมือชื่อนักศึกษา_____

ปีการศึกษา 2553 ลายมือชื่ออาจารย์ที่ปรึกษา_____

COL. PARINYA CHAYAPONG : SPATIAL ANALYSIS OF URBAN HEAT ISLAND PHENOMENON AND ITS RELATIONSHIP WITH LAND USE AND LAND COVER AND ELETRICAL ENERGY CONSUMPTION: A CASE STUDY IN BANGKOK METROPOLITAN AREA. THESIS ADVISOR : ASST. PROF. SONGKOT DASANANDA, Ph.D. 136 PP.

SURFACE TEMPERATURE/ HEAT ISLAND/ UHI/ URBAN GROWTH/ NDBI

Main objectives of this research are to examine relationships of the observed land surface temperature (LST) and land use/land cover (LULC) components in the Bangkok Metropolitan Administration (BMA) region. Influencing of rising air temperature on the electrical demand was also assessed. In the first part of the research, substantial growth of urban/built-up area (of about 92.5%) was seen during the 16-year period (1992-2008) in expenses of the original vegetation and bare land area. The highest increasing rate was found during 1996-2000 (31.62%) and 2004-2008 (32.38%). The urban expansion occurs mostly from central Bangkok to its satellite cities nearby and within Bangkok outskirt in nearly all directions. Information from the derived LST maps indicate strong urban heat island (UHI) phenomenon over BMA region. In central Bangkok, only Bang Krajao sub-district is still not experienced much of the severe UHI. It was found that different LULC types have different impacts on the UHI intensity. In general, the increase of urban/built-up space can notably enhance UHI intensity while green vegetation tends to reduce UHI severity as well as large water body.

In the second part, moderate negative correlation was discovered between LST data and their corresponding NDVI data at pixel scale (R^2 of 0.408) while strong positive correlations were found between LST and %ISC or NDBI (with R^2 of 0.836 and 0.734, respectively). The strong positive correlation between %ISC and NDBI was also found (R^2 of 0.922). In the third part, all three chosen public parks expressed different degrees of influences on ambient temperature data from which the largest park (Chatuchak Park Complex) generated most obvious impact with temperature dropping of about 4°C over distance of about 1.6 km away from the its center. The other two parks did comparably well with temperature dropping of 0.5-1.0^{o}C over distances of 0.5-0.7 km from their centers. In the fourth part, strong positive correlation was evidenced between monthly electrical loading data and mean air temperature over the BMA region, especially for the residential and small-general-service sections (with R^2 of 0.937 and 0.843, respectively).

School of Remote Sensing   Student's Signature_____

Academic Year 2010   Advisor's Signature_____

ACKNOWLEDGEMENTS

CONTENTS

CONTENTS (Continued)

CONTENTS (Continued)

LIST OF TABLES

LIST OF TABLES (Continued)

LIST OF FIGURES

LIST OF FIGURES (Continued)

LIST OF FIGURES (Continued)

LIST OF FIGURES (Continued)

LIST OF ABBREVIATIONS

ΔT	=	Intensity of the UHI phenomenon
AGC	=	Responsible Agency
BARE	=	Bare Land
BLHI	=	Boundary Layer Heat Island
BMA	=	Bangkok Metropolitan Administration
CBD	=	Central Business District
CLHI	=	Canopy Layer Heat island
CPC	=	Chatuchak Park Complex
CUS	=	Customer
DN	=	Digital Number
DOPA	=	Department of Provincial Administration Department
DST	=	District
EGAT	=	Electricity Generating Authority of Thailand
GCP	=	Ground Control Point
GISTDA	=	Geo-Informatics and Space Technology Development Agency
GOV	=	Governmental and Non-profit Organizations
GW	=	Gigawatt
ISC	=	Impervious Surface Cover
L/CUS	=	Electrical Loading Per Customer
LGS	=	Large General Service

LIST OF ABBREVIATIONS (Continued)

LST	=	Land Surface Temperature
LULC	=	Land Use and Land Cover
LUT	=	Look-up Tables
MEA	=	Metropolitan Electricity Authority
MGS	=	Medium General Service
NDBaI	=	Normalized Difference Bareness Index
NDBI	=	Normalized Difference Built-up Index
NDVI	=	Normalized Difference Vegetation Index
NHA	=	National Housing Authority
NIR	=	Near Infrared
NPO	=	Non-profit Organization
NSMA	=	Normalized Spectral Mixture Analysis
PCD	=	Pollution Control Department
PRV	=	Province
RES	=	Residential
SBU	=	Specific Business
SGS	=	Small General Service
ST	=	Station
SUHI	=	Surface Urban Heat Island
TG	=	Average Ground-based Temperature Data
TIR	=	Thermal Infrared
TM	=	Thematic Mapper

LIST OF ABBREVIATIONS (Continued)

TMD   =   Thai Meteorological Department

TS   =   Average Satellite-based Temperature Data

U/B   =   Urban and Built-up

UBL   =   Urban Boundary Layer

UCL   =   Urban Canopy Layer

UHI   =   Urban Heat Island

VEG   =   Vegetation

V-I-S   =   Vegetation, Impervious Surface and Soil Endmembers

WAT   =   Water Body
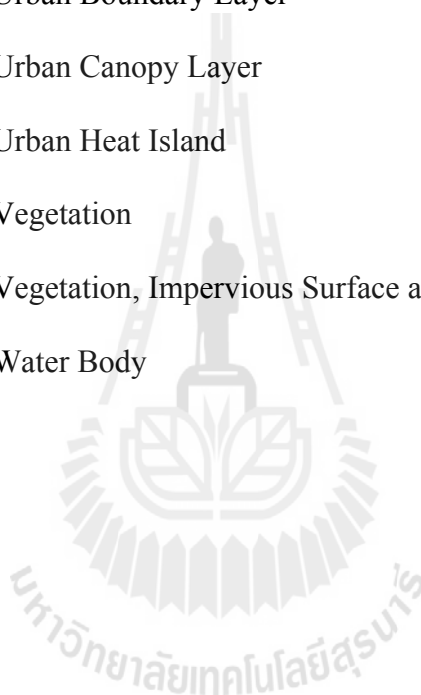
CHAPTER I

INTRODUCTION

1.1 Background Problem

Urban heat island (UHI) is a well-known phenomenon which has been evidenced globally, especially in the megacities around the world (Weng, 2001; Streutker, 2002; Hung et al., 2006; Kataoka et al., 2008). This phenomenon is characterized by noticeable increase of urban temperatures compared to those of the surrounding rural or suburban area (like in Figure 2.1). As Bangkok is the famous megacity and is home to several millions of residences at present, these make it prone to having severe urban heat island phenomenon as a result. General characteristics of the Bangkok UHI have been investigated in some recent researches. For examples, Boonjawat et al. (2000) and Hung et al. (2006) found that UHI intensities in Bangkok vary considerably from daytime to nighttime and between seasons where the variation range between 2-8°C was reported. Kataoka et al. (2008) concluded in their study that the average UHI intensity value in Bangkok increases about 2°C in the past 50 years. The uses of Landsat TM and ETM+ images for the analysis of UHI in Bangkok were also reported in Komolveeraket (1998) and Tonsuwonnont (2006).

Through, the intense UHI phenomenon in Bangkok area are well-recognized in recent years as stated earlier, however, it still lacks of known researches that thoroughly analyze its characteristics, especially, its relationship with urban growth, urban green areas, and land use/land cover (LULC) components in general. Also, impacts of UHI on electricity consumption in Bangkok Metropolitan Administration (BMA) area are still not fully assessed so far. All these addressed shortages are substantially fulfilled in this thesis based on the LULC and temperature data derived from the proper satellite imagery.

It is hoped that the significant results obtained from this work can provide us better understanding of the UHI characteristics within BMA region and LULC factors that influence UHI intensification over the area in recent years. This knowledge can benefit responsible local authorities and the government in planning more effective UHI mitigation programs for the BMA area in the future.

1.2   Research Objectives

Principal objective of this research is to analyze relationship between Bangkok UHI characteristics and LULC components during 1992-2008 whereas impact of the UHI on electricity consumption is also examined. Based on these intentions, there are four specific objectives proposed for this thesis:

1.2.1 To examine relationship between observed LST data (and UHI intensity) in the BMA area and LULC components during years 1992-2008.

1.2.2 To quantify influences of the vegetation cover, impervious surface, and bare soil on the variation of LST data derived from satellite thermal images.

1.2.3 To investigate effect of urban green area in the reduction of ambient air temperature.

1.2.4 To evaluate relationships of the temperature variation and the electricity consumption.

1.3 Scope and Limitations

1.3.1 The study area is 5 provinces within the BMA area including Bangkok, Nonthaburi, Samut Sakhon, Pathum Thani and Samut Prakan Provinces (Figure 1.1).

1.3.2 Temperature data are acquired from several sources; which are

1.3.2.1 LST derived from Landsat-TM and MODIS instruments.

1.3.2.2 Recorded near ground air temperature data from responsible agencies (Thai Meteorological Department and Pollution Control Department).

1.3.2.3 In situ measurements conducted during field observations.

1.3.3 Period of the satellite-based LST analysis covers 16 years from 1992 to 2008 but the MODIS-based LST analysis was conducted in 2008 only.

1.3.4 LULC data are broadly divided into 4 main categories: (1) urban/built-up, (2) vegetation, (3) bare land, and (4) water body.

1.4   Benefits of the Study

1.4.1 Better understanding on relationship of LST and UHI characteristics in BMA and its LULC pattern and trends of the UHI intensity during 1992-2008.

1.4.2 Having relationships between vegetation, impervious surface, and bare soil and the LST derived from satellite thermal images.

1.4.3 Knowledge on effects of the urban green areas (with different sizes) in the reduction of ambient air temperature in BMA area.

1.4.4 Knowledge on the relationship of temperature variation and electricity consumption in BMA area.

1.4.5 Suggestions about proper plan to mitigate present UHI situation within the BMA area.

1.5   Study area

The study area resides within Bangkok Metropolitan Administration (BMA) area covering area of 5593.332 km^2 in five provinces: Bangkok, Nonthaburi, Samut Sakhon, Pathum Thani, and Samut Prakan Provinces (Figure 1.1 and Table 1.1).
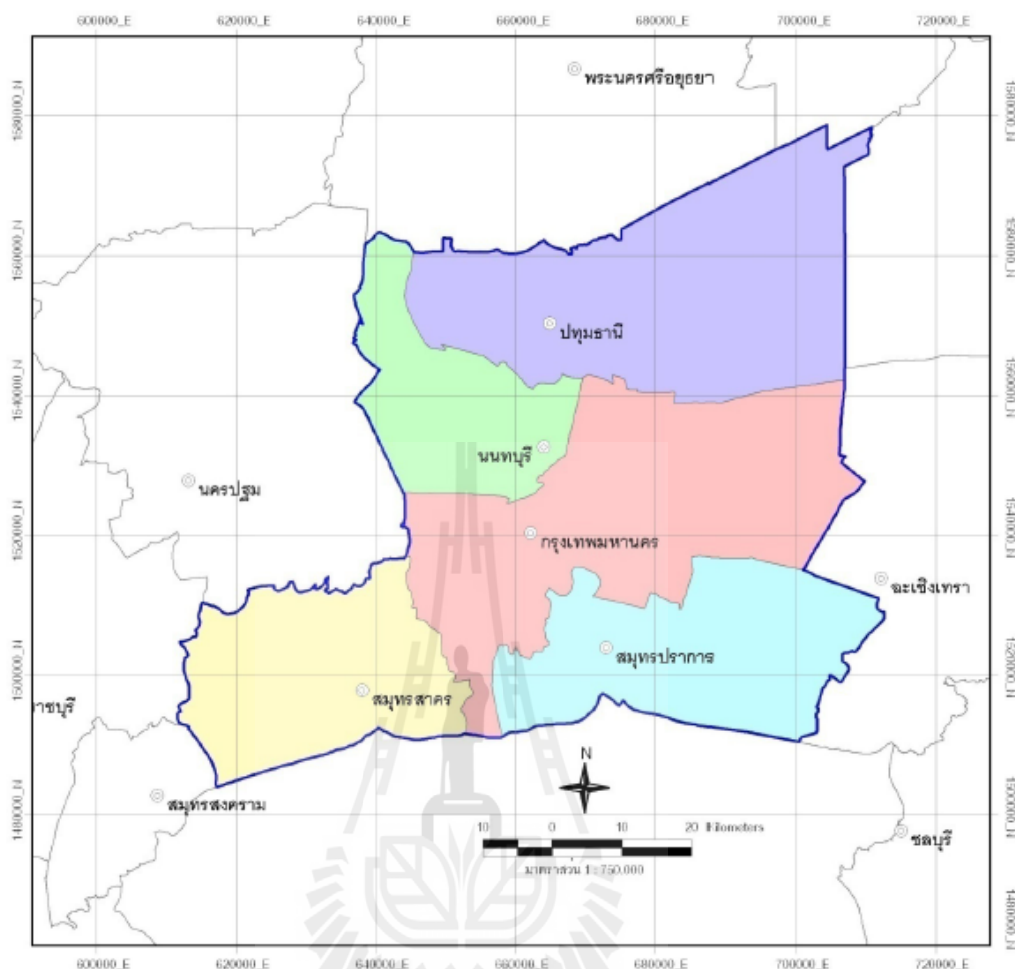
Figure 1.1 Map of the study area (five provinces within the BMA region).

Table 1.1 General data for the BMA region (listed by province).

Official name		Province code	Area (km^2)	Population (2009)	Population density (per km^2)	Number of districts
English	**Thai**					
Bangkok	กรุงเทพมหานคร	BKK	1,568.74	5,702,595	3,635.15	50
Nakhon Pathom	นครปฐม	NPT	2,168.33	851,426	392.66	7
Nonthaburi	นนทบุรี	NBR	622.30	1,078,071	1,732.39	6
Pathum Thani	ปทุมธานี	PTN	1,525.86	956,376	626.78	7
Samut Prakan	สมุทรปราการ	SPK	1,004.09	1,164,105	1,159.36	6
Samut Sakhon	สมุทรสาคร	SSK	872.35	484,606	555.52	3
	Total		**7,761.67**	**10,237,179**	**1,318.94**	**79**

CHAPTER II

LITERATURE REVIEW

2.1   Urban Heat Island Characteristics

Urban heat island (UHI) is a well-known phenomenon that has been evidenced globally, especially in the megacities around the world (Weng, 2001; Streutker, 2002; Hung et al., 2006; Stathopoulou and Cartalis, 2006; Kataoka et al., 2008). The phenomenon is evidenced by a notable increase of the urban temperatures compared to temperatures of the surrounding rural or suburban area (Figures 2.1 and 2.2). Primary cause of UHI in the cities is due to the absorption of solar radiation by building structures, roads, and other hard surfaces during daytime. Then, part of the absorbed heat is subsequently re-radiated to the atmosphere in form of the thermal infrared wave which can substantially increase ambient temperature in the urban area. This process keeps urban lands warmer than surrounding areas during both daytime and nighttime (IAUC, 2011).

Intensity of the UHI phenomenon (ΔT) is usually measured by the temperature differences between urban locations and some refereed rural sites, or,

$$\text{UHI Intensity} (\Delta T) = T_{urban} - T_{rural\,(reference)} \qquad (2.1)$$

In general, UHI intensities for a particular city will have distinct spatial and temporal variations depending on several factors, e.g. size, population, industrial development,

topography, physical layout, regional climate system, and meteorological conditions. Particular meteorological conditions, including the high temperature, low cloud cover, and low average wind speed, tend to intensify the effect.
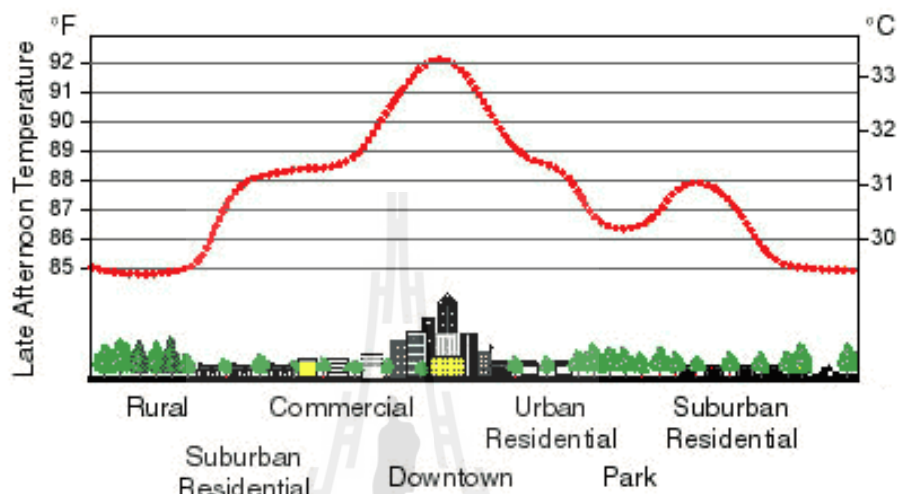
Figure 2.1   Typical temperature profile represents the urban heat island phenomenon.

From: http://www.eoearth.org/article/Heat_island.
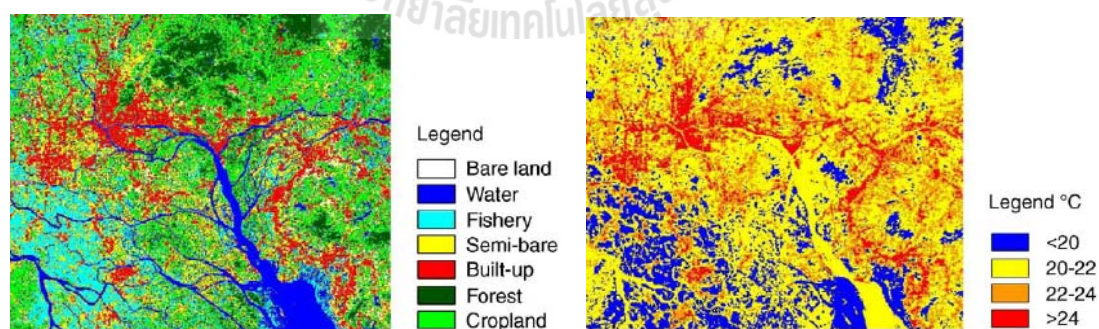
Figure 2.2   LULC pattern and land surface temperature (LST) distribution in the China's PRD (Pearl River Delta) region on November 1, 2000.

From: Chen et al. (2006).
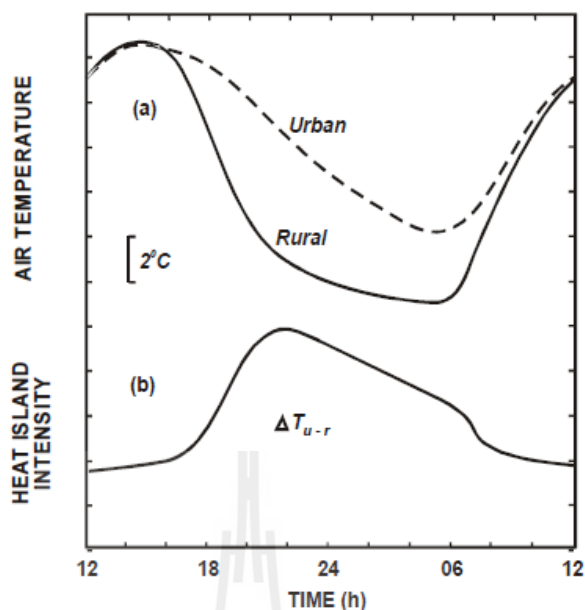
Figure 2.3 Typical diurnal variations of air temperature under calm/clear air.

From: http://www.epa.gov/heatisland/resources/pdf/HeatIslandTeachingResource.pdf.

The UHI intensity is usually found greatest at night under clear skies and calm air (Figure 2.3) as under such conditions, surface cooling is directly associated with radiation exchange. This is because while exposed rural sites cool rapidly after sunset, urban sites cool more slowly. The difference between urban and rural sites grows with time after sunset and reaches a peak value after about 4 hours. Maximum data is usually found in centre of the settlement (the larger indicates the higher). In addition, average UHI intensity may be enhanced during daytime due to the artificial heat released by the combustive processes from vehicles and industrial activities. Heats originating from commercial and domestic air conditioning systems also contribute to higher air temperatures within the urban area. But if consider all year round, average maximum UHI intensities are weakest in summer time and strongest in autumn and winter (Memon et al., 2009; Lee and Baik, 2010).

2.1.1 Types of the UHI Phenomenon

Conventionally, three types of heat islands are recognized in literature: (1) canopy layer heat island (CLHI), (2) boundary layer heat island (BLHI), and (3) surface urban heat island (SUHI) (Yuan and Bauer, 2007). The first two types are atmospheric heat islands produced mainly by the urbanization. They are theoretically defined by the warming of urban atmosphere at two different levels which are (1) the urban canopy layer (UCL), which extends upwards from ground to approximately mean building height, and (2) the urban boundary layer (UBL), which situates directly above the canopy layer (Figure 2.4).

These two distinct layers and the associated heat islands are governed by different processes; UBL is dominated by processes acting at local or meso-scale levels, whereas UCL is a micro-scale concept where its climate is strongly affected by nature of the immediate sites. Finally, the surface UHI refers to the relative warmth of the urban surfaces compared to their non-urbanized surroundings.

As seen in Figure 2.4, there are three spatial scales normally utilized for studying urban environments: (1) micro-scale (10^1-10^2 m) which involves spatial differences in response to individual roughness elements (e.g. variability in building or canyon dimensions or trees) and proximity to the localized emissions sources (e.g. roads and vegetation); (2) local-scale (10^2-10^4 m) which represents integrated response of an array of roughness elements with spatial variability showing unique characteristics of different land-uses or neighborhoods; and (3) meso-scale (10^4-10^5 m) which looks a city in its entirely, and differentiated from its surroundings, areas of the forest, and agriculture, etc.
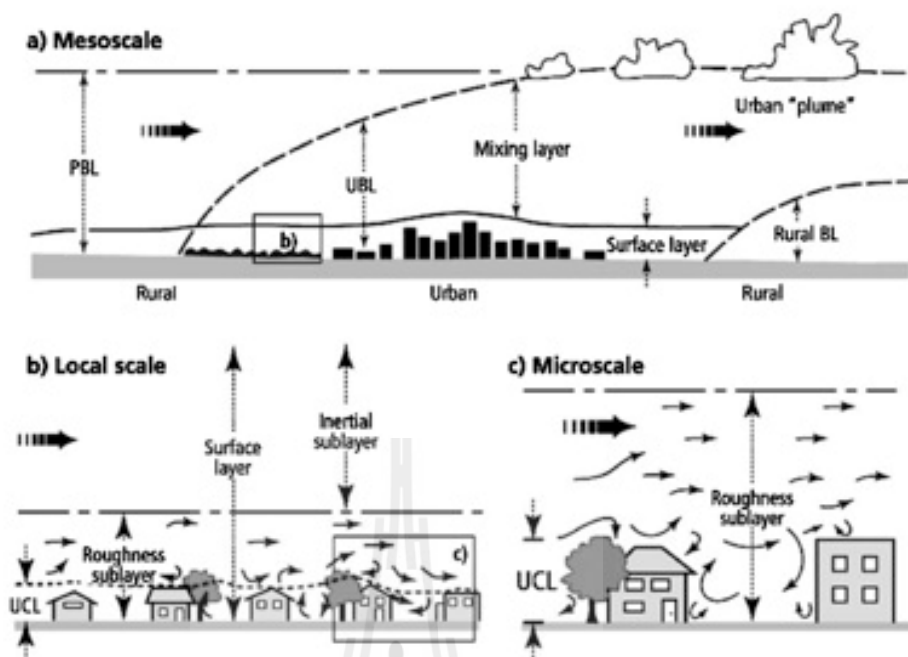
Figure 2.4 Three spatial scales usually utilized for studying urban environments.

From: http://co2montreal.blogspot.com/2010/10/principles-of-urban-meteorology-re.html.

The urban canopy layer (UCL) is defined as being from the ground to the mean height of the roughness elements, usually just below roof-level, where the micro-scale effects of site characteristics are dominated. It is most clearly delineated in high building density areas and may be sparse or absent in less densely developed suburban areas. And the layer extending from top of the UCL, to a height where urban surface influences are no longer perceptible, is called urban boundary layer (UBL). It includes roughness sub-layer immediately affected by individual roughness elements, turbulent surface layer (local-scale), and the outer mixed layer (meso-scale).

2.1.2   UHI impacts and mitigation approaches

The development of urban heat island phenomenon can be attributed to a number of factors, including: (1) urban construction materials of high heat capacity and low solar reflectivity such as asphalt and concrete, (2) reduced turbulent heat transfer and long-wave radiative heat loss due to the street canyons geometry, (3) reduced latent heat loss by evaporating due to the replacement of the natural green surfaces with dry surfaces, and (4) increased of anthropogenic heat emission into the atmosphere. All these factors could produce and enhance the formation of UHI in the cities (Stathopoulou and Cartalis, 2006).

Typically, heat islands have several profound impacts on health and welfare of the urban residences through their influences on the local urban climate and state of natural environment (EPA, 2011). Severe UHI can introduce vital heat-related illness, produce unpleasant living situation, accelerate smog formation that increases air pollution in urban area, and generate higher demand for cooling energy consumed (especially for air-conditioning systems). UHIs also have strong influence on patterns of tree and crop growth (Zhang et al., 2002, 2004; Fisher et al., 2006).

To reduce the UHI intensity, several mitigation techniques have been proposed, for examples, using more of white or reflective materials to build houses, pavements, and roads, and increasing more large green areas, such as parks or pacts of large trees, within city area. Urban trees and green areas can reduce UHI impact in two different aspects. First, they reduce air temperature and increases humidity from the evapotranspiration in vegetation foliage where heat in surrounding environment is converted to latent heat thereby lowering neighborhood temperature. And second, they provide more shaded surfaces to the cities. The solar radiation intensity in the trees'

shade could be reduced by up to 10-50% under crowd of the dense trees (Avissar, 1996; Georgi and Zafiriadis, 2006). In addition, trees also reduce adjacent wind speeds which can lower the amount of energy demand for cooling (Huang et al., 1990). It was found that areas with mature tree canopies were about 2.7-3.3^{o}C cooler than areas with no trees (US-EPA 1992).

In case of large green areas such as parks, vegetation affects the air above it and thus improve thermal environment of urban area. Cooling effect of park was investigated by several researchers with several values of temperature difference found. According to previous studies, large number of trees and urban parks can reduce local air temperature by 0.5-5.0^{o}C. The influencing distances of a park on the surrounding area were also investigated in several reports and usually found that the lager parks have longer distance impact than the smaller ones (Wong and Yu, 2005).

2.2   UHI Measurements

History of UHI research began in early 19th century by pioneering examination of London's climate by Luke Howard (Howard, 1818). This type of research continues and there is now a large body of data on UHI characteristics from cities globally. UHIs have long been assessed by the ground-based observations taken from fixed thermometer networks or by traverses with used sensor mounted on vehicles. With the advent of thermal remote sensing technology, remote observations of UHI became possible using satellite and aircraft platforms and have provided new avenues for the observation of UHI and the study of their causation through combination of thermal remote sensing and urban micro-meteorology.

2.2.1   Applications of thermal remote sensing to UHI research

In the past, most UHI studies were conducted based on temperature data obtained from the in situ measurements which have advantage of a high temporal resolution and a long historical data record. But these data also have poor spatial resolution. In contrast to the ground-based measurements that mostly record the near-surface air temperature data, the satellite thermal radiometers are able to detect land surface temperature (LST) data at larger spatial coverage but less temporal frequency than in typical situ measurements. These data can give better spatial characterization of urban-nonurban surface heating differences that are necessary for the analysis of the surface UHIs.

Therefore, the remotely sensed thermal data become a unique source of information to define surface heat islands because it can provides a continuous and simultaneous view of the whole region which is of prime importance for detailed investigation of urban surface climate. Rao (1972) was the first to demonstrate that urban surface temperatures could be identified from the analysis of thermal infrared data acquired by the satellite. Since then, a variety of sensor-platform combinations (satellites, aircrafts, ground-based) have been used to carry out remote observations of the urban surface temperatures that contribute to SUHI over a ranges of scales. Broad reviews of satellite perspective on the assessment of UHI were given by Gallo et al. (1995) and Voogt and Oke (2003). Studies on UHIs, by using satellite-based thermal images to extract land surface temperature data, have been primarily used with low resolution NOAA-AVHRR thermal data. The obtained LST data were proved to be effective for regional the urban temperature mapping (Kidder and Wu, 1987; Gallo et al., 1993). However, Landsat-TM/ETM+ and MODIS/ASTER instruments can also

provide surface thermal infrared data with better spatial resolution than those of NOAA-AVHRR. These make their LST products more appropriate for local-scale studies of the UHIs (Weng, 2001; Chen et al., 2002; Gluch et al., 2006). The MODIS images are also available on the internet which makes them more attractive for general use.

Several published researches have demonstrated that Landsat-TM/ETM+ imagery are highly applicable for general uses in UHI investigations over megacities around the world (e.g. Aneiallo et al., 1995; Stathopoulou and Cartalis, 2006; Zhangyan et al., 2006; and Adinna et al., 2009). However, as the instruments provide only daytime image during their late morning pass-over of the area, therefore, the analysis may be more completed if thermal data obtained from other sources (with different observing schedules) or from field surveys are included as the supplement data for the UHI study of interest.

Voogt and Oke (2003) had reviewed the use of thermal remote sensing for the study of urban climates with respect to the UHI and then described prominent distinctions between atmospheric and surface UHIs. Atmospheric UHIs are normally detected by ground-based air temperature measurements taken from the standard meteorological stations, where surface UHIs are mainly recognized from the thermal remote sensors which record upwelling thermal radiance emitted by observed surface area that lies within instantaneous field of view (IFOV) of the sensors. In contrast to the atmospheric UHI that is evidenced under calm and clear conditions at night, surface UHI is usually examined by using satellite or aircraft thermal data of high spatial resolutions (≤100 m) acquired at daytime when heat island intensities are greatest. Many surface UHI studies have been done using thermal data from satellite

observations which give a spatially continuous SUHI over large urban areas than is feasible using data from in situ station networks.

Voogt and Oke (2003) had also suggested three major applications of thermal remote sensing to improve the study of the UHI: (1) determine appropriate surface radiative (e.g. emissivity) and structural parameters from remote sensing to better describe urban surface, and to ensure their appropriateness for further use in urban atmospheric models; (2) couple canopy radiative transfer models with both sensor view models and the surface energy balance models to better simulate and understand urban thermal anisotropy and the link between surface temperatures, the surface energy balance and air temperature in and above the urban canopy layer; and (3) perform observational studies with ultimate goal of obtaining better independent validations of the surface effective parameters derived from remote thermal sensors.

2.3   Influence of LULC on UHI Characteristics

Researches on UHIs have shown that the modification of land use and land cover (LULC) in urban areas can result in the notable increase of both local air and surface temperatures. This is due to the differences in thermal properties of surface areas which are resulting from changing characters of the urban landscape. As a result, a large number of studies have been devoted to find relationships between land surface temperature and LULC characteristics such as composition of vegetation, water, and urban/built-up land and their changes, e.g., in Dousset and Gourmelon (2003), Weng et al. (2004), Chen et al. (2006), and Jasuf et al. (2007).

Knowledge on the relationship between LULC and LST can help us devise more sustainable land use planning and assist the effective UHI mitigation planning.

Figure 2.2 shows examples of LULC pattern and LST distribution in the China's PRD (Pearl River Delta) region on November 1, 2000.

    2.3.1   Impacts of vegetation and impervious surface

          Among the studies about impact of LULC on UHI characteristics, much emphasis has been placed on the roles of vegetation cover and impervious surfaces in the formation and intensification of UHIs. Increased green vegetation covers, like having more parks, normally lead to less intense UHI while having more impervious surfaces, like increasing urban/built-up lands, could induce more intense UHIs (Figures 2.5 and 2.6). Impervious surfaces are surfaces which water cannot infiltrate and are primarily associated with the transportation (e.g. street, parking lot, or sidewalk) and rooftop. Amount of impervious surfaces is related to urban growth and is an important indicator of environmental quality.
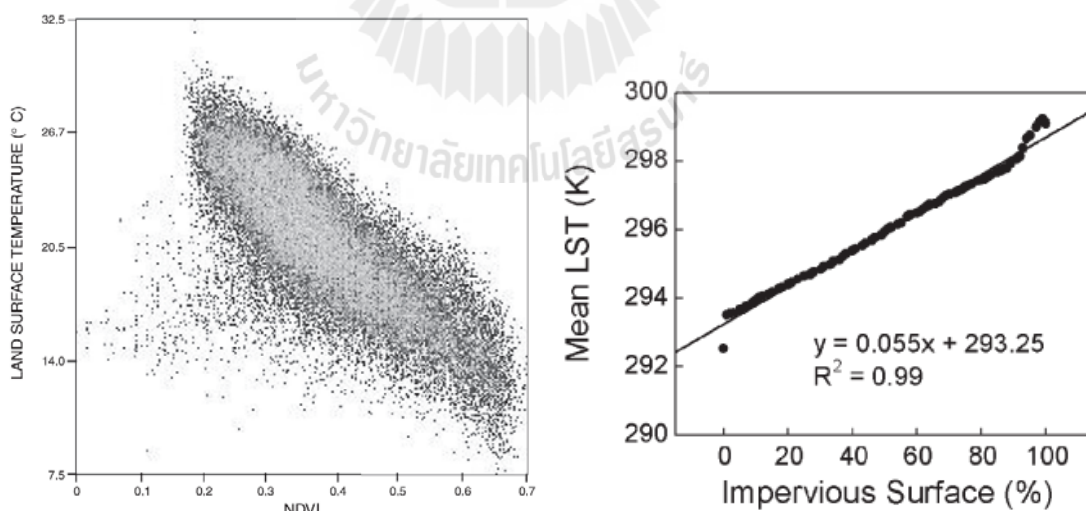
(a) LST and NDVI   (b) LST and %ISC

Figure 2.5   Relationships found between (a) LST and NDVI and (b) LST and %ISC.

From: (a) Dousset and Gourmelon (2003) and (b) Yuan and Bauer (2007).
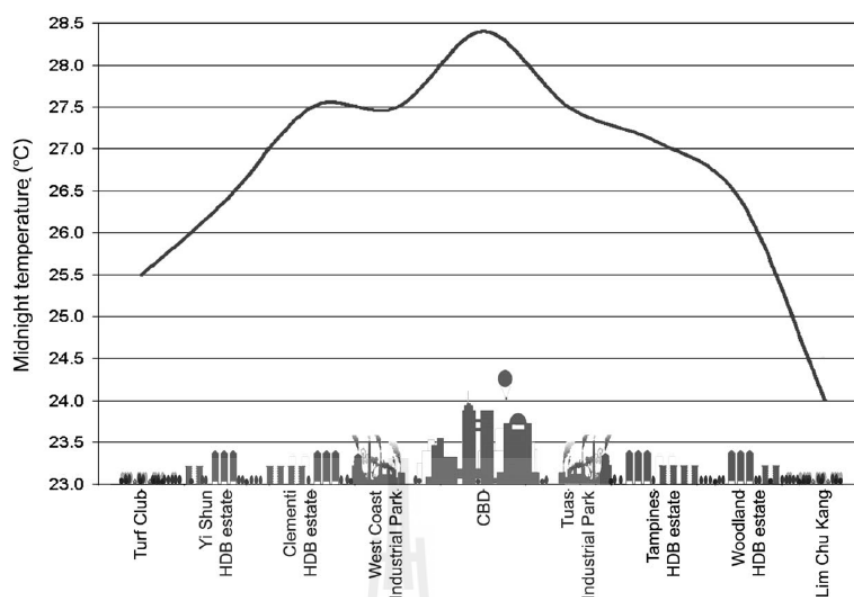
Figure 2.6   Profile of air temperature data along the selected route in Singapore.
From: Wong and Yu (2005).

In most studies, amount of vegetation cover is usually described in terms of some specific parameter called "NDVI" (normalized difference vegetation index). The NDVI values could be found directly from satellite image with red and NIR observing channels using simple equation like one shown in Eq. 3.4 (for Landsat-TM/ETM+ images). NDVI values range between -1 to 1 where the positive values closer to 1 indicate larger fraction of vegetation cover in a considered pixel. The negative correlation was often experienced between NDVI and LST where lower LSTs are usually found in areas with high NDVI. Gallo and Owen (1999) evaluated seasonal trends in temperature and NDVI and found that differences in NDVI and satellite-based LST accounted for 40% of the variation in urban-rural temperature differences.

However, there are two main difficulties in using NDVI as LST indicator which are arisen from nature the NDVI data themselves. First, measurements of NDVI data are subject to seasonal variations which may introduce an uncertainty in

the interpretation of surface UHI found. Second, the relationship between NDVI and LST is well known to be rather non-linear and the mixed-up with bare soil may complicate the gained results more (Figure 2.5a). The variability and non-linearity suggest that NDVI alone is not suitable to be a sufficient parameter to examine SUHI quantitatively (Yuan and Bauer, 2007).

On the other hand, SUHI phenomena have been investigated by analyzing the relationship between the LST and urbanization, which is described in term of the percent impervious surface cover (%ISC). In remote sensing aspect, classification of impervious surface cover is being used to quantify urbanization intensity and map extension of the urban land use which relies principally on population growth. Therefore, identification of percent impervious surface cover can lead to the understanding of both urban expansion and SUHI. Previous studies have shown that LST data usually increase (in linear fashion) with more %ISC found (Figure 2.5b). When compared to NDVI, %ISC is more stable all year round, therefore, it might be introduced as a complement to NDVI as indicators of the LSTs which are necessary for the study of SUHI in the urban environment.

Usually, there are two normal approaches found in extracting %ISC from satellite images. The first approach uses the sub-pixel classification technique called normalized spectral mixture analysis (NSMA) model (as described in Section 3.2.1; Wu, 2004; Yuan and Bauer, 2007). The second approach uses some pre-defined indices to identify %ISC implicitly (Zha et al., 2003; Chen et al., 2006).

2.4 Impact of UHI on Energy Consumption

Heat island phenomenon can lead directly to the higher electrical energy consumption mostly due to heavier uses of cooling system appliances, especially air-conditioners. But they significantly reduce need for heating in the winter also. These facts were emphasized in several published studies, for examples, Franco and Sanstad (2008) found that there is a high correlation between simple average daily temperature from four selected sites and daily electricity demand in CalISO region that comprises most of California (Figure 2.7). Kolokotroni et al. (2007) found that the urban cooling load in London area is 25% higher than the rural load over the year, and the annual heating load is reduced by 22% due to the local urban heat island phenomenon.
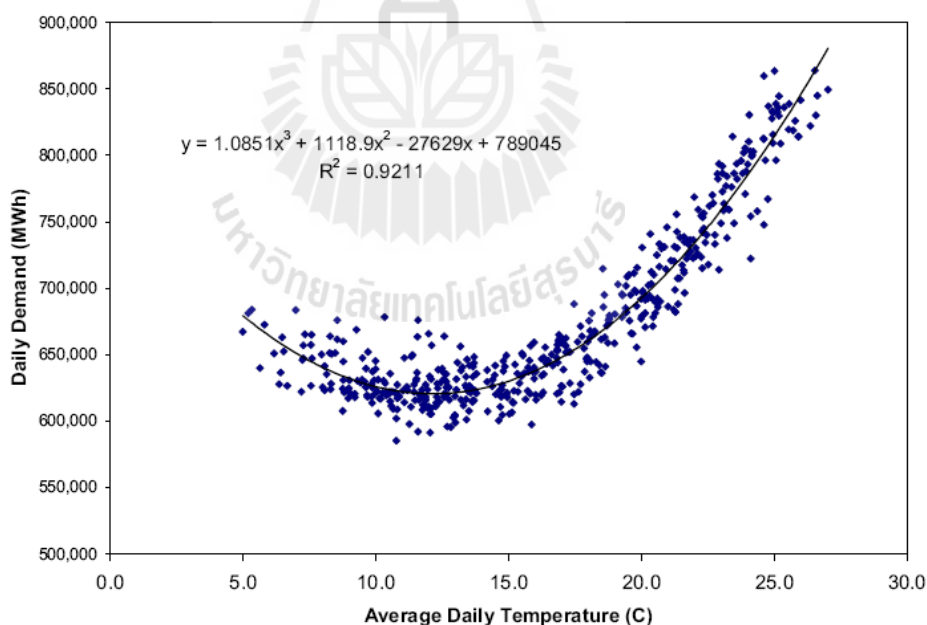
Figure 2.7 Electricity demand in the CalISO area, California, as being function of average daily temperatures during period 2004-2005.

From: Franco and Sanstad (2008).

Also in Athens, where the mean UHI intensity exceeds 10°C, it was found that the cooling load of the urban buildings might be doubled and the peak electricity load for cooling purposes may be tripled especially for locations with higher temperatures. During the winter, the heating loads of central urban buildings were found to be reduced up to 30% (Santamouris et al., 2001). Akasaka et al. (2002) showed that due to the heat island, the cooling load of Tokyo has increased about 20% since 1900 whereas its corresponding heating load decrease by about 40%. To overcome this problem, strategies to reduce cooling energy loads in the buildings were proposed by Akbari and Konopacki (2005). These were classified to direct (reducing heat gain through building shell) and indirect (reducing ambient air temperature). Knowledge of energy demand that varies with air temperature is necessary for planning sufficient energy supply by the responsible agencies.

2.5   Heat Island Phenomena in Bangkok

Bangkok is one of the most famous mega cities in the world which becomes home to several millions of residences. Due to rapid expansion of the urban and built-up areas along with dramatic rise in its population in recent decades, Bangkok has greatly suffered from UHI phenomenon. General characteristics of Bangkok UHI have been investigated in some recent studies, for examples, Boonjawat et al. (2000) and Hung et al. (2006) found that UHI magnitudes in Bangkok vary considerably from daytime to nighttime (Figure 2.8) and between seasons. The variation range between 2-8°C was reported and Kataoka et al. (2008) concluded that the average UHI intensity in Bangkok increased about 2°C in the past 50 years. The uses of Landsat TM/ETM+

images for the analysis of UHI in Bangkok were reported in Komolveeraket (1998) and Tonsuwonnont (2006).
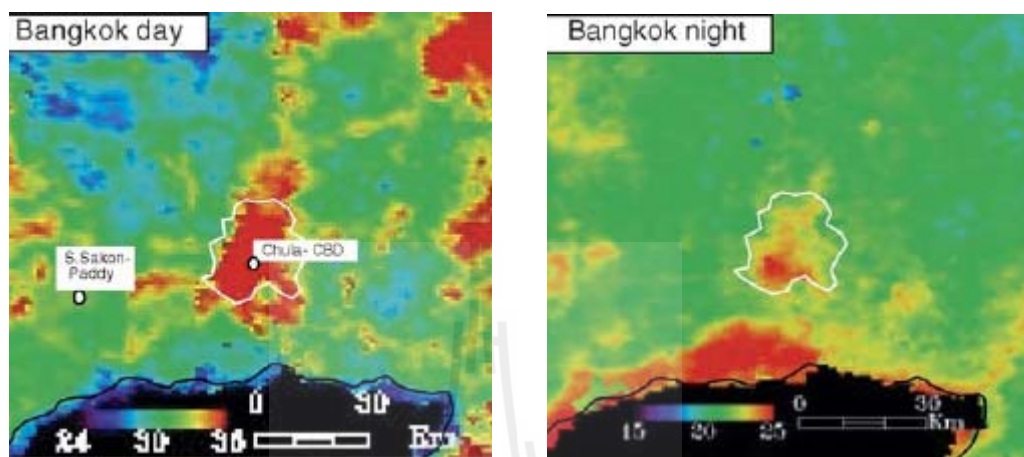
Figure 2.8 MODIS-based LST maps of Bangkok in dry season (February 2002, white polygons indicate the central business district, or CBD, location).

From: Hung et al. (2006).

Through, the UHI phenomena in Bangkok are well-recognized to be more intense in recent years; however, it is still lack of researches that fully analyze characteristics of the Bangkok UHI thoroughly, especially, the relationship with urban growth, urban green areas, and LULC pattern in general. Also, impact of UHIs on observed electricity consumption in Bangkok Metropolitan Area (BMA) is still not fully examined so far. All these addressed shortages are substantially fulfilled in this thesis. It is hoped that the results found can provide us with better understanding of the UHIs characteristics in BMA and LULC factors that relate to their intensification in recent years. This knowledge can benefit responsible authorities and government in planning more effective UHI mitigation programs in the future.

CHAPTER III

RESEARCH METHODOLOGY

3.1   Conceptual Framework

This research has been divided into 4 principal parts based on objectives stated in Chapter 1 (see work flowchart in Figure 3.1). The first part focuses on the analysis of relationship between satellite-based observed land surface temperature (LST) maps (and their associated UHI maps) and urban growth pattern (or other LULC classes) in BMA region during years 1992-2008. The analysis was based on LST and LULC maps for years 1992, 1996, 2000, 2004, and 2008 produced from the Landsat TM imagery. The prior assumptions of this work are that the UHI phenomenon should be more intensified as urban/built-up area expanding with time and its existences can be effectively observed by the satellite images in use and the relevant ground-based measurements. There are four main LULC categories being identified in the classified LULC maps, which are (1) urban/built-up, (2) vegetation, (3) bare land, and (4) water body.

In the second part, influences of each LULC component on the observed LST data were determined quantitatively by using appropriate indices for each LULC type. These are (1) NDVI (for vegetation), (2) NDBI (for urban/built-up), (3) NDBaI (for bare land), and (4) %ISC (for impervious surface). The relationships of these index values with their corresponding LST data (at pixel scale) were assessed and obtained results were presented in form of linear regression form (for each relevant index). The linear

relationship was primarily assumed based on extensive literature review on this issue.

The third part contains the evaluation on effect of existing public parks within BMA region in the reduction of observed ambient air temperature. This analysis was conducted based on both field observation data and satellite-based temperature data. The primary assumption is that, green parks with different sizes should have different impact on ambient air temperature. There were three parks with different sizes (small, medium, and large) chosen for the detailed analysis on this topic.

In the fourth part, relationships between observed temperature variation (from both ground-based and satellite-based measurements) and amount of electricity consumption in BMA region in year 2008 were examined. The strong linear relationships were assumed to be evidenced from the study as well as distinct impacts of different LULC types on amount of consumed electricity. To achieve these, different groups of the MEA registered customers were examined and reported separately.

3.2   Research Methodology

According to the earlier stated conceptual framework, the entire work process can be divided into 4 main sections as follows (see Figure 3.1 for flowchart):

3.2.1   Data preparation

This section concentrates on the acquiring and preparing of essential data for the subsequent analyzing process. The priority was given to the preparation of used satellite data (Landsat TM). This includes 5 main steps (Figure 3.2):

(1)   Relevant data were acquired from the responsible sources (listed in Table 3.1), then categorized and kept in form of the GIS-based database. Some general data of the study area have already been presented in Chapter I.
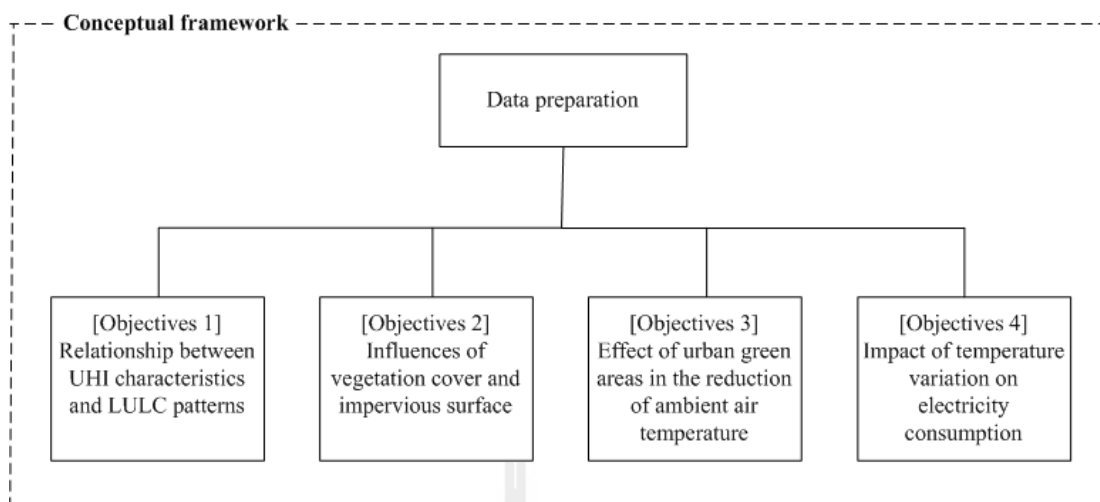
Figure 3.1   Conceptual framework of the study.

Table 3.1   Information of the essential data required in the research.

Data category	Data type/origin	Scale/format	Source	Date/year
Satellite imagery	Landsat TM	25x25m	GISTDA	20/11/1992 (09:58:43 AM) 15/11/1996 (09:58:33 AM) 10/11/2000 (10:16:38 AM) 21/11/2004 (10:22:55 AM) 02/12/2008 (10:21:35 AM)
	MODIS	1x1km	Internet	2008
	Ikonos	1x1m	Internet	2008
Temperature data	Landsat TIR	120x120m	GISTDA	As listed above
	MODIS TIR	1x1km	Internet	2008
	Ground-based	Point map	TMD, PCD	1996-2009
	Field surveys	Point map	-	2009
LULC data	TM	25x25m	GISTDA	As listed above
Secondary data	Electricity consumption	Point map	MEA	2008
	Administrative data	Line/polygon/attribute	DOPA	2003

Note: 1.   GISTDA ≡ Geo-Informatics and Space Technology Development Agency,
           MEA   ≡ Metropolitan Electricity Authority, TMD ≡ Thai Meteorological Department,
           DOPA   ≡ Department of Provincial Administration Department,
           PCD   ≡ Pollution Control Department
        2.   MODIS website ≡ http://webmodis.iis.u-tokyo.ac.jp.
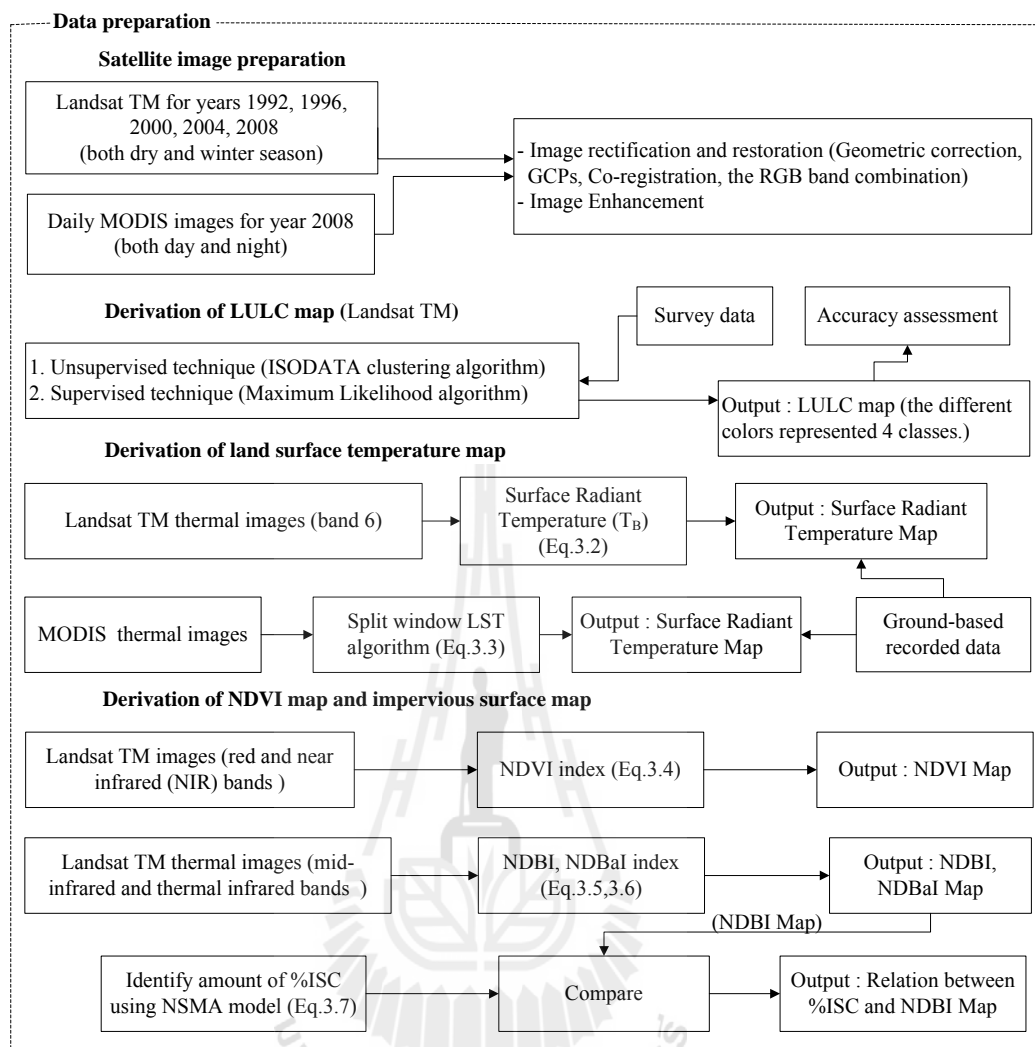
Figure 3.2   Flowcharts of the data preparation part.
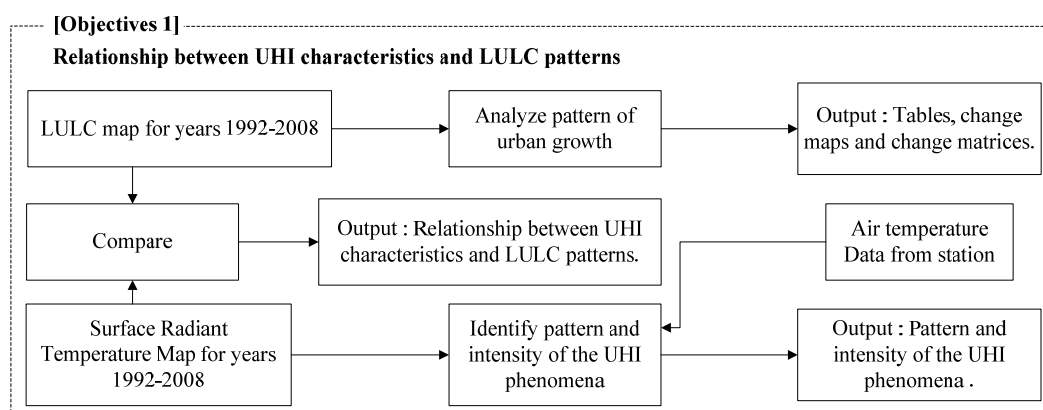
Figure 3.3 Flowcharts of Objectives 1 (relationship between UHI characteristics and LULC patterns).
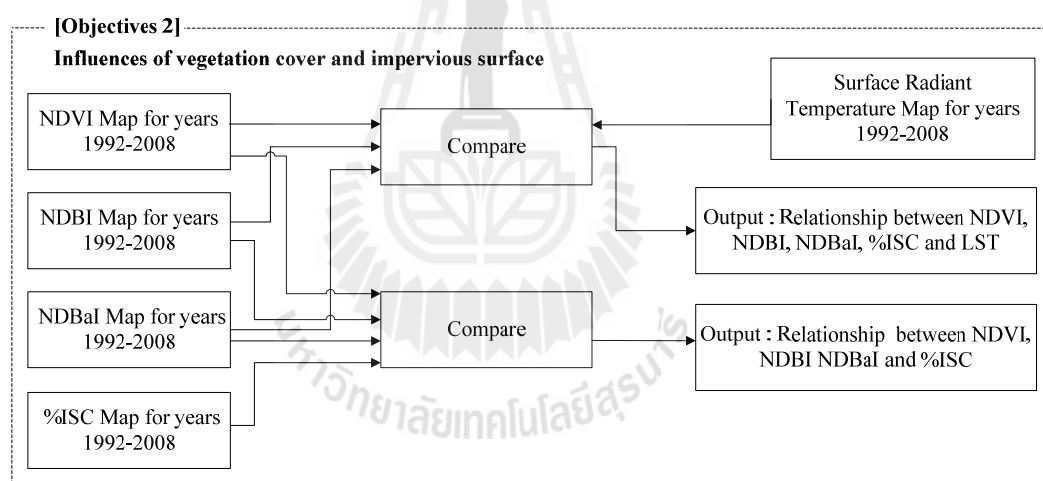
Figure 3.4 Flowcharts of Objectives 2 (influences of vegetation cover and impervious surface).
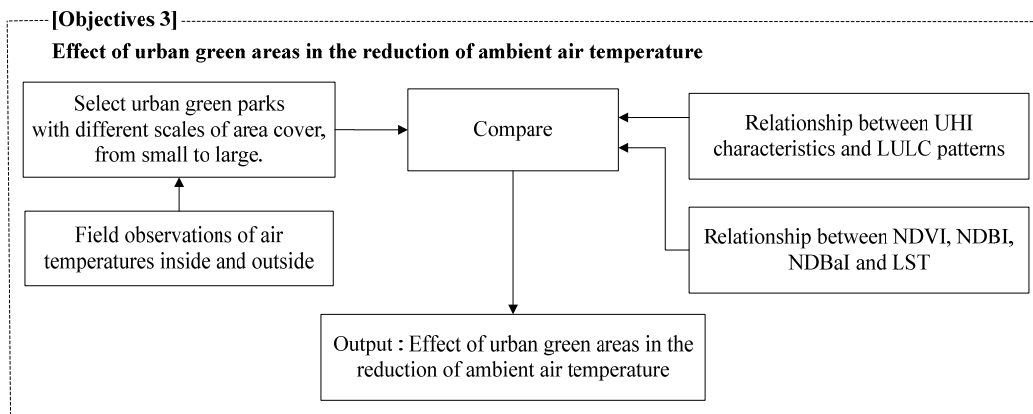
Figure 3.5   Flowcharts of objectives 3 (effect of urban green areas in the reduction of ambient air temperature).
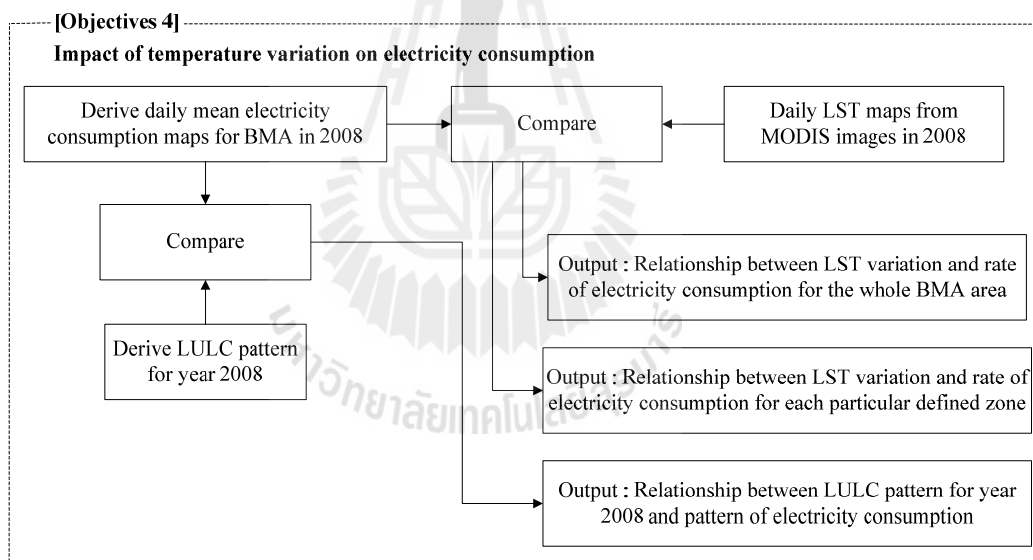
Figure 3.6   Flowcharts of objectives 4 (impact of temperature variation on electricity consumption).

(2)   Landsat TM images for BMA region in years 1992, 1996, 2000, 2004, and 2008 (winter dates) were provided from GISTDA while MODIS images were downloaded from its website (Table 3.1). Only winter TM images were used in this research due to their potentially less cloud cover and more visible vegetation cover.

The original satellite images were enhanced and geo-rectified using set of the ground control points (GCP) whose coordinates are acquired by GPS devices. Then, NIR false-color-composite satellite images (for years 1990, 1994, 1996, 2000, 2004, and 2008) were produced (RGB = 453 for TM imagery) (see Figure 3.7 for an example).
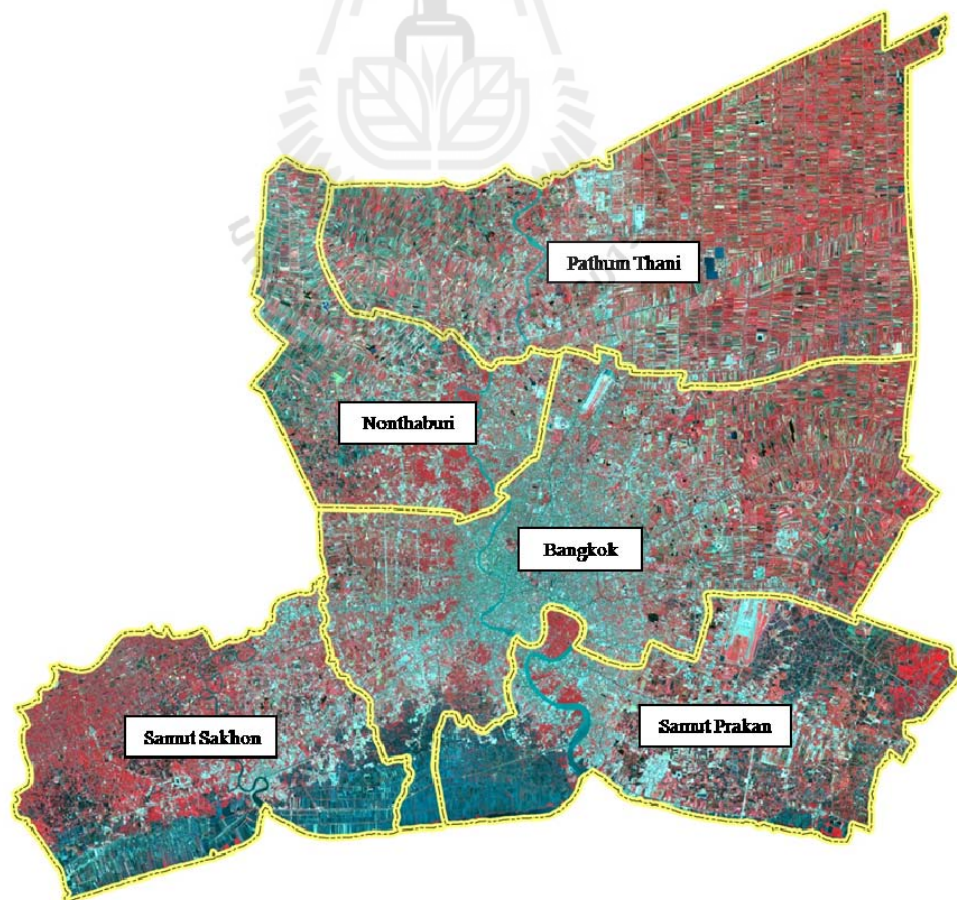
Figure 3.7   TM false color composite image (RGB = 432) of the BMA area (2008).

(3)　The composite images synthesized in step (2) were then digitally classified to create associated LULC map (for a given year) based on hybrid classifying method. The procedure began by applying the unsupervised classifying algorithm (ISODATA) to extract prior knowledge of possible LULC components within the images. Then, the supervised classifying algorithm (Maximum Likelihood) was applied to reclassify the primarily LULC components into 4 dominant categories, which are, (1) urban/built-up area, (2) vegetation, (3) bare land, and (4) water body.

In addition, the accuracy assessment was also conducted (for the 2008 LULC map) based on known LULC data of 440 reference locations distributing within the study area that were chosen using stratified sampling approach.

(4)　The LST maps were generated from Landsat TM thermal images (band 6) based on the following formula (pixel-based calculation):

$$L_0 = \frac{\left(L_{max} - L_{min}\right)}{255} \times DN + L_{min} \tag{3.1}$$

$$T_B = \frac{k_2}{\ln\left(\dfrac{k_1}{L_0} + 1\right)} \tag{3.2}$$

where, L_0 is the sensor's observed radiance, DN is the digital number of the observed pixel, L_{min} and L_{max} are spectral radiance of the used thermal band at DN = 0 and 255 respectively. T_B is derived LST in Kelvin unit, k_1 and k_2 are the pre-launch calibration constants of sensors. For Landsat-5 TM, $k_1 = 607.76$ W/(m^2.sr.μm) and $k_2 = 1250.56$ K (Rong-bo et al., 2007; Yuan and Bauer, 2007).

The MODIS LST data were derived from observed radiances at TIR bands 31 and 32 using the split-window algorithm that described in Wan and Dozier (1996) and Wan et al. (2002) that was reported to have errors of less than 1 K. In this method, the surface temperature (T_S) is estimated by the following relation:

$$T_s = C + \left(A_1 + A_2 \frac{1-\varepsilon}{\varepsilon} + A_3 \frac{\Delta\varepsilon}{\varepsilon^2} \right) \frac{T_{31}+T_{32}}{2} + \left(B_1 + B_2 \frac{1-\varepsilon}{\varepsilon} + B_3 \frac{\Delta\varepsilon}{\varepsilon^2} \right) \frac{T_{31}-T_{32}}{2} \quad (3.3)$$

where $\varepsilon = 0.5(\varepsilon_{31} + \varepsilon_{32})$ and $\Delta\varepsilon = 0.5(\varepsilon_{31} - \varepsilon_{32})$ are mean and difference of the surface emissivities in MODIS bands 31 and 32. T_{31} and T_{32} are the brightness temperatures in these two split windows bands. The coefficients C, A_i and B_i (i = 1, 2, 3) are given by interpolation on a set of multi-dimensional look-up tables (LUT). These LUTs were acquired by the linear regression of MODIS simulation data from radiative transfer calculations over wide ranges of surface and atmospheric conditions.

In order to have more conformity between the satellite-based LST mentioned above and their corresponding ground-based measurements, the relations between these two groups of data were identified (separately done for TM), then all the acquired satellite-based LST data were transformed to be their equivalent ground-based LST data by using the previously-derived relationships as being a standard transformation formula (see more details in Section 3.3).

(5)   The NDVI map was derived using DN data from the red and near infrared (NIR) bands of the used satellite images based on the following formula:

$$NDVI = \frac{R_{NIR} - R_{red}}{R_{NIR} + R_{red}} \quad (3.4)$$

where R_{NIR} and R_{red} are DN values in red and NIR bands, respectively. NDVI values range between -1 to 1 where large positive values indicate high vegetation cover.

Amount of impervious surface and bare land were implicitly quantified using the "normalized difference built-up index" (NDBI) and "normalized difference bareness index" (NDBaI) defined as follows (Chen et al., 2006):

$$NDBI = \frac{R_{MIR} - R_{NIR}}{R_{MIR} + R_{NIR}} \tag{3.5}$$

$$NDBaI = \frac{R_{MIR} - R_{TIR}}{R_{MIR} + R_{TIR}} \tag{3.6}$$

where R_{MIR} and R_{TIR} are pixel's DN values in mid-infrared and thermal infrared bands of the sensors, respectively.

Amount of the %ISC was quantified by using a normalized spectral mixture analysis (NSMA) model (described in Wu, 2004; Yuan and Bauer, 2007). The NSMA is a usual approach to sub-pixel classification whereby it can find percent impervious surface by modeling a mixed spectrum (at pixel scale) as being a linear combination of three common components: vegetation, impervious surface and soil endmembers (V-I-S). To determine fractional cover of each given endmember within a given pixel, following equation must be solved for all image bands simultaneously (pixel-based), using least squares approach:

$$R_b = \sum_{i=1}^{3} f_i R_{i,b} + e_b \tag{3.7}$$

Here, R_b is the reflectance value of the considered pixel at band b, f_i is the proportion of endmember i within the pixel, $R_{i,b}$ is the reflectance of endmember i for band b (as a pure pixel) and e_b is the error of fit for band b in use. Inverting this relationship of mixing equations can retrieve each endmember fraction (f_i) that best fits the observed mixed reflectances (ones with minimum error). This process implies determining of the optimal location of endmembers in feature space.

    3.2.2   Determination on relationship between LST and LULC components

        This section examines influences of the LULC components: vegetation cover, urban/built-up, impervious surface, and bare land, on the variations of satellite-based LST data. This objective was fulfilled by formulating proper relationships between the observed LST data and associated indices of the LULC components: (1) NDVI (for vegetation), (2) NDBI (for urban/built-up), (3) NDBaI (for bare land), and (4) %ISC (for the impervious surface), as formerly detailed in 3.2.1(5). This work was carried out in 5 steps as follows (see Figure 3.3-3.4 for flowchart):

        (1) Patterns of urban growth during 1992-2008 were analyzed using classified LULC maps gained from 3.2.1(3) and the obtained results were displayed in form of tables, change maps and change matrices.

        (2) Pattern and intensity of the SUHI phenomena in BMA region during 1992-2008 were identified using classified LST maps gained from 3.2.1(4).

        (3) Relations between UHI data and LULC patterns were identified by comparing the derived LULC maps and their corresponding UHI maps.

        (4) Relations between LST data and NDVI, NDBI, NDBaI, and %ISC indices were assessed by comparing values of these indices and their corresponding LST data. The linear form was assumed for all relationships under consideration.

(5) The internal relationships among NDVI, NDBI, NDBaI, and %ISC indices were investigated based on their observed values at pixel-based scale.

3.2.3 Impact of urban green areas on ambient air temperature reduction

This section devotes to the evaluation on effect of existing public parks within BMA area in ambient air temperature reduction based on both field observation data and satellite-based temperature data. The initial assumption was that urban parks can notably reduce ambient air temperature. This work consists of 4 steps as follows (see Figure 3.5 for flowchart):

(1) Information about public parks located in the BMA region was accumulated to identify some interesting places for further analysis. At present, there are 25 public parks distributed within the Bangkok Province (as listed in Table 3.2) and three of them were chosen for the subsequent detailed analysis.

(2) Three group of parks listed in Table 3.2 were chosen according to their reported sizes: Santipap Park (small), Lumpini Park (medium), and Chatuchak Park Complex (CPC) (large). The CPC comprises of Chatuchak Park, Queen Sirikit Park and Wachirabenchathat Park which locate close to each other in Chatuchak District. The general components of these parks are illustrated in Figures 3.8 and 3.9.

(3) Field measurements of air temperature data inside and outside each park mentioned in (2) were conducted during mid-daytime (within radius distance of about 3 km from park's center) on several bright and calm days during May-October 2009. The measurements were made just above ground to be resembled LST the most. There are 1249, 1634, and 1724 sampling points for the Santipap Park, Lumpini Park, and Chatuchak Park Complex (CPC), respectively (Figures 4.16).

(4) Impact of the chosen parks on the measured ambient temperature in (3) was evaluated based on spatial distributing pattern of the observed LST data within the prescribed radius form each park's center.

Table 3.2 List of official public parks located in Bangkok Province (in order of size).

No.	Name	Size (rai)	District	No.	Name	Size (rai)	District
1.	Suan Luang Rama IX Park	500	Prawet	14.	Nong Chok Park	35	Nong Chok
2.	Wachirabenchatat Park	375	Chatuchak	15.	Public Park in Commemoration of H.M. the King's 6th Cycle Birthday	29	Bang Kho Laem
3.	Lumphini Park	360	Pathum Wan	16.	Rommaninat Park	29	Phra Nakhon
4.	Seri Thai Park	350	Bueng Kum	17.	Benchasiri Park	29	Khlong Toei
5.	Queen Sirikit Park	196	Chatuchak	18.	Saranrom Park	23	Phra Nakhon
6.	Chatuchak Park	155	Chatuchak	19.	Suan Luang Rama VIII Park	24	Bang Phlat
7.	Benchakitti Park	130	Khlong Toei	20.	Maha Chakri Sirindhorn's 50th Birthday Park	20	Prawet
8.	Thonburirom Park	63	Thung Khru	21.	Santiphap Park	20	Ratchathewi
9.	Ram Indra Sports Park	59	Bang Khen	22.	Rommani Thungsikan Park	15	Don Mueang
10.	Her Majesty the Queen's 60th Birthday Park	52	Lat Krabang	23.	Phanphirom Park	14	Huai Khwang
11.	Tawiwanarom Park	51	Thawi Watthana	24.	Chaloem Phrakiat Kiakkai Public Park	10	Dusit
12.	Phra Nakhon Park	50	Lat Krabang	25.	Santichaiprakan Public Park	8	Phra Nakhon
13.	Wanadharm Park	38	Prawet				

Note: 1 rai = 1,600 m^2, 1 km^2 = 625 rai

From: http://minpininteraction.com/bkk_static/park22.asp.

Figure 3.8a   Environmental settings of the Santipap Park.

Figure 3.8b   Environmental settings of the Lumpini Park.

Figure 3.8c   Environmental settings of the Chatuchak Park Complex (CPC).

(a) General structure of the Lumpini Park.

(b) General structure of the H.M. Queen Sirikit Park.

Figure 3.9   General structures of (a) Lumpini Park and (b) H.M. Queen Sirikit Park.

From: http://www.parzapark.ob.tc/index.html.

3.2.4   Impact of temperature variation on electricity consumption

In this section, relationships between temperature variation (based on available ground-based data and satellite-based data) and amount of electricity consumption in BMA region in 2008 were examined. There are 2 steps included in this work (see Figure 3.6 for flowchart):

(1)   Electricity consumption data within the BMA region reported by the MEA in 2008 were acquired and their relationships with mean temperature recorded in the BMA area were assessed. Different groups of the MEA registered were examined and reported: (a) residential (RES), (b) small general service (SGS), (c) medium general service (MGS), (d) large general service (LGS), (e) governmental office (GOV), (f) specific business (SBU), and (g) non-profit organization (NPO). Example of report on electricity consumption issued by the MEA is shown in Table 3.3.

(2)   Relationships between MODIS-based LST data with amount of electricity consumption within BMA area (at districts with different LULC environment) were examined to identify impact of LULC components on electricity consumption.

Table 3.3   Report on the electricity consumption provided by the MEA (April 2008).

CLASS	Kilowatt hours	Coincident Peak at 14:30		Sector Diversified Demand		
		MW	Contribution (%)	Max MW.	Date	Time
RES	900,304,509	932.19	13.01	2,243.29	19 Apr 08	22:00
SGS	546,699,582	1,225.96	17.12	1,309.36	9 Apr 08	11:45
MGS	630,622,529	1,610.45	22.48	1,729.01	21 Apr 08	14:15
LGS	1,257,125,660	2,509.40	35.03	2,613.47	8 Apr 08	16:00
SBU	158,312,270	291.21	4.07	293.75	22 Apr 08	13:30
GOV and NPO	93,810,638	382.32	5.34	471.86	22 Apr 08	10:30
Public Lighting	19,064,076	0.00	0.00	53.27	-	-
Loss	102,617,598	211.13	2.95	211.13	22 Apr 08	14:30
Total	3,708,556,862	7,162.65	100	7,162.65	22 Apr 08	14:30

3.3   Construction of the Equivalent Ground-Based LST Maps

In this study, the LST maps were originally generated from the chosen satellite imagery sources (Landsat TM and MODIS) based on formulas described by Eq. 3.2 (for TM data) and Eq. 3.3 (for MODIS data). Then, these LST maps were transformed to become equivalent ground-based LST maps based on known relationships between extracted satellite-based LST and their associated ground-based temperatures. This procedure was introduced to reduce discrepancies between these two groups of LST data found within the study area. Detail of the procedure is as follows.
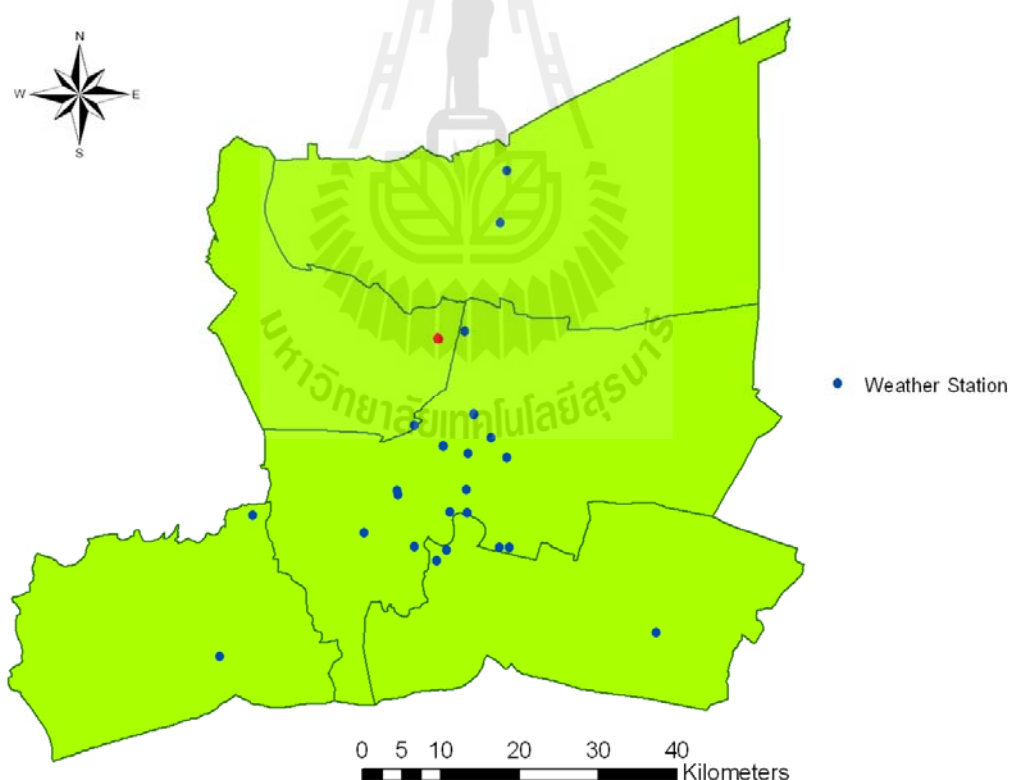
Figure 3.10   Location map of the used ground-based temperature measuring stations.

3.3.1 Ground-based temperature data

Ground-based temperature data were acquired from two responsible agencies, the Thai Meteorological Department (TMD) and the Pollution Control Department (PCD), including 26 measuring stations (Figure 3.10 and Table 3.4).

Table 3.4 General information of the selected temperature measuring stations.

Code	Location (UTM zone 47)				Name/Responsible agency			Data begin
	Easting	Northing	DST	PRV	code	Name	AGC	
ST1	669401	1518780	KTO	BKK	455201	Bangkok Metropolis	TMD	1991
ST2	669269	1539070	DMU	BKK	455601	Bangkok Airport	TMD	1991
ST3	674858	1511450	BNA	BKK	455301	Bang Na	TMD	2006
ST4	669567	1515860	KTO	BKK	455203	Klong Toei	TMD	2001
ST5	660676	1518679	TBR	BKK	02T	Bansomdejchaopraya Rajabhat U	PCD	1996
ST6	662861	1511566	RBU	BKK	03T	Rat Burana Post Office	PCD	1996
ST7	673673	1511376	BNA	BKK	05T	TMD, Bangna	PCD	1996
ST8	670334	1528374	CTC	BKK	07T	Chandrakasem Rajabhat U.	PCD	1996
ST9	670332	1528372	BKP	BKK	10T	NHA-Klongjun	PCD	1996
ST10	669612	1523437	HKW	BKK	11T	NHA Stadium-Huaykwang	PCD	1996
ST11	667326	1515973	YNW	BKK	12T	Nonsi Withaya School	PCD	1996
ST12	656379	1513271	BKT	BKK	15T	Singharaj Pittayakom School	PCD	1996
ST13	660743	1518091	TRR	BKK	52T	Thonburi Power Substation	PCD	1997
ST14	672535	1525366	BKP	BKK	53T	Chokechai 4 Police Box	PCD	1996
ST15	666527	1524284	DDG	BKK	54T	NHA-Dindaeng	PCD	1996
ST16	666523	1524294	PTH	BKK	59T	Public Relations Department	PCD	2004
ST17	674551	1522837	WTL	BKK	61T	Badindecha School	PCD	2005
ST18	662820	1526910	BKR	NBR	13T	EGAT	PCD	1996
ST19	665920	1538067	PKR	NBR	22T	Sukhothai Thammathirat U.	PCD	1996
ST20	666931	1511101	PPD	SPK	08T	Prabadang Disable Rehabitation	PCD	1997
ST21	693623	1500626	BST	SPK	19T	NHA-Bangplee	PCD	1996
ST22	665688	1509780	PPD	SPK	17T	The Residental House of DMR	PCD	1996
ST23	638074	1497609	MSS	SSK	27T	SSK Provincial Administration	PCD	1996
ST24	642271	1515539	KTB	SSK	14T	SSK Highway District	PCD	1997
ST25	673719	1552775	KLG	PTN	20T	Bangkok U., Rangsit Campus	PCD	1995
ST26	674534	1559398	KLG	PTN	419301	Pathum Thani Agromet	TMD	2006

Note: 1. DST ≡ District, PRV ≡ Province, AGC ≡ Responsible agency
2. NHA ≡ National Housing Authority, EGAT ≡ Electricity Generating Authority of Thailand, DMR ≡ Department of Mineral Resources, TMD ≡ Thai Meteorological Department. PCD ≡ Pollution Control Department
3. ST19 was used as a reference station for the temporal UHI analysis in this chapter.

3.3.2   Relationships between ground-based and satellite-based temperature data

As discussed earlier, the preferred LST maps for further UHI analysis are the equivalent ground-based LST maps generated based on knowledge of the relationship between original satellite-based LST and their associated ground-based temperatures. These relationships were determined for the TM case only as it is most crucial to our research and both temperature dataset are appropriate to be compared with each other. In the MODIS case, pixel-based LST map has relatively large scale (1km) that makes it not being suitable for the comparison with the point-based ground measurement. Example of the obtained MODIS-LST map is shown in Figure 3.13.

The first step was acquiring reference ground-based LST data along with their corresponding LST data that were obtained from the satellite-based LST maps. Using data during the year 1992 to 2008, about 159 pairs of these temperature data were accumulated and then rearranged in order of ground-based LST values from minimum to maximum. Then, average values of these ground-based LST and their associated satellite-based data were calculated at ranging step of 1°C each (e.g. at 20-21°C, 21-22°C, and 22-23°C, etc.).

These pairs of the average values (for each defined LST step value) were then plotted against each other to identify the existing relationships and results are reported in Figures 3.11. The plotting result indicates strong linear relationship between average ground-based temperature and its average satellite-based counterpart at the correlation coefficient (R^2) of 0.8355. The found relationship is expressed by:

$$\text{TM case:} \quad T_G = 1.4238\ T_S + 10.53 \tag{3.8}$$

where T_G and T_S are the average ground-based and satellite-based LST, respectively.

This relation was assumed to valid for normal LST range of interest (at 20-35°C).
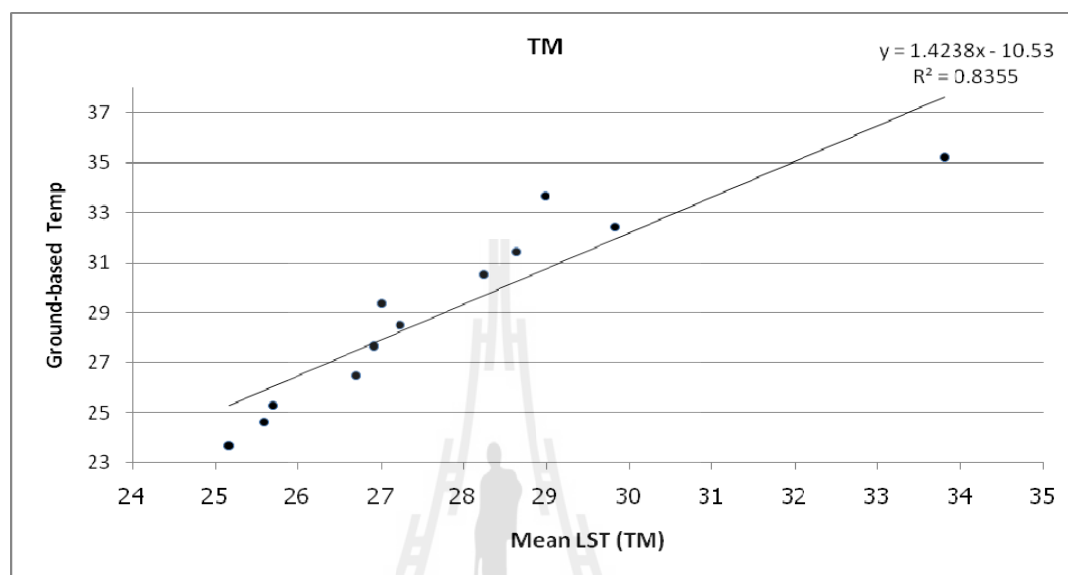
Figure 3.11   Relation of average ground-based and satellite-based LST data (TM case).

The known relation described by Eq. 3.8 was then used as essential tool

for the construction of equivalent LST ground-based LST map from the original

satellite-based LST map. Example of this task is presented in Figures 3.12. Table 3.5

provides data of the TG/TS pairs used in Figure 3.11.

Table 3.5   Values of TG and TS pair (in ^{o}C) used in Figure 3.11.

$\mathbf{T_G}$	23.67	24.63	25.29	26.49	27.66	28.49	29.37	30.52	31.42	32.43	33.65	35.21
$\mathbf{T_S}$	25.15	25.58	25.69	26.70	26.91	27.23	27.00	28.23	28.63	29.82	28.97	33.80

Note: $T_G \equiv$ Average ground-based temperature data (data during 1992 to 2008.)

$T_S \equiv$ Average satellite-based LST data (data during 1992 to 2008.)
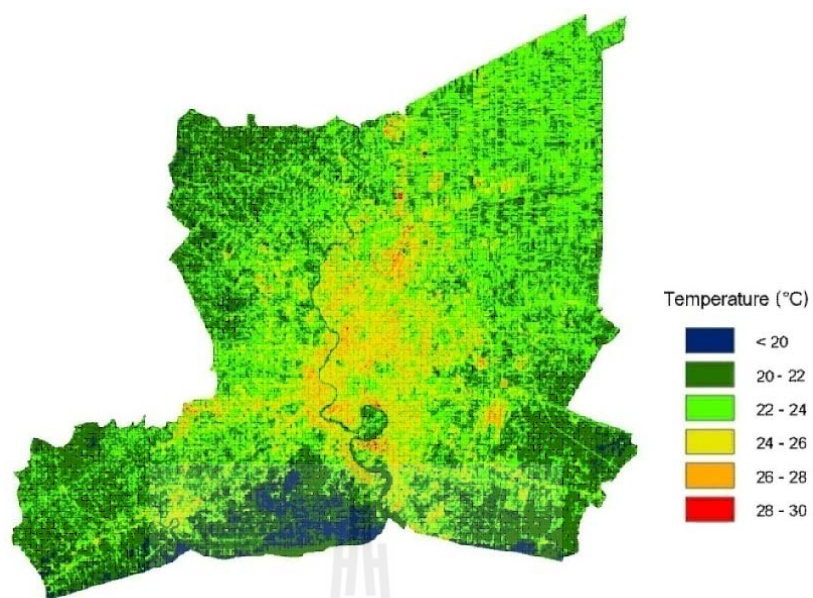
(a) Original TM-based LST map of 2008 (on 02/12/2008 at 10:21:35 AM)
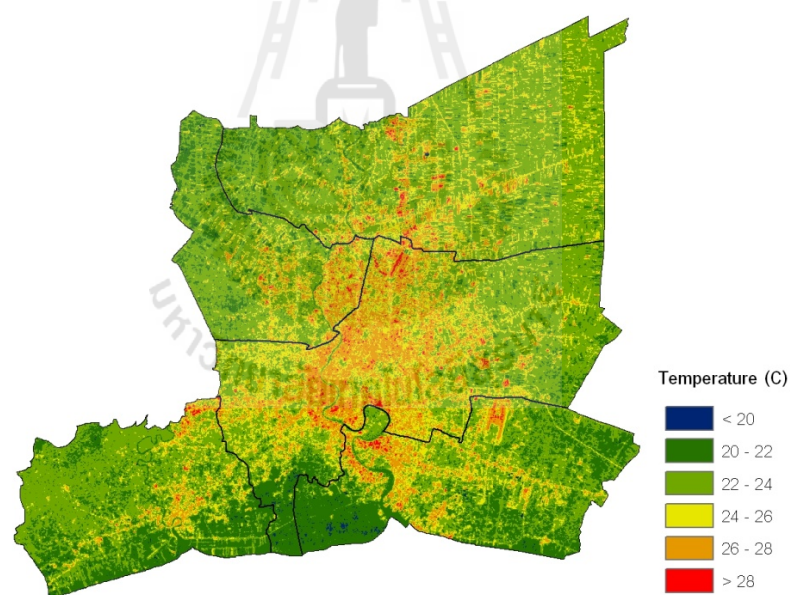
(b) Equivalent ground-based LST map of 2008 (on 02/12/2008 at 10:21:35 AM).

Figure 3.12   Comparison between original LST maps and their equivalent ground-based LST maps for the TM case.
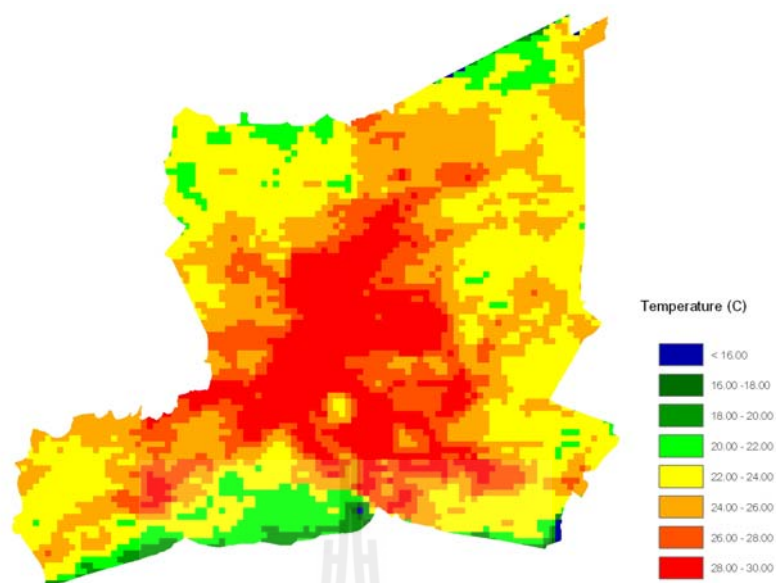
Figure 3.13   Example of the daytime MODIS-based LST map for the BMA region.

3.4   Field Measurements of Air Temperature Data

As mentioned earlier, field measurements of air temperature data inside and outside each chosen park were conducted during mid-daytime (within radius distance of about 3 km from the park's center) on several bright and calm days during May-October 2009. The measurements were made just above ground surface so that the recorded data can be confidentially resembled the actual LST data of the studied area. Group of trained staffs (Figure 3.14) were organized the measurements using devices like GPS receivers, the VelociCalc 9555 (for mobile measurements) and QUESTemp 34 (for stationary measurements) as seen in Figure 3.15. For stationary measurements, air temperature data were recorded at three different heights above ground surfaces: (1) at surface level, (2) at ~0.5 m height, and (3) at ~1 m height. The obtained datasets from these methods have similar patterns of variation and the obtained data at surface level were used for the formation of temperature maps presented in Chapter IV.

Figure 3.14   Group of trained staffs that organized field measurements.

(a) QUESTemp 34 (for stationary measurements).

(b) 9555-VelociCalc (for mobile measurements).

Figure 3.15 Photos of the temperature sensors used in field measurements.

CHAPTER IV

RESULTS AND DISCUSSION

This chapter reports significant results obtained from the research as described in the research procedure stated in Chapter III. Its content composes of four principal works: (1) urban expansion and its impact on the UHI phenomenon, (2) relationships of LULC indices and LST data, (3) influence of the urban green area on ambient air temperature, and (4) relations of air temperature variation and electricity consumption in the BMA region. Details of each aforementioned issue are as follows.

4.1 Variation Patterns of the Ground-Based Temperature Data

The acquired ground-based data stated in Section 3.3 can be readily applied to examine variation pattern of the near surface temperature records within BMA region, for examples, daily/monthly/annual variation. Some interesting issues were explored and their results are demonstrated here as follows.

4.1.1 Diurnal variation patterns

As being a tropical country, Thailand usually has a large gap between minimum and maximum daily temperature data (about 10-15°C) but this gap is less pronounced within the BMA region (about 7-10°C) (TMD, 2011). This phenomenon can be seen in Figure 4.1 wherein the diurnal variation of the recorded air temperature over four selected days at ST1 station (Bangkok Metropolis location) are presented

(2 days each for summer and winter seasons). From Figure 4.1, it was found that the variation patterns of the observed temperature data over all four days are rather similar to each other with peak values appear around 15.00-16.00 PM and the lowest values occur at around 6.00-7.00 AM. However, the hourly data in winter are usually lower than those in summer (at the same time period) around 5-8°C. The peak values in summer are at 35-36°C and lowest values at about 27-28°C whereas these values in winter are at about 27-28°C and 19-20°C, respectively. The increasing rate of temperature during daytime (7.00 AM - 4.00 PM) is about 1°C /hour. More relevant data are given in Table 4.1.

In term of the UHI intensity, the differences between observed temperature at Station 1 (urban) and Station 19 (reference) on chosen days are most pronounced at nighttime (around 19.00-21.00 PM) in summer with peak at around 3-4°C (Figure 4.2). But on winter days, peak spots of 1-3°C appear in the morning (around 8.00-10.00 AM). However, during daytime, trends of UHI intensity are still uncertain in both seasons. And to have more precise conclusion on the diurnal UHI characteristics of both seasons, more reference temperature data must be used.
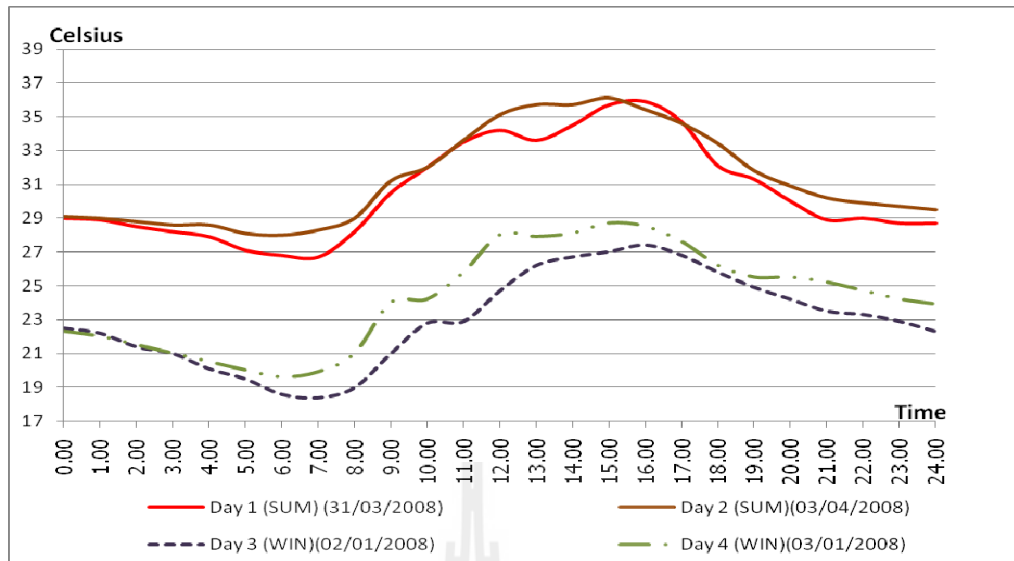
(a) Diurnal variation of the ground-based temperature profiles on four selected days at ST1 station (Bangkok Metropolis location).
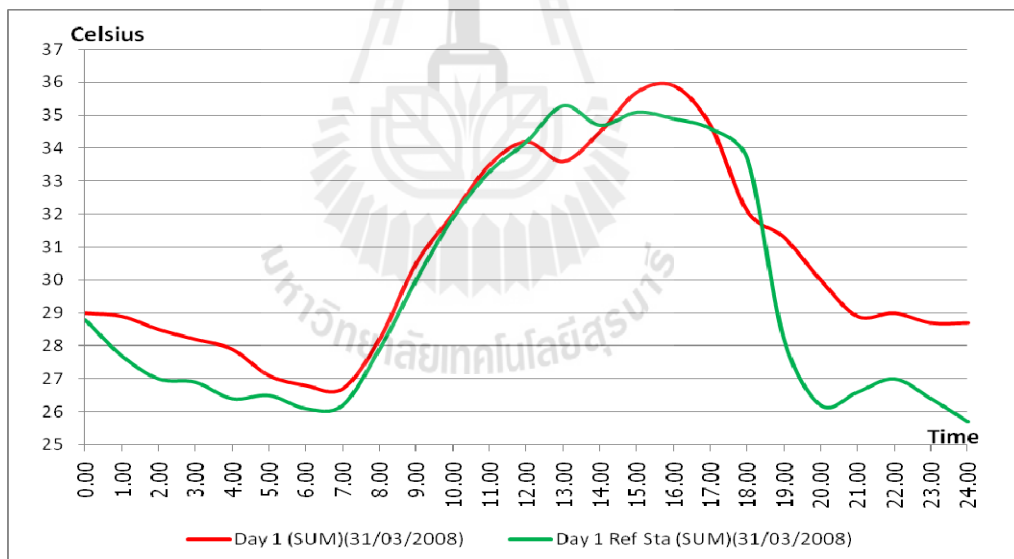
(b) Diurnal variation of ground-based temperature on a selected day at two stations, the ST1 station at Bangkok Metropolis location (urban) and Station 19 at Sukhothai Thammathirat University (reference station).

Figure 4.1   Diurnal temperature variations on selected winter and summer days.
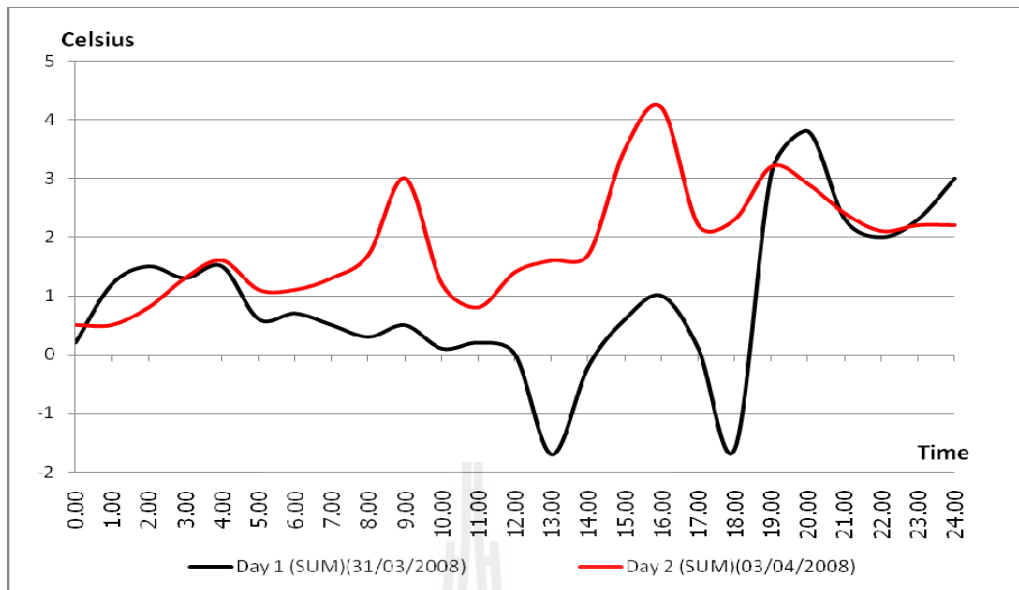
(a) Diurnal variation of the UHI intensity on two selected summer days.
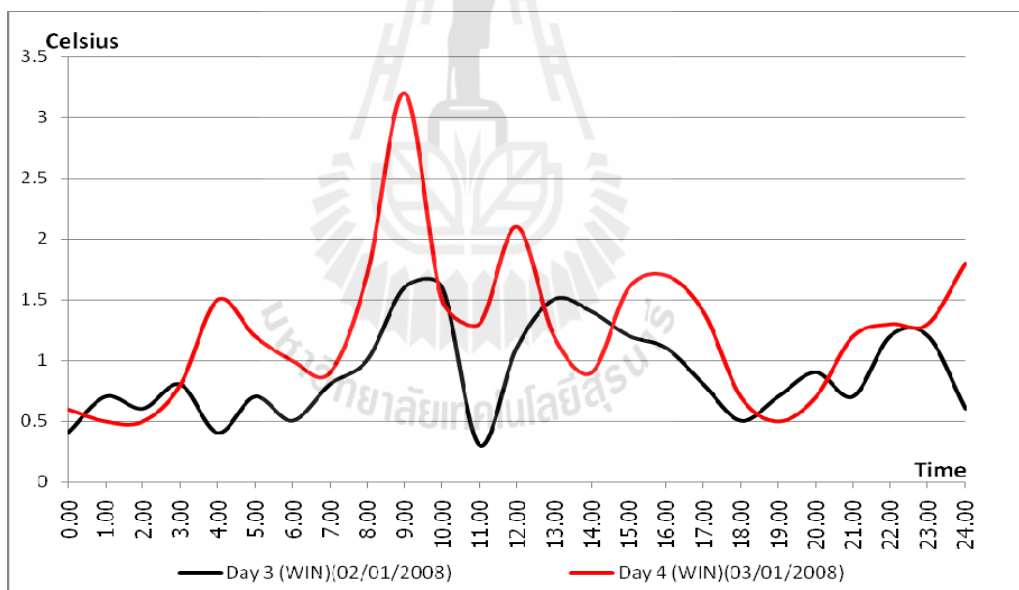
(b) Diurnal variation of the UHI intensity on two selected winter days.

Figure 4.2   Diurnal variations of the UHI intensity on selected winter/summer days, the differences between observed temperature of ST1 station at Bangkok Metropolis location (urban) and Station 19 at the Sukhothai Thammathirat ᴜniversity (reference).

Table 4.1   Diurnal temperatures and their UHI intensity (ΔT) on four chosen days at the ST1 station.

Time	Summer (ST1)				Winter (ST1)			
	Day 1 (31/03/2008)		Day 2 (03/04/2008)		Day 3 (02/01/2008)		Day 4 (03/01/2008)	
	T	ΔT	T	ΔT	T	ΔT	T	ΔT
0.00	29.0	0.2	29.1	0.5	22.5	0.4	22.3	0.6
1.00	28.9	1.2	29.0	0.5	22.2	0.7	22.0	0.5
2.00	28.5	1.5	28.8	0.8	21.4	0.6	21.5	0.5
3.00	28.2	1.3	28.6	1.3	21.0	0.8	21.0	0.8
4.00	27.9	1.5	28.6	1.6	20.1	0.4	20.5	1.5
5.00	27.1	0.6	28.1	1.1	19.5	0.7	20.0	1.2
6.00	26.8	0.7	28.0	1.1	18.6	0.5	19.6	1.0
7.00	26.7	0.5	28.3	1.3	18.4	0.8	19.9	0.9
8.00	28.2	0.3	29.0	1.7	19.0	1.0	21.0	1.7
9.00	30.5	0.5	31.2	3.0	21.0	1.6	24.0	3.2
10.00	32.0	0.1	32.0	1.2	22.8	1.6	24.2	1.5
11.00	33.5	0.2	33.6	0.8	22.9	0.3	25.8	1.3
12.00	34.2	0.0	35.1	1.4	24.7	1.1	28.0	2.1
13.00	33.6	-1.7	35.7	1.6	26.2	1.5	27.9	1.2
14.00	34.5	-0.2	35.7	1.7	26.7	1.4	28.1	0.9
15.00	35.7	0.6	36.1	3.5	27.0	1.2	28.7	1.6
16.00	35.9	1.0	35.4	4.2	27.4	1.1	28.5	1.7
17.00	34.7	0.1	34.6	2.2	26.8	0.8	27.6	1.4
18.00	32.1	-1.6	33.4	2.3	25.8	0.5	26.2	0.7
19.00	31.3	3.1	31.8	3.2	24.9	0.7	25.5	0.5
20.00	30.0	3.8	30.9	2.9	24.2	0.9	25.5	0.7
21.00	28.9	2.3	30.2	2.4	23.5	0.7	25.2	1.2
22.00	29.0	2.0	29.9	2.1	23.3	1.2	24.7	1.3
23.00	28.7	2.3	29.7	2.2	22.9	1.2	24.2	1.3
24.00	28.7	3.0	29.5	2.2	22.3	0.6	23.9	1.8

Note: Temperature data from the ST19 station were used as reference (not shown here).

4.1.2   Monthly variation patterns

The monthly-mean temperature data in the BMA region can vary greatly from season to season as seen in Figure 4.3a at four selected stations (ST1, ST2, ST4, and ST19) over period of 48 months (January 2006-December 2009). It is obvious that lowest values usually exhibit in winter months (mostly December) and highest values are often visible in summer months (mostly April). The highest average values were found at the ST4 station (Klong Toei) followed by ST1 station (Bangkok Metropolis), ST2 (Bangkok Airport), and ST19 (Sukhothai Thammathirat University), respectively. The cooler environment evidenced at the ST19 station is probably due to the existing agricultural and open space surroundings.

In term of the UHI intensity, the differences between monthly observed mean temperature at the selected stations and station 19 (reference) are most pronounced during wintertime (around November-January) and least pronounced during monsoon season (around July-September) (Figure 4.3b). Peak values at around 1.5-2.5°C were found at the ST4 station (Klong Toei) while the other stations usually have peak of less than 1°C. In addition, it seems that the UHI intensity tend to noticeably decline in later years at the ST1 station (Bangkok Metropolis) and ST2 (Bangkok Airport). But at the ST4 station (Klong Toei), the UHI trend seems rather stable over period of the study, especially on the later years (e.g. during years 2008-2009).
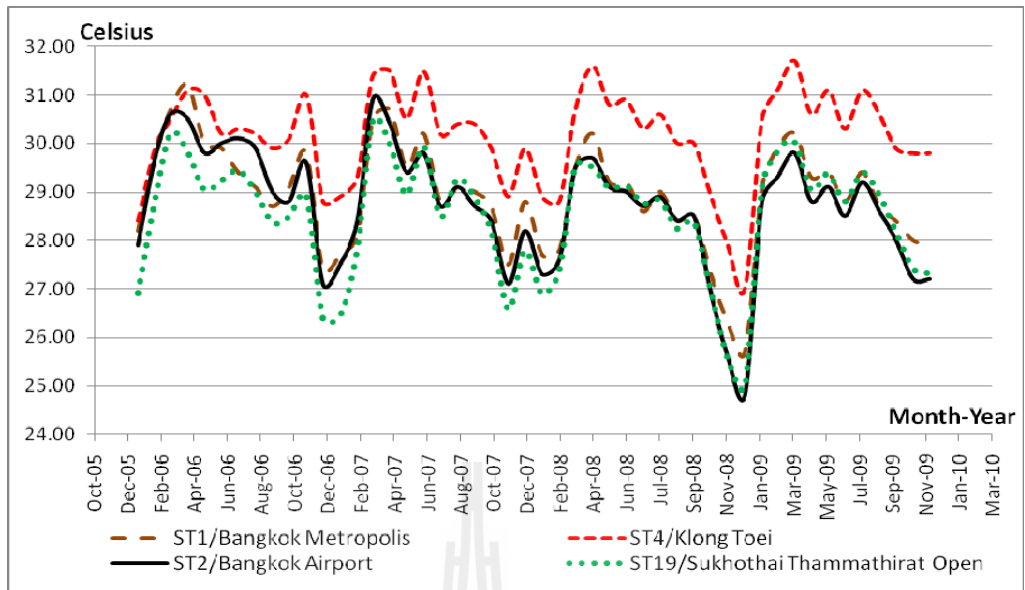
(a) Monthly-mean temperature.
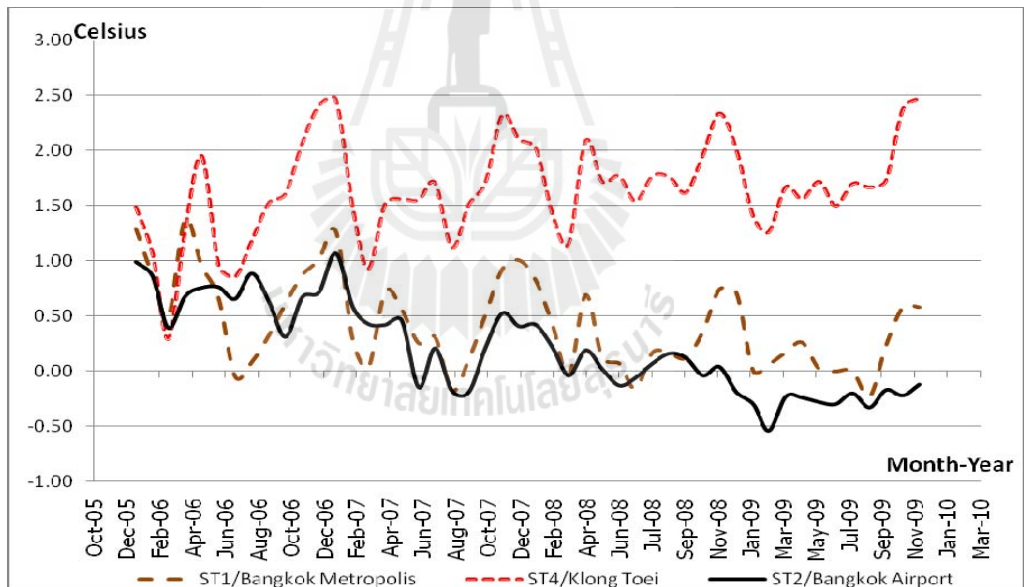
(b) Associated UHI intensity [from (a)].

Figure 4.3   Variation patterns of (a) monthly mean temperature data (2006-2009) and (b) their associated UHI intensity (from Table 4.2).

Table 4.2   Monthly mean temperatures and their UHI intensity (2006-2009) (in ^{o}C).

Month	2006						2008					
	ST1		ST4		ST2		ST1		ST4		ST2	
	T	ΔT	T	ΔT	T	ΔT	T	ΔT	T	ΔT	T	ΔT
Jan	28.20	1.29	28.40	1.49	27.90	0.99	27.70	0.82	28.90	2.02	27.30	0.42
Feb	29.70	0.86	29.90	1.06	29.70	0.86	27.80	0.41	28.80	1.41	27.60	0.21
Mar	30.70	0.49	30.50	0.29	30.60	0.39	29.50	-0.04	30.70	1.16	29.50	-0.04
Apr	31.20	1.38	31.10	1.28	30.50	0.68	30.20	0.69	31.60	2.09	29.70	0.19
May	30.00	0.95	31.00	1.95	29.80	0.75	29.20	0.12	30.80	1.72	29.10	0.02
Jun	29.90	0.66	30.20	0.96	30.00	0.76	29.20	0.07	30.90	1.77	29.00	-0.13
Jul	29.40	-0.05	30.30	0.85	30.10	0.65	28.60	-0.16	30.30	1.54	28.70	-0.06
Aug	29.10	0.08	30.20	1.18	29.90	0.88	29.00	0.17	30.60	1.77	28.90	0.07
Sep	28.70	0.33	29.90	1.53	29.00	0.63	28.40	0.16	30.00	1.76	28.40	0.16
Oct	29.10	0.61	30.10	1.61	28.80	0.31	28.50	0.12	30.00	1.62	28.50	0.12
Nov	29.80	0.87	31.00	2.07	29.60	0.67	27.30	0.36	28.90	1.96	26.90	-0.04
Dec	27.40	1.01	28.80	2.41	27.10	0.71	26.30	0.74	27.90	2.34	25.60	0.04
Month	2007						2009					
	ST1		ST4		ST2		ST1		ST4		ST2	
	T	ΔT	T	ΔT	T	ΔT	T	ΔT	T	ΔT	T	ΔT
Jan	27.70	1.27	28.90	2.47	27.50	1.07	25.70	0.71	27.00	2.01	24.80	-0.19
Feb	28.10	0.28	29.30	1.48	28.40	0.58	29.10	0.00	30.50	1.40	28.80	-0.30
Mar	30.50	0.03	31.40	0.93	30.90	0.43	29.90	0.06	31.10	1.26	29.30	-0.54
Apr	30.70	0.72	31.50	1.52	30.40	0.42	30.20	0.17	31.70	1.67	29.80	-0.23
May	29.50	0.56	30.50	1.56	29.40	0.46	29.30	0.26	30.60	1.56	28.80	-0.24
Jun	30.20	0.25	31.50	1.55	29.80	-0.15	29.40	0.02	31.10	1.72	29.10	-0.28
Jul	28.80	0.31	30.20	1.71	28.70	0.21	28.80	0.00	30.30	1.50	28.50	-0.30
Aug	29.10	-0.18	30.40	1.12	29.10	-0.18	29.40	0.00	31.10	1.70	29.20	-0.20
Sep	29.00	0.11	30.40	1.51	28.70	-0.19	28.70	-0.23	30.60	1.67	28.60	-0.33
Oct	28.70	0.51	29.90	1.71	28.40	0.21	28.40	0.23	29.90	1.73	28.00	-0.17
Nov	27.50	0.93	28.90	2.33	27.10	0.53	28.00	0.58	29.80	2.38	27.20	-0.22
Dec	28.80	1.01	29.90	2.11	28.20	0.41	27.90	0.58	28.90	2.48	27.20	-0.12

Note: Temperature data from the ST19 station were used as reference (not shown here).

4.2   Urban Growth and Its Impact on UHI Phenomenon

As described earlier in Chapter II, it was found from many researches about strong impact of urban growth on intensity of the UHI phenomenon at several megacities around the world. However, for the BMA region, such impact was still not examined thoroughly by known previous works. To gain more concrete knowledge on this important issue over BMA area, the systematic examination about relations of urban/built-up expansion and the UHI characteristics was carried out. This work was achieved based on the comparison between two associated data maps: satellite-based LULC maps and their corresponding LST maps. Both products were constructed from the Landsat TM imagery and the important results gained in this work are as follows.

4.2.1   Urban growth and LULC changing pattern

To quantify pattern or rate of urban growth effectively, the temporal LULC maps of the area (with urban/built-up as a main LULC component) must be synthesized first. This was accomplished by generating classified LULC maps during 1992-2008 of BMA region based on Landsat TM imagery (as described in Section 3.2.1). There are four main components presented on these maps: (1) urban/built-up (U/B), (2) vegetation (VEG), (3) bare land (BARE), and (4) water body (WAT) (Figures 4.4a-e). Accuracy assessment of the obtained 2008 classified LULC map was computed based on 440 stratified sampling points. This number is derived from the multinomial distribution theory with a level of confidence of 90% and a precision of 5% (Jensen, 2005). In this case, the overall accuracy of 84.55% with Kappa index of 0.7902 were achieved indicating satisfied result of the gained LULC map for further use, especially the fairly high accuracy of the urban/built-up class (Table 4.3).
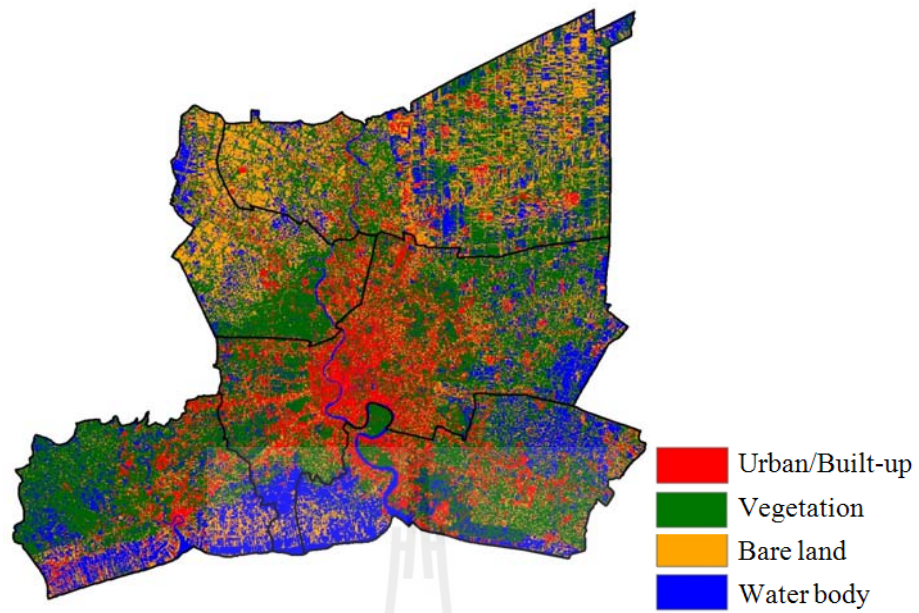
(a) Classified LULC map (20/11/1992).
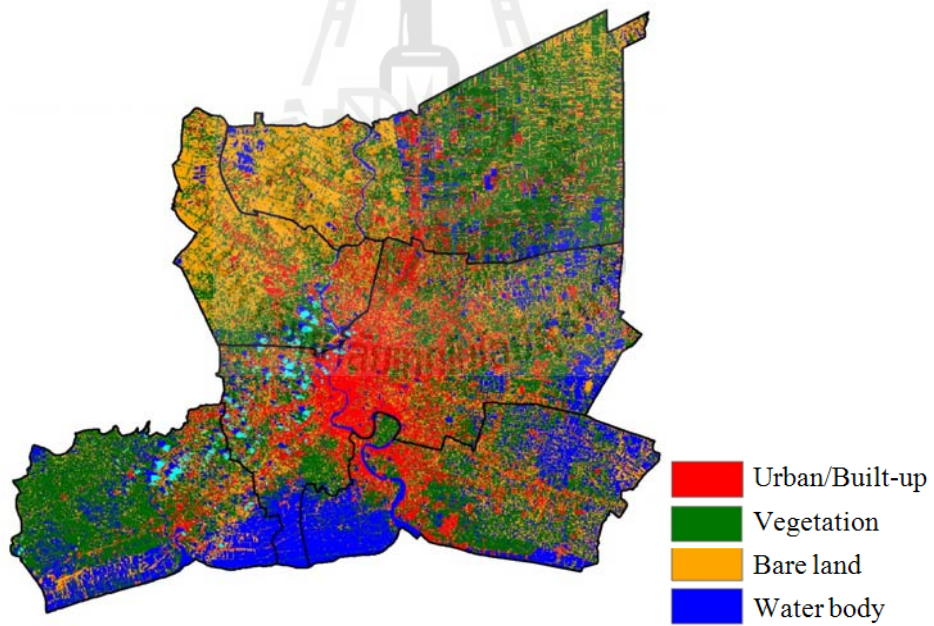
(b) Classified LULC map (15/11/1996).

Figure 4.4 Classified BMA LULC of (a) 1992, (b) 1996, (c) 2000, (d) 2004, (e) 2008.
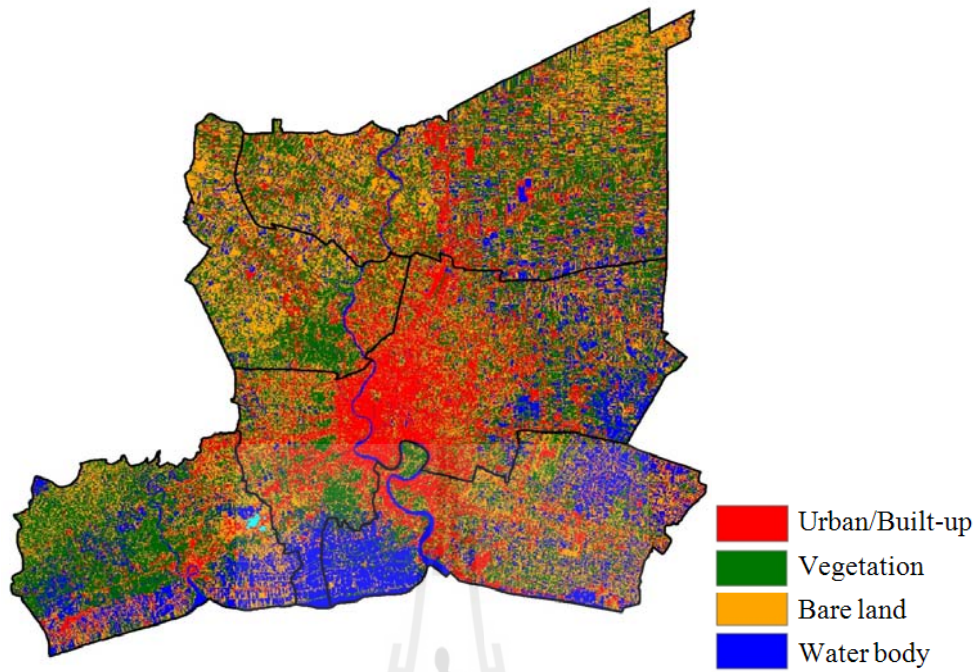
(c) Classified LULC map (10/11/2000).
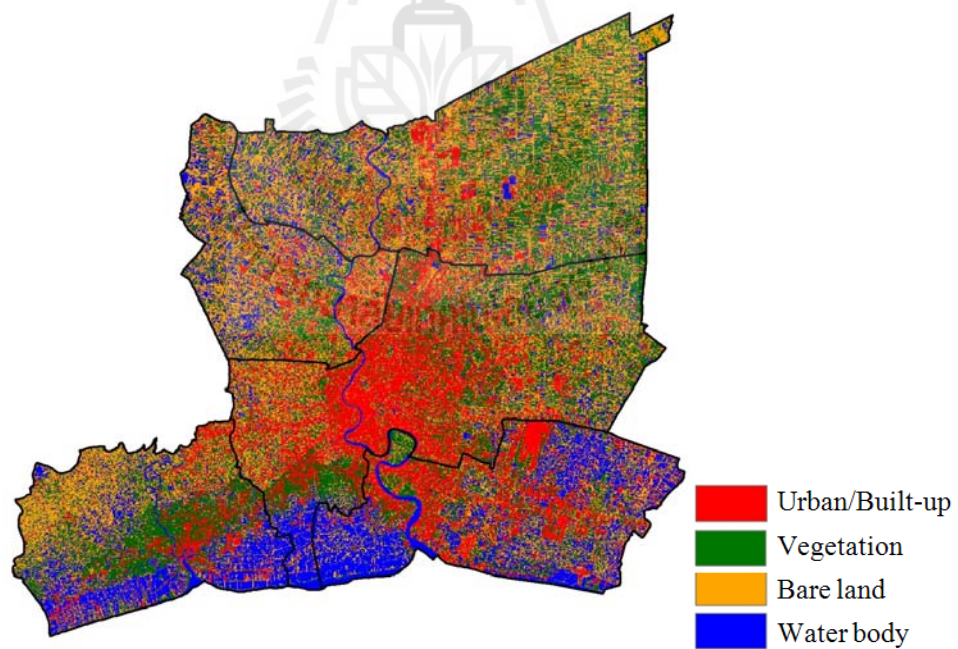
(d) Classified LULC map (21/11/2004).

Figure 4.4   Classified BMA LULC of (a) 1992, (b) 1996, (c) 2000, (d) 2004, (e) 2008 (Continued).
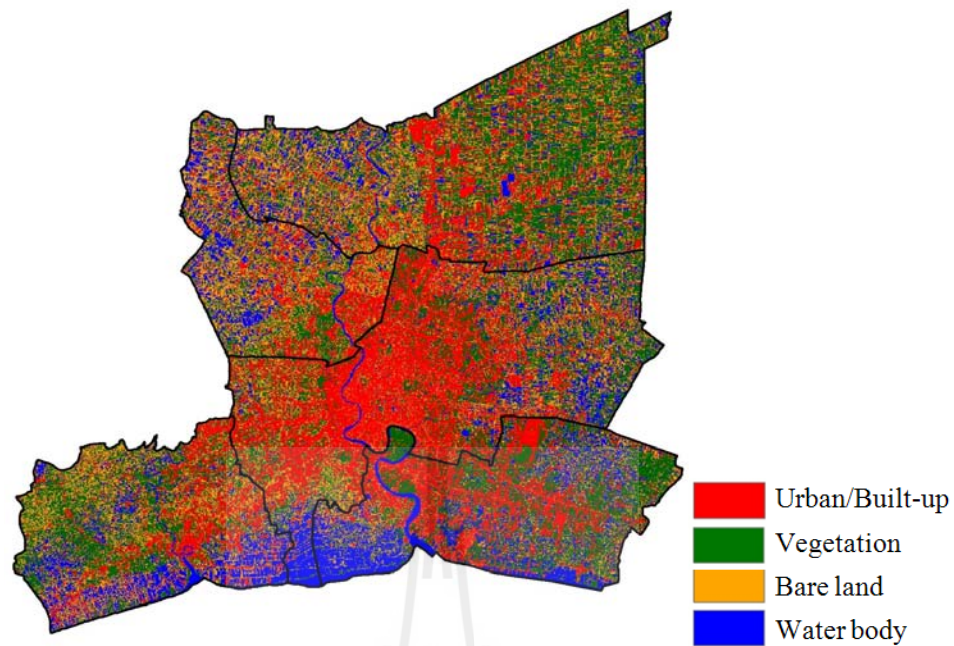
(e) Classified LULC map (02/12/2008).

Figure 4.4   Classified BMA LULC maps of (a) 1992, (b) 1996, (c) 2000, (d) 2004,

(e) 2008 (Continued).

Table 4.3   Error matrix for the 2008 classified LULC map (in Figure 4.4e).

	LULC Class	Classified data				Total (pixel)	EO	PA
		U/B	VEG	BARE	WAT			
Reference data	U/B	106	8	8	1	123	5.36	94.64
	VEG	3	114	26	0	143	14.93	85.07
	BARE	3	10	91	0	104	31.06	68.94
	WAT	0	2	7	61	70	1.61	98.39
Total (pixel)		112	134	132	62	440	-	-
EC		13.82	20.28	12.5	12.86	-	-	-
CA		86.18	79.72	87.5	87.14	-	-	-

Note: Overall accuracy = 84.55 and Kappa index = 0.7902

Table 4.4   Proportion of LULC components in 1992, 1996, 2000, 2004, and 2008.

LULC Class	1992		1996		2000		2004		2008	
	km^2	%	km^2	%	km^2	%	km^2	%	km^2	%
U/B	806.38	14.49	831.91	14.95	1095.01	19.67	1172.46	21.06	1552.14	27.88
VEG	2352.96	42.27	2255.86	40.53	1819.03	32.68	1590.86	28.58	1811.94	32.55
BARE	1315.93	23.64	1475.31	26.50	1747.94	31.40	1808.17	32.48	1310.73	23.55
WAT	1091.15	19.60	946.08	17.00	900.51	16.18	994.92	17.87	891.59	16.02
Cloud	0.00	0.00	57.26	1.03	3.91	0.07	0.00	0.00	0.00	0.00
Total	5566.4	100	5566.4	100	5566.4	100	5566.4	100	5566.4	100
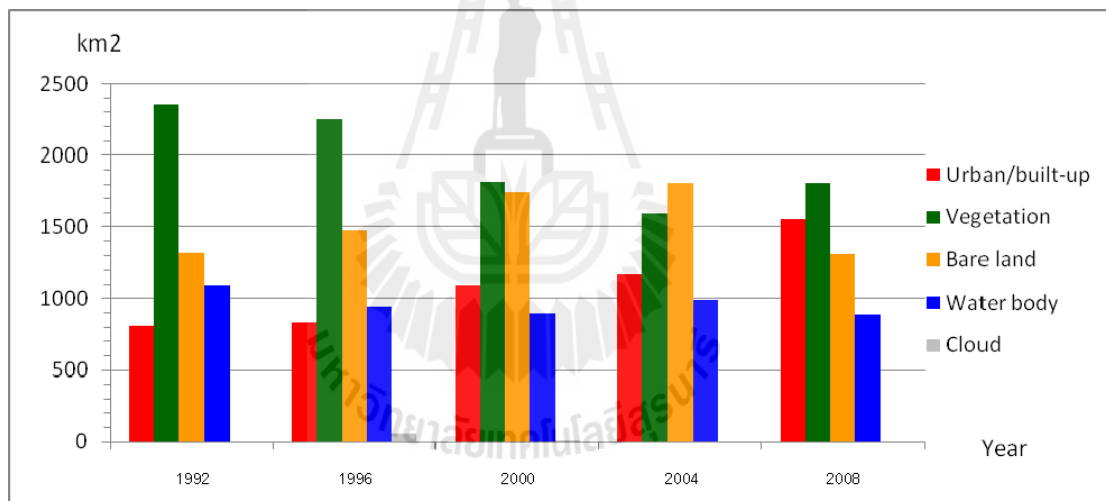
Figure 4.5   Proportion of LULC components in 1992, 1996, 2000, 2004, and 2008.

Table 4.5 Periodic change rates (gain/loss) of LULC components during 1992-2008.

Period	Class	U/B	VEG	BARE	WAT
1992-1996	km^2(total)	25.53	-97.10	159.38	-145.08
	% (total)	3.21	-4.13	12.11	-13.30
1996-2000	km^2(total)	263.10	-436.82	272.63	-45.56
	% (total)	31.62	-19.36	18.48	-4.82
2000-2004	km^2(total)	77.45	-228.18	60.23	94.41
	% (total)	7.07	-12.54	3.45	10.48
2004-2008	km^2(total)	379.68	221.09	-497.44	-103.33
	% (total)	32.38	13.90	-27.51	-10.39
1992-2000	km^2(total)	288.64	-533.92	432.01	-190.64
	% (total)	35.79	-22.69	32.83	-17.47
	km^2(annual)	36.08	-66.74	54.00	-23.83
	% (annual)	4.47	-2.84	4.10	-2.18
2000-2008	km^2(total)	379.68	221.09	-497.44	-103.33
	% (total)	34.67	12.15	-28.46	-11.47
	km^2(annual)	47.46	27.64	-62.18	-12.92
	% (annual)	4.33	1.52	-3.56	-1.43
1992-2008	km^2(total)	745.77	-541.01	-5.20	-199.56
	% (total)	92.48	-22.99	-0.40	-18.29
	km^2(annual)	46.61	-33.81	-0.32	-12.47
	% (annual)	5.78	-1.44	-0.025	-1.14

Note: % (total) $= \dfrac{\text{Year2} - \text{Year1}}{\text{Year1}} \times 100$; % (annual) $= \dfrac{\% \, (\text{total})}{\text{Number of years}}$

From the LULC maps depicted in Figure 4.4a-e and their associated descriptive data provided in Tables 4.4 and 4.5, it can be primarily concluded that, among all the known LULC classes, the vegetation cover has highest proportion of occupying area for all years of interest followed by the bare land and water body, or urban/built-up, classes respectively. However, percentages in area cover of vegetation have dropped continuously, in general, from 42.27% in 1992 to 32.55% in 2008 (about 23% decreased from its original area in 1992). But, during the same period, urban/built-up area has substantially expanded from about 14.49% in 1992 to 27.88% in 2008 (about 92.5% increased from the original area in 1992). The highest increasing rate of urban and built-up was found during periods of 1996-2000 (31.62% increased) and 2004-2008 (32.38% increased). No obvious changing trends appear for water body and bare land classes during period of the study.

The expansion of urban/built-up area (at about 46.61 km^2 per year) occurs mostly along major roads traversing from central Bangkok to its satellite cities nearby and within Bangkok outskirt in nearly all directions (Figure 4.7a). Mixed classes of vegetation, bare-land, and inland water body usually signify agricultural zone (paddy fields in particular) surrounding the more developed urban/built-up space. The vegetation areas observed in the urban environment are mostly public green areas, e.g. urban parks or reserved forests. The most prominent one seen in the middle of the lower part of Figure 4.4 is the reserved green area in Bankrajao sub-district of Samut Prakarn Province. Many water bodies were readily evidenced along the border of Thai Gulf in the southern most of study area. These areas might be used for operating vast aquatic farms for commercial purposes. The inland water bodies are mostly indicating the inundated paddy fields.

It should be noted here that, the total vegetation and bare-land areas have changed noticeably from year to year. This should due mainly to the different amount of agricultural plantations utilized each year by local farmers (at times that satellite images were taken). In addition, it is still difficult to differentiate between bare lands for agricultural purposes and those for commercial purposes from satellite images in use (Landsat-TM). Therefore, to define definite space for agricultural area on these images is often not straightforward. In term of the changing pattern, out of about 1552.15 km^2 found of urban/built-up area in 2008, just only 518.19 km^2 that was existing in 1992 while the rest was converted from the other LULC classes. These are vegetation (530.91 km^2), bare land (350.63 km^2), and water body (152.22 km^2) (Table 4.6c).

The notable changes of the urban/built-up land to other LULC classes were also observed, especially to the vegetation and bare land. These findings usually occur at remote areas far from the city centers. These situations should not occur much in reality, however, there might be two main sources being responsible for these unusual LULC changing pattern, which are,

(1) the possible similarity of spectral reflectance characteristics of the bare land and the open urban/built-up area,

(2) the existing of mixed pixels that have more than one LULC classes contained inside, e.g. U/B and vegetation or U/B and bare land.

These two scenarios may lead to some classification errors by the used algorithm (hybrid classification), especially at the LULC-mixed areas far from city centers and result in the observed significant changes of urban/built-up land to other LULC classes (or other way round) as reported in Tables 4.6a-c.

Table 4.6a LULC change matrix (from 1992 to 2000) (in km^2).

	LULC Class	LULC 2000					Total (1992)
		U/B	VEG	BARE	WAT	Cloud	
LULC 1992	U/B	473.45	110.29	191.54	30.81	0.29	806.38
	VEG	285.17	1120.79	732.44	212.49	2.07	2352.96
	BARE	249.24	385.28	523.16	157.27	0.96	1315.93
	WAT	87.15	202.67	300.80	499.94	0.59	1091.15
	Cloud	0.00	0.00	0.00	0.00	0.00	0.00
Total (2000)		1095.01	1819.03	1747.94	900.51	3.91	5566.41

Table 4.6b LULC change matrix (from 2000 to 2008) (in km^2).

	LULC Class	LULC 2008					Total (2000)
		U/B	VEG	BARE	WAT	Cloud	
LULC 2000	U/B	696.27	163.11	182.86	52.77	0.00	1095.01
	VEG	315.16	887.48	462.65	153.74	0.00	1819.03
	BARE	437.77	573.86	476.80	259.51	0.00	1747.94
	WAT	101.15	186.95	186.98	425.43	0.00	900.51
	Cloud	1.80	0.54	1.44	0.14	0.00	3.91
Total (2008)		1552.14	1811.94	1310.73	891.59	0.00	5566.41

Table 4.6c LULC change matrix (from 1992 to 2008) (in km^2).

	LULC Class	LULC 2008					Total (1992)
		U/B	VEG	BARE	WAT	Cloud	
LULC 1992	U/B	518.39	138.82	115.94	33.25	0.00	806.40
	VEG	530.91	1013.03	591.93	217.08	0.00	2352.95
	BARE	350.63	391.30	359.28	214.71	0.00	1315.92
	WAT	152.22	268.8	243.58	426.54	0.00	1091.14
	Cloud	0.00	0.00	0.00	0.00	0.00	0.00
Total (2008)		1552.15	1811.95	1310.73	891.58	0.00	5566.41

The dynamic exchanges between vegetation lands and bare lands were also found at all considered time periods as shown in Table 4.6a-c. This phenomenon

indicates the highly convertible between bare land and vegetation cover within the agricultural scenery of the BMA region. As paddy fields are the most dominant crop covers of the study area, actual amount of the bare lands can substantially vary from season to season, or from year to year, depending on the associated planting calendar and decision of farmers how to utilize their agricultural fields each year.

Figure 4.6 and 4.7 illustrate the loss and gain spaces of main LULC classes: urban/built-up, vegetation, bare land and water body. As stated earlier, urban loss/gain areas appear mostly in the suburban region far from city centers (under agricultural environment). And they are normally resulted from dynamic changes in occupying land with vegetation and bare land classes. Great losses in green area were also found at nearly every studied province, especially Nonthaburi and Samut Sakorn.

Figure 4.6 illustrates the changing status (from/to basis) of the U/B class during 1992-2008. It was found that the converting of U/B to other classes appeared mostly over transitional zone of urban and agricultural spaces (or the city's suburb). Often, the mixed-nature of main LULC components (urban/built-up, bare land, and vegetation) within this zone can make precise separation of their individual existing based on moderate resolution satellite image, like Landsat-TM or ETM+, rather difficult. This could result in the relatively high rate of conversion from one class to the other (like seen in Table 4.6c). To have more accurate LULC map of the mixed-area, fine resolution satellite image may be more appropriate to fulfill the task (e.g. Ikonos, QuickBird, and THEOS).
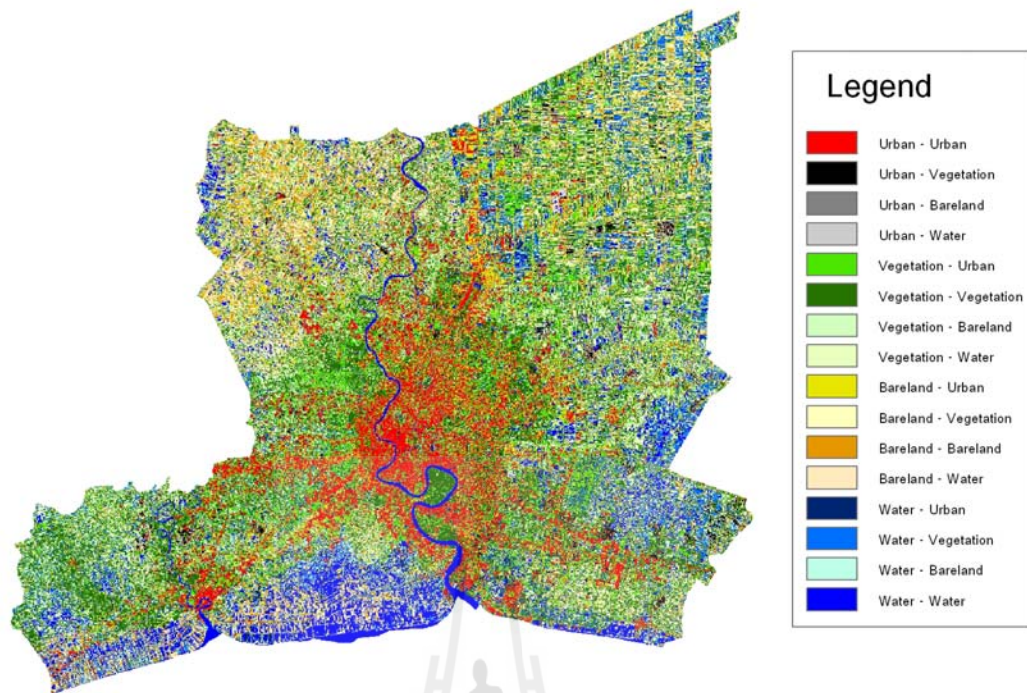
Figure 4.6 Change patterns of the U/B class during 1992-2008.
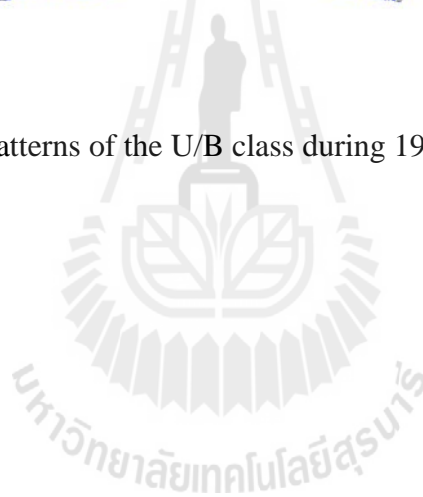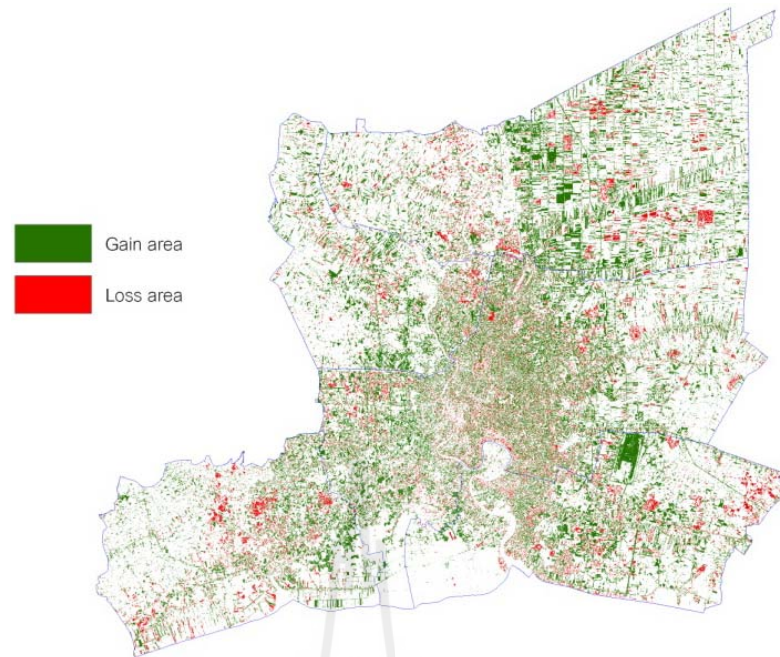
(a) Urban/built-up.
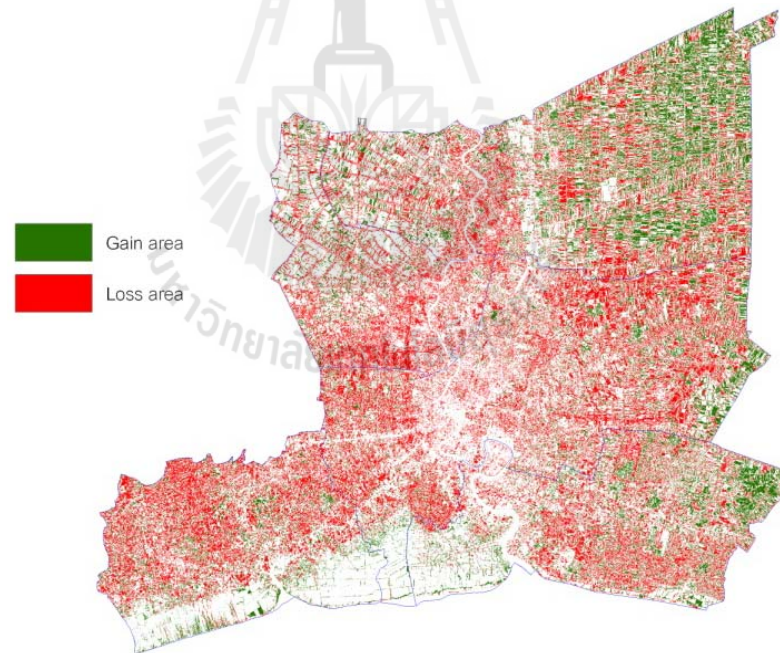
(b) Vegetation.

Figure 4.7   Loss/gain areas for different LULC classes during period of 1992-2008

for (a) urban/built-up, (b) vegetation, and (c) water body.
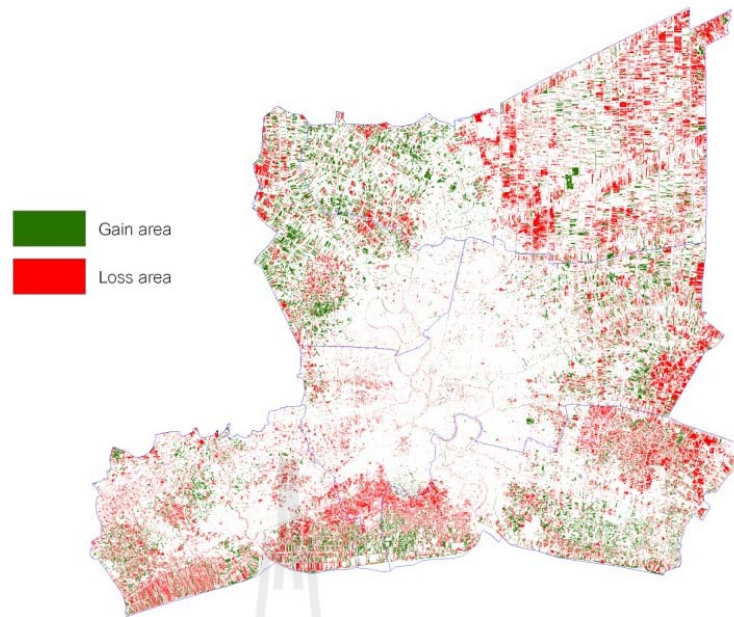
(c) Water body.

Figure 4.7 Loss/gain areas for different LULC classes during period of 1992-2008 for (a) urban/built-up, (b) vegetation, and (c) water body (Continued).
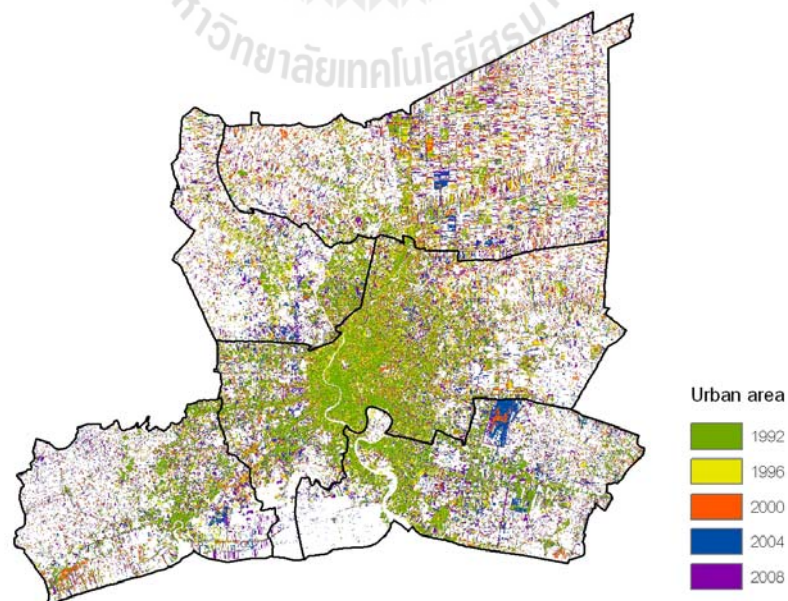
Figure 4.8 Urban/built-up map during 1992-2008.

4.2.2   Intensification of the UHI phenomenon

The LST maps of years 1992, 1996, 2000, 2004, and 2008 were derived from Landsat TIR imagery, based on Eqs. 3.1 and 3.2, along with their UHI intensity maps and results are presented in Figure 4.9 (a-e). The calculation of UHI intensity was done based on the definition given in Eq. 2.1. The reference rural data were taken from the ST19 station for each chosen year due to their relatively colder environment when compare to the warmer urban atmosphere in the BMA inner area. The reference data for each year are as follows: 22.58^{o}C (1992), 25.5^{o}C (1996), 21.71^{o}C (2000), 24.74^{o}C (2004), and 23.45^{o}C (2008).

Figure 4.9 shows that, in 1992, the highest values of LST data were found mostly around core area of Bangkok but in 2008 the peak values have spread outward to occupy most areas in central Bangkok and also moved across to the adjacent areas of its satellite provinces, especially Nonthaburi and Samut Prakarn. And when compared these maps to their corresponding LULC maps in Figure 4.4, it was found that the most intense UHI phenomenon occur at core urban area of central Bangkok (like the LST). Impact of UHI on LST variation is less visible at the rural area far from the central Bangkok or from the dense urban area as the dominant land classes there are vegetation and bare land, which are theoretically less vulnerable to the UHI phenomenon than the urban area.

In addition, low UHI intensity is clearly seen in coastal areas along the Thai Gulf in the south, that also have lowest average LST data. The LST data shown on these maps usually have peak values around $26\text{-}30^{o}$C and associated peak UHI more than about 2°C. However, the UHI map of 1996 is still unrealistic, which is probably due to the unusually high reference temperature data applied in that year (25.5^{o}C).
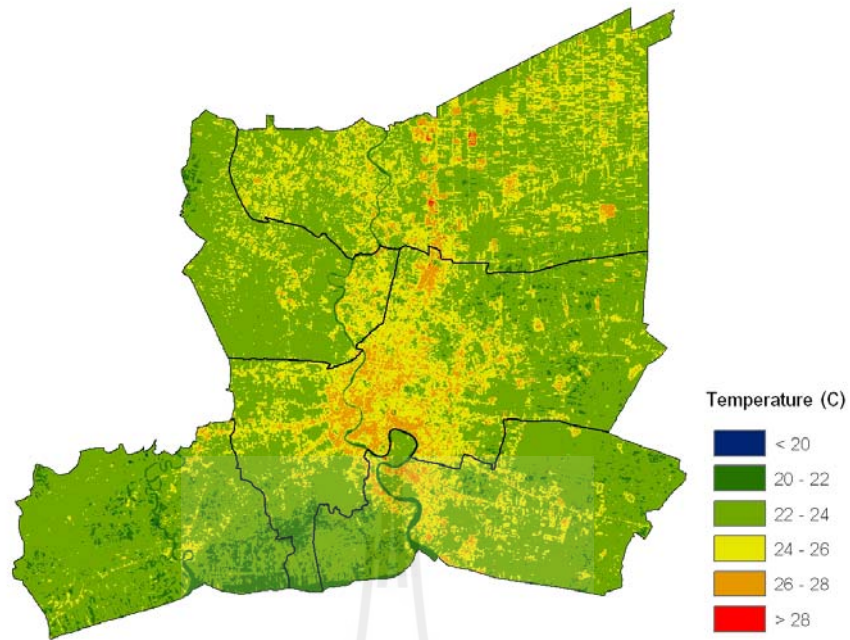
(a1) LST map (20/11/1992).
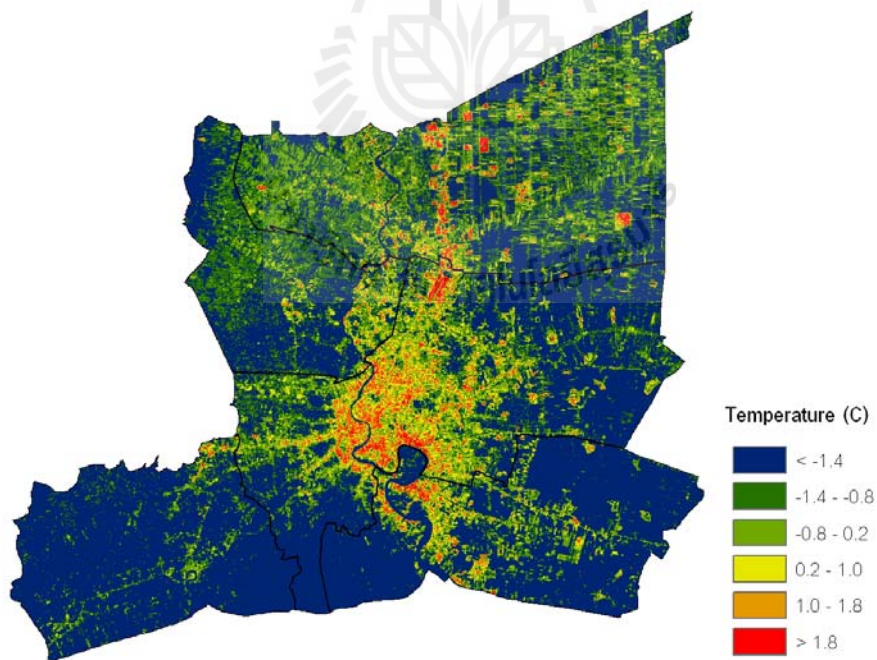
(a2) UHI intensity map (20/11/1992).

Figure 4.9   LST and UHI maps in (a) 1992, (b) 1996, (c) 2000, (d) 2004, and (e) 2008.
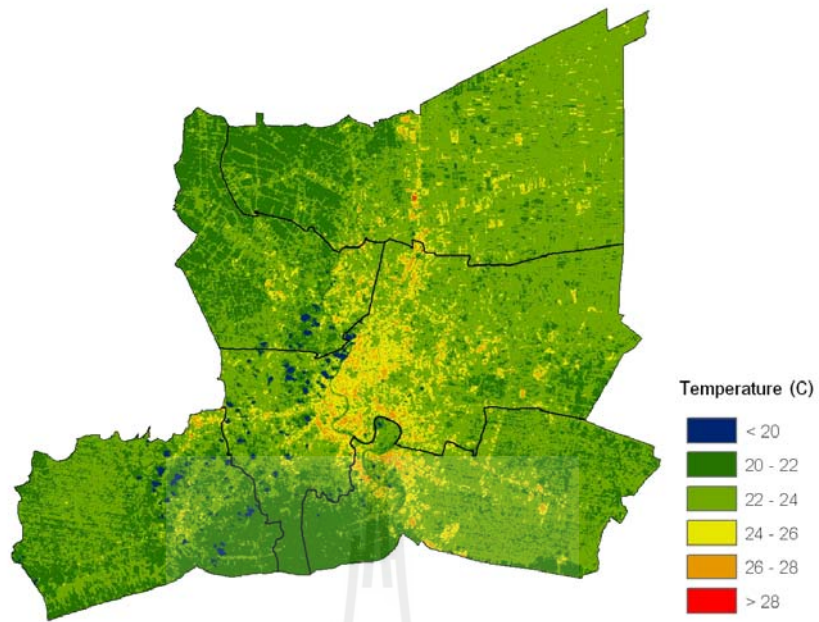
(b1) LST map (15/11/1996).
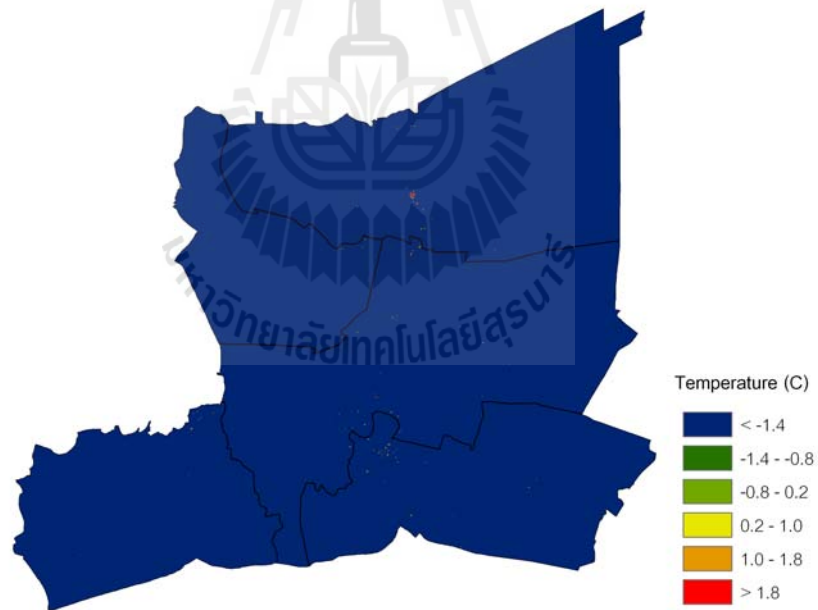
(b2) UHI intensity map (15/11/1996).

Figure 4.9 LST and UHI maps in (a) 1992, (b) 1996, (c) 2000, (d) 2004, and (e) 2008
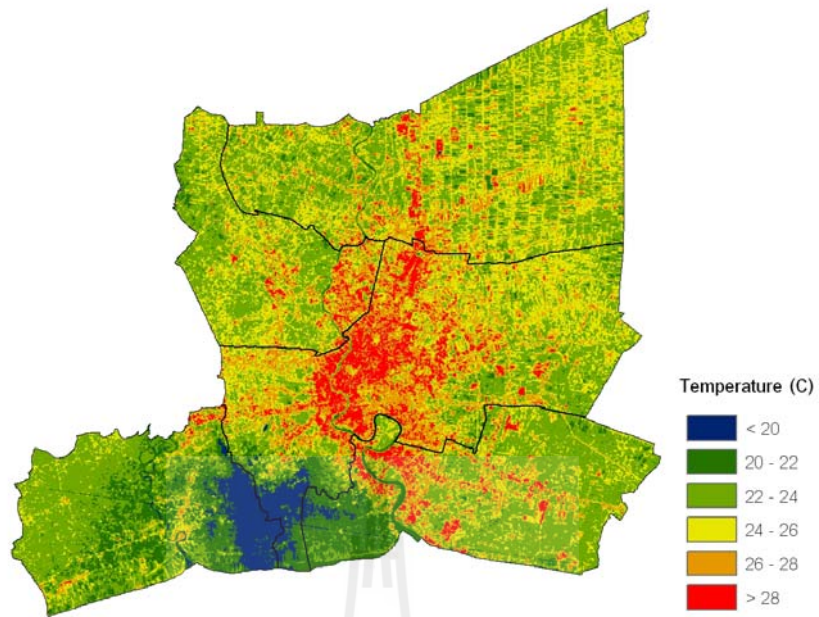
(Continued).

(c1) LST map (10/11/2000).
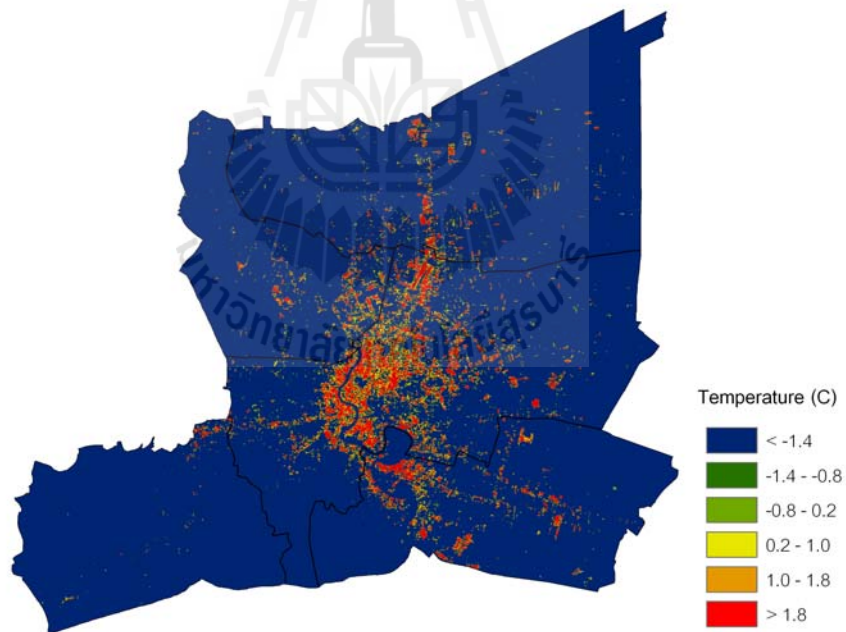
(c2) UHI intensity map (10/11/2000).

Figure 4.9   LST and UHI maps in (a) 1992, (b) 1996, (c) 2000, (d) 2004, and (e) 2008
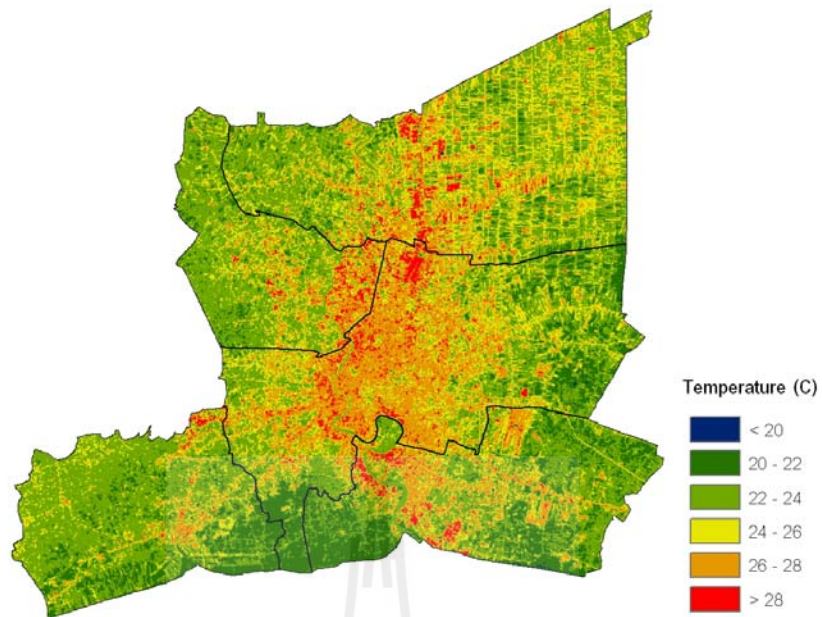
(Continued).

(d1) LST map (21/11/2004).
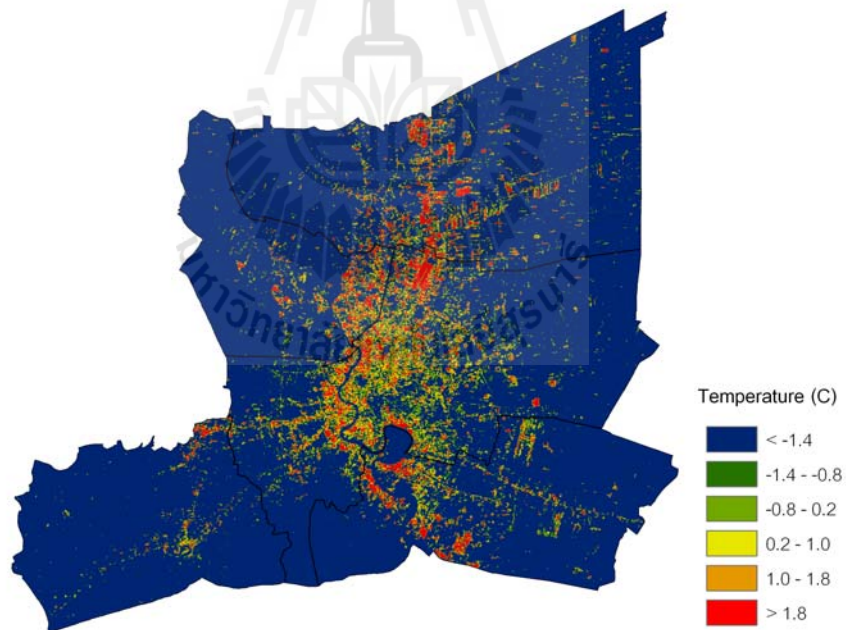
(d2) UHI intensity map (21/11/2004).

Figure 4.9　　LST and UHI maps in (a) 1992, (b) 1996, (c) 2000, (d) 2004, and (e) 2008
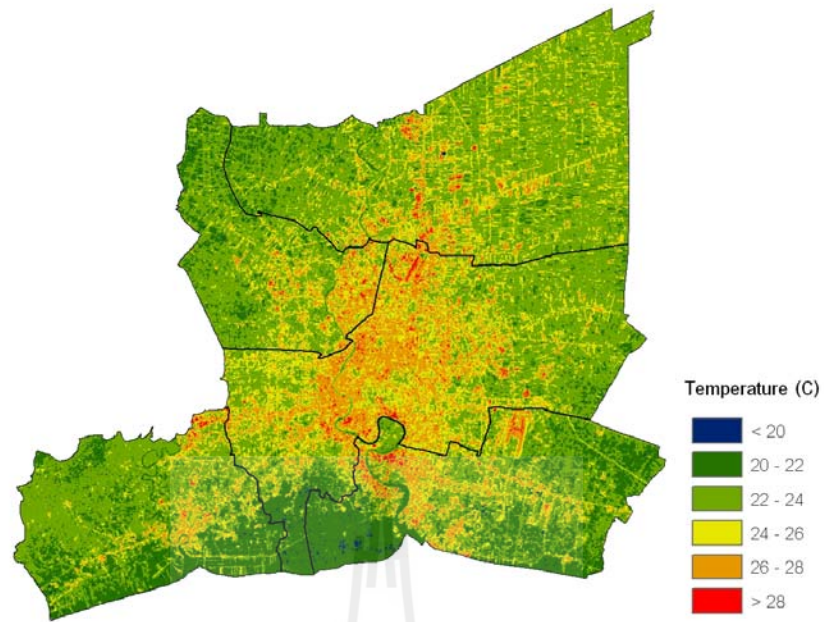
(Continued).

(e1) LST map (02/12/2008).
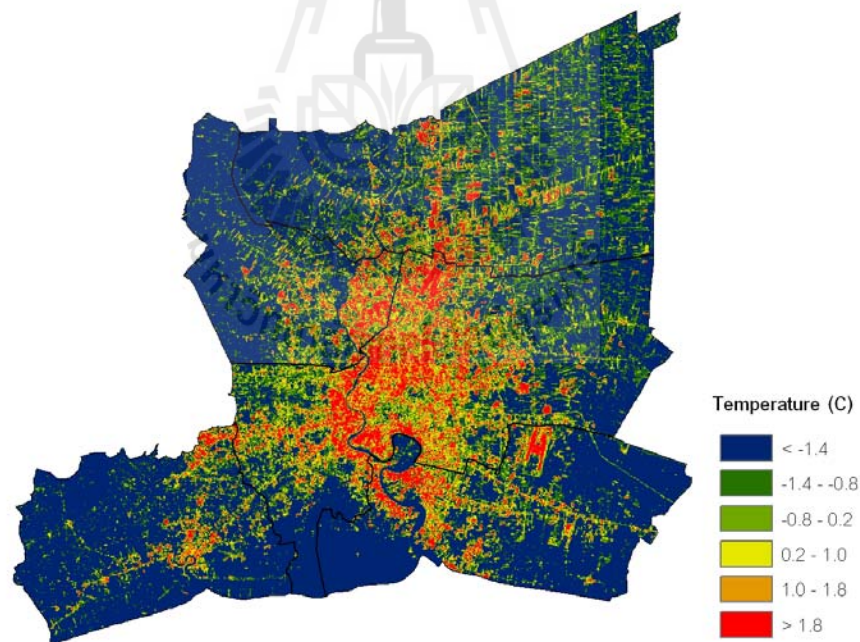
(e2) UHI intensity map (02/12/2008).

Figure 4.9   LST and UHI maps in (a) 1992, (b) 1996, (c) 2000, (d) 2004, and (e) 2008.

(Continued).

Table 4.7   Area coverage of LST and UHI classes (in %) in 1992 and 2008.

Year	LST Class (in ^oC)							Total
	< 20	20-22	22-24	24-26	26-28	28-30	> 30	
1992	0.03	4.91	70.16	21.58	3.26	0.06	0	100
2008	0.48	15.82	53.74	19.19	9.72	1.02	0.03	100

Year	UHI Class (in ^oC)							Total
	< -1.4	-1.4--0.7	-0.7-0	0-0.7	0.7-1.4	1.4-2.1	> 2.1	
1992	51.89	23.2	15.25	3.87	4.14	0.95	0.7	100
2008	50.91	19.13	10.66	4.55	7.27	4.48	3	100

From Table 4.7, it was found that most area in 1992 (about 70.16%) has the LST of between 22-24^oC while about 21.58% has LST between 24-26 ^oC. But in 2008, these numbers have changed to become 53.74% and 19.19% respectively. If consider only for those areas with LST higher than 26^oC, the numbers are 3.32% (in 1992) and 10.77% (in 2008), respectively. This result indicates the notable increase in number of the relatively high LST area which might lead to the more severe UHI situation over the BMA region as a consequence. This fact is obviously demonstrated in data of areas with different classes of UHI intensities. It was found that, in 1992, areas with ΔT higher than 0^oC are at 9.66% of the total area but, in 2008, this number rises to 19.3%. The very interesting result is that area with $\Delta T > 2.1^oC$ covers about 0.7% only in 1992 but it has expanded to become 3% in 2008 which indicate great rise in areas with high UHI intensity over BMA region. These areas should be of great concerned if the trend of UHI intensification is still continuing without any mitigation plan implemented by the government of responsible local agencies.

4.3 Relationships of LULC Components and LST Data

In this part, the observable influences of main LULC components: vegetation cover, urban/built-up, impervious surface, and bare land, on variation of the satellite-based LST data were assessed based on relationships between the chosen index for each LULC type and their associated LST data. These indices are (1) NDVI (for vegetation), (2) NDBI (for urban/built-up), (3) NDBaI (for bare land), and (4) %ISC (for impervious surface) where their definitions are given by Eqs. 3.4 (NDVI), 3.5 (NDBI), 3.6 (NDBaI), and 3.7 (%ISC), respectively.

4.3.1 General characteristics

As stated in Section 2.3, different LULC components have different impact on UHI intensity. In general, the increase of urban/built-up area can enhance UHI intensity considerably (like in Figure 4.9) while green vegetation tends to reduce the UHI severity noticeably (like at Bang Krajao sub-distict). Large water body also substantially helps to diminish UHI intensity for the surrounding environment.

Table 4.8 presents examples of descriptive relations between LULC components in the study area (from Figure 4.4) and their observed LST data and the UHI intensity (from Figure 4.9). It was found that the relatively high temperature pixels tend to locate within the urban/built-up class (with average values of 25.11°C in 2008) while colder pixels were significantly found within the vegetation and water body classes (with the average values of 22.96°C and 22.09°C in 2008). These results strongly support the fundamental believes on roles of these LULC fractions in UHI study mentioned above.

Table 4.8 Area coverage of LST class (in %) over LULC map (2008).

LULC	LST Class (in ^{o}C)							Average LST
	< 20	20-22	22-24	24-26	26-28	28-30	> 30	
U/B	0.06	0.31	7.19	11.11	8.22	0.96	0.03	25.11
VEG	0.03	4.93	23.33	3.76	0.5	0.01	0	22.96
BARE	0.03	3.24	15.53	3.74	0.95	0.05	0	23.21
WAT	0.35	7.34	7.69	0.58	0.06	0	0	22.09
Total	0.47	15.82	53.74	19.19	9.73	0	0	100

Influence of large water body on the reduction LST within the urban environment was also investigated by considering variation of mean LST (of different LULC classes) with distance away from the Thai Gulf and results are shown in Table 4.9 and Figure 4.10. From this figure, it is obvious that large portion of the sea water (in Thai Gulf) has great effect on reduction of LST data of up to 30 km deep inland. The less dense urban/built-up space away from Bangkok center shall have lower UHI intensity also.

Table 4.9 Variation of average LST data with distances (in km) from the Bangkok center (Victory Monument) and from sea water (Thai Gulf) (as shown in Figure 4.10).

Distance from BKK center	Average LST	Distance from sea	Average LST (^{o}C)			
			U/B	VEG	BARE	Average
0-2.5	25.56	0-5	24.32	22.13	22.18	22.07
2.5-5.0	25.69	5-10	24.74	22.54	22.35	22.85
5.0-7.5	25.88	10-15	24.82	22.77	22.66	23.29
7.5-10.0	25.22	15-20	25.10	22.86	23.08	23.55
10.0-12.5	24.98	20-25	25.53	22.98	23.36	24.07
12.5-15.0	24.88	25-30	25.83	23.50	23.99	24.57
15.0-17.5	24.46	30-35	25.50	23.56	23.92	24.36
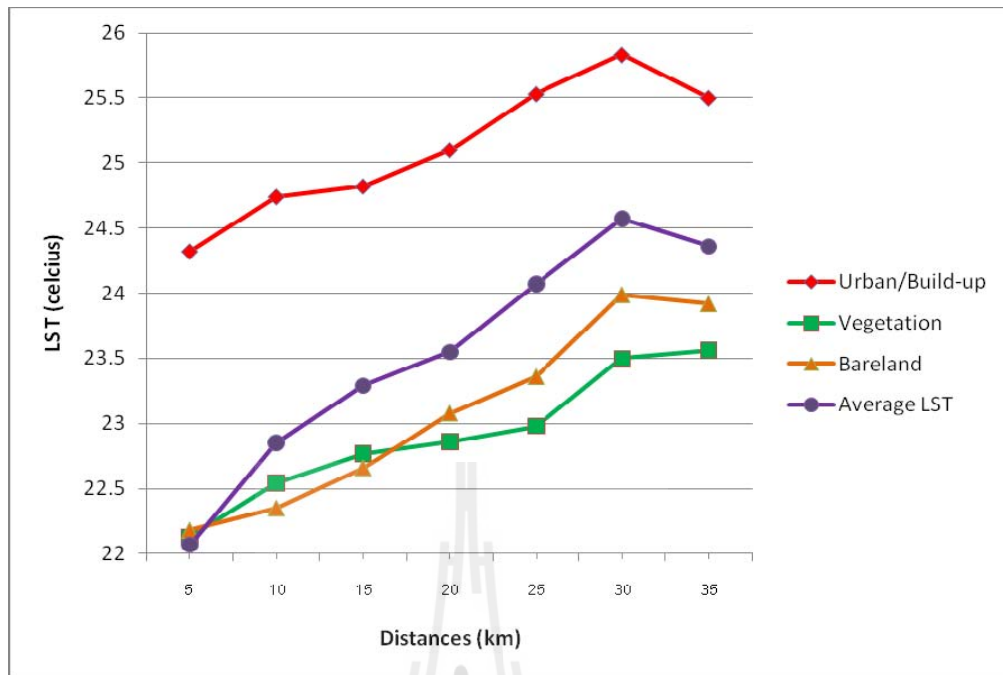
(a)   Temperature variation with distances from the Thai Gulf.
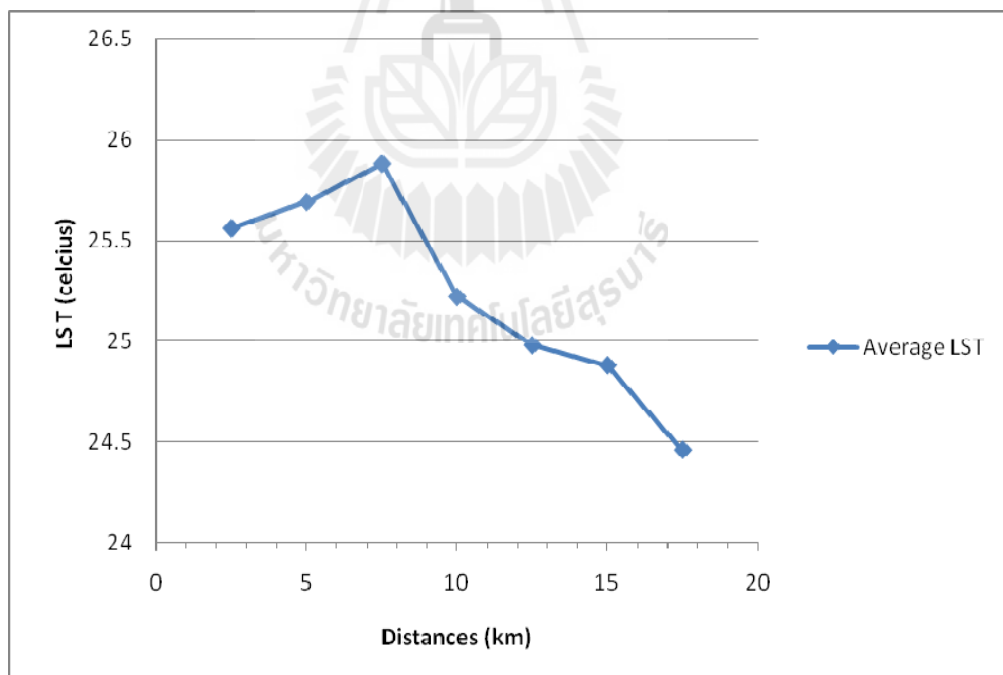
(b)   Temperature variation with distances from BKK center.

Figure 4.10   Variation of the average LST data with distances from (a) the Thai Gulf and (b) the Bangkok urban center (from data in Table 4.9).

4.3.2   Applications of LULC indices

The formerly-stated LULC indices, especially NDVI, have been used fruitfully in several published researches (as described in Chapter II) to quantify the relative amount of a specific LULC component (at pixel scale) over the interested area. These indices can be readily derived from the Landsat TM/ETM+ imagery (at some appropriate bands) and results can be expressed as a map. Examples of these maps for the NDVI, NDBI, NDBaI, and %ISC for BMA region in 2008 are presented in Figure 4.11a-d. Basic interpretation of the derived index values is that higher value of a specific index indicate higher amount of the LULC component (over the considered pixel) it represents.

The derived NDVI, NDBI, NDBaI and %ISC maps in 2008 were compared with the corresponding LULC map (Figure 4.4e) and the LST/UHI maps (Figure 4.9e) of the study area in 2008. It was found that, the NDVI map can represent the vegetation class fairly well, especially at those areas with NDVI $\geq$ 0.4. The NDBI map also resembles the %ISC map and both can signify the urban/built-up class on LULC map pretty well.

The landmarks for urban green area, especially Bang Krajao sub-district and some parts of Nonthaburi Province are distinctively visible on the gain NDVI map. Similarly, landmarks of the urban/built-up area, especially Bangkok inner zone and Suvarnbhumi Airport, were also readily detected on the gain NDBI map of the BMA area. In addition, the negative values of NDVI were associated mostly to the water body class, especially those situate close to the border with Thai Gulf. The NDBaI map here does not exhibit any outstanding features on its content, dissimilar to those of NDVI and NDBI maps.

The comparison of the NDVI and NDBI maps with their corresponding LST map emphasizes the conventional believe that higher NDVI values are associated with lower LST values, but higher NDBI values are associated with higher LST values (Table 4.10). More explicit relationships of the NDVI and NDBI variation with LST data are examined later in this section (Figure 4.12 and Table 4.11).

However, it is interesting to find that the NDBI and NDBaI values have saturated at rather low values (about 0.2-0.3) of their possible scale (from -1 to 1) only. This means the presently used definitions of both indices are still not suitable to represent the whole range of their possible values as expected (compared to the NDVI that normally saturates at value of about 0.7-0.8 over the same possible scale range of -1 to 1). This problem was also evidenced in several works published earlier (Chen et al., 2006; Zhang et al., 2009; Yongnian et al., 2010). Therefore, it might be more useful if formal definitions of both indices are modified to reflect the full scale range on their outcome maps.
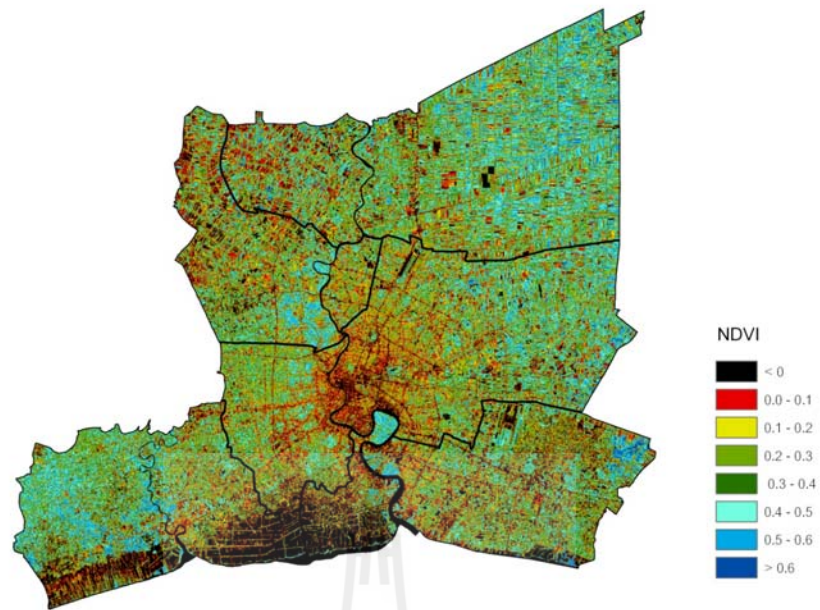
(a)　　NDVI map (02/12/2008).
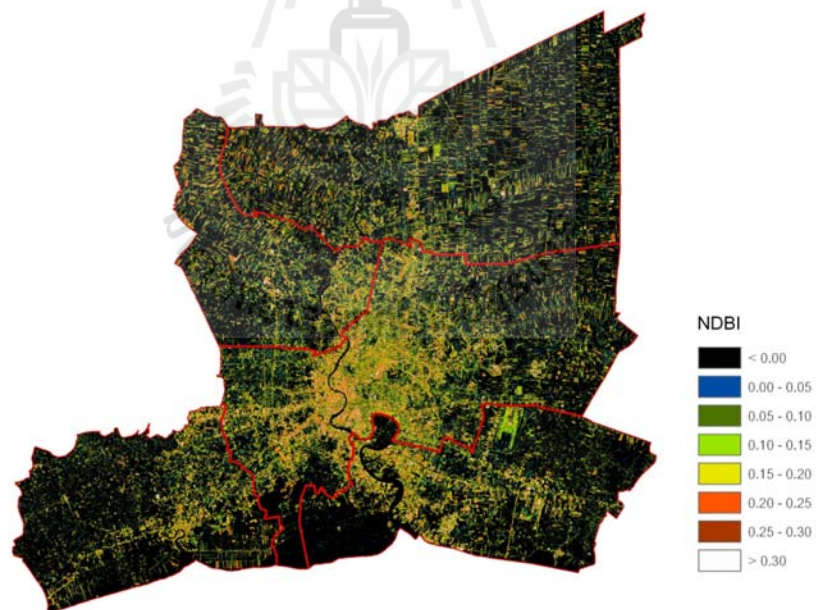
(b)　　NDBI map (02/12/2008).

Figure 4.11　　LULC index maps in 2008 of (a) NDVI, (b) NDBI, (c) NDBaI, and
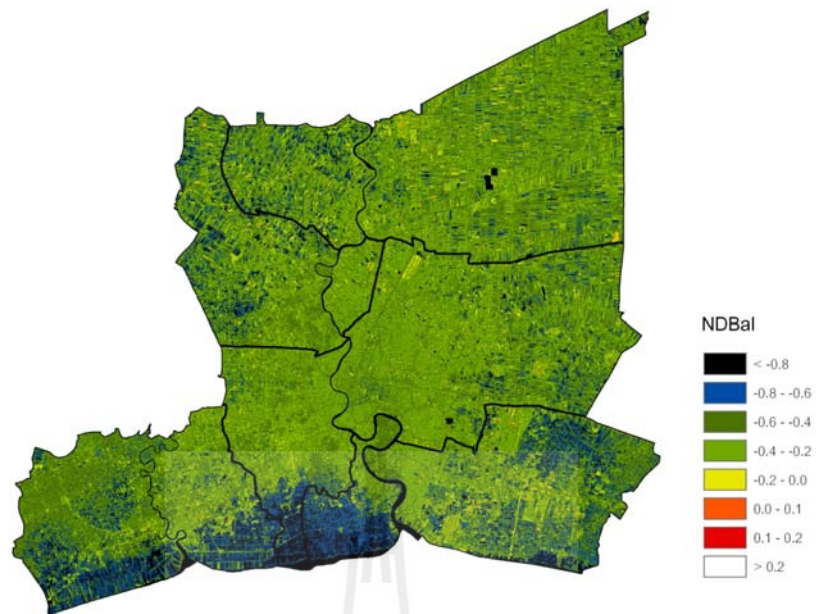
(d) %ISC.

(c)   NDBaI map (02/12/2008).
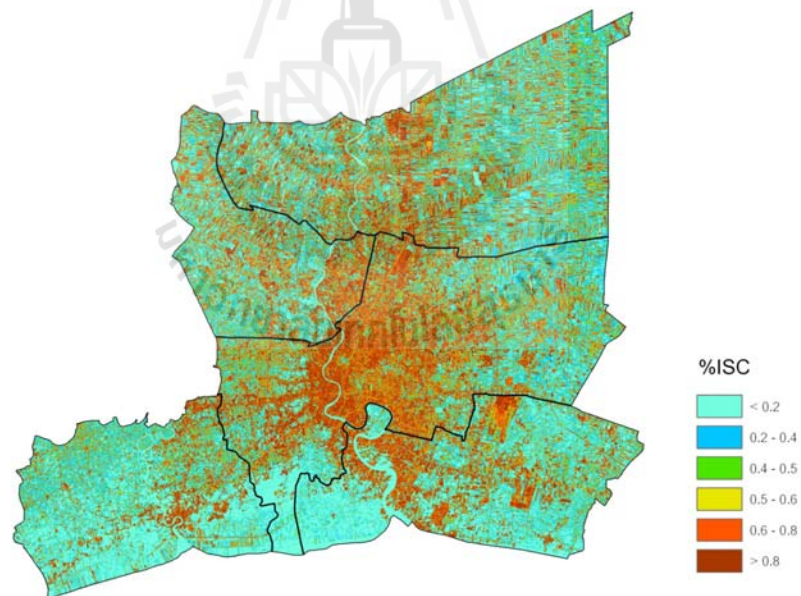
(d)   %ISC map (02/12/2008).

Figure 4.11   LULC index maps in 2008 of (a) NDVI, (b) NDBI, (c) NDBaI, and (d) %ISC (Continued).

Table 4.10a Area coverage and average LST for different NDVI classes.

Class	NDVI Class							
	-1.0/-0.4	-0.4/-0.2	-0.2/0.0	0.0/0.2	0.2/0.4	0.4/0.6	0.6/0.8	0.8/1.0
Area (km^2)	10.6	183.7	510.9	1621.6	1788.6	1400.4	50.1	0.0
Area (%)	0.2	3.3	9.2	29.1	32.1	25.2	0.9	0.0
LST (^{o}C)	21.74	21.37	23.24	24.28	23.54	22.90	22.12	-

Table 4.10b Area coverage and average LST for different NDBI classes.

Class	NDBI Class							
	-1.0/-0.4	-0.4/-0.2	-0.2/0.0	0.0/0.2	0.2/0.4	0.4/0.6	0.6/0.8	0.8/1.0
Area (km^2)	202.11	880.23	2224.84	1725.16	528.67	5.57	0.05	0.0
Area (%)	3.63	15.81	39.97	30.99	9.50	0.10	0.00	0.0
LST (^{o}C)	21.77	22.11	23.00	24.38	25.47	26.04	-	-

Table 4.10c Area coverage and average LST for different %ISC classes.

Class	%ISC Class									
	0-10	10-20	20-30	30-40	40-50	50-60	60-70	70-80	80-90	90-100
Area (km^2)	900.5	558.79	634.24	628.52	587.86	550.05	524.59	479.80	363.03	339.25
Area (%)	16.18	10.04	11.39	11.29	10.56	9.88	9.42	8.62	6.52	6.09
LST (^{o}C)	22.21	22.66	22.89	23.12	23.39	23.77	24.18	24.55	25.01	25.45

Relationships of LST and LULC indices

The relationships of each LULC index mentioned earlier and their associated LST data (pixel-based) were evaluated and their results are reported in Figures 4.12 and 4.13 and Table 4.11. Figure 4.12 exhibits relationships between known LST data and their associated LULC indices (pixel-based) in 2008. It was found that trends of the relationship between each LULC index and the LST data were clearly seen (positive or negative correlation). However, the correlation level is rather moderate for the NDVI (negative correlation with R^2 = 0.408) but rather high

(positive correlation) for the other indices with R^2 = 0.734 (NDBI), 0.670 (NDBaI), and 0.836 (%ISC). The explicit relations in term of the linear regression formula are described in Table 4.11.

The strong negative correlations of NDVI with NDBI and %ISC, R^2 = 0.7703 and 0.5651 respectively, are as expected because they signify different groups of surfaces that are not generally coexistence. This means in dense urban area, healthy green vegetation (with high NDVI values) should be hard to find, and the opposite is true for dense green vegetation zone (e.g. mature crop fields).

In addition, the high positive correlation between %ISC and NDBI (with R^2 of 0.9221) should be of a particular interest here. This is because %ISC is regarded as being crucial indicator for the determination of urban/built-up expansion space in urban growth analysis, but finding its valid values is still a somewhat complicated task so far (typically relying on some chosen sub-pixel classification scheme as stated earlier in Section 3.2.1). Therefore, due to significantly high correlation between %ISC and NDBI, the NDBI, which is much easier to be found at pixel scale, can potentially be used as an effective replacement of well-acknowledged %ISC in the study of urban growth in the near future. However, NDBI is still not as good as the %ISC in term of correlation to LST (with R^2 of 0.7342), therefore, it may not be very effective in telling small-scale impact of urban expansion on its associated LST changes as %ISC does.

However, as mentioned earlier, because NDBI values (and NDBaI), by its present definition given in Eq. 3.5, have usually saturated at rather low values (about 0.2-0.3) of their possible scale (from -1 to 1) only. This means the presently used definitions of both indices are still not suitable to represent the whole range of

possible values as expected. Therefore, it might be more useful if formal definitions

of both indices are modified to reflect the full-scale range on their derived maps.

Table 4.11 Linear relationships of %ISC, NDVI, NDBI, NDBaI, and LST.

Index pair		Linear relationship formula	Correlation coefficient (R^2)
X	**Y**		
%ISC	LST	Y = 16.693X + 15.327	0.8367
NDVI	LST	Y = -5.8186x + 26.149	0.4080
NDBI	LST	Y = 8.0277X + 22.795	0.7342
NDBaI	LST	Y = 7.1832X + 25.519	0.6704
%ISC	NDVI	Y = -0.3658X + 0.5819	0.5651
%ISC	NDBI	Y = 2.0229X – 1.0087	0.9221
%ISC	NDBaI	Y = 1.7009X – 1.236	0.6536
NDBI	NDVI	Y = -0.7342X + 0.2043	0.7703
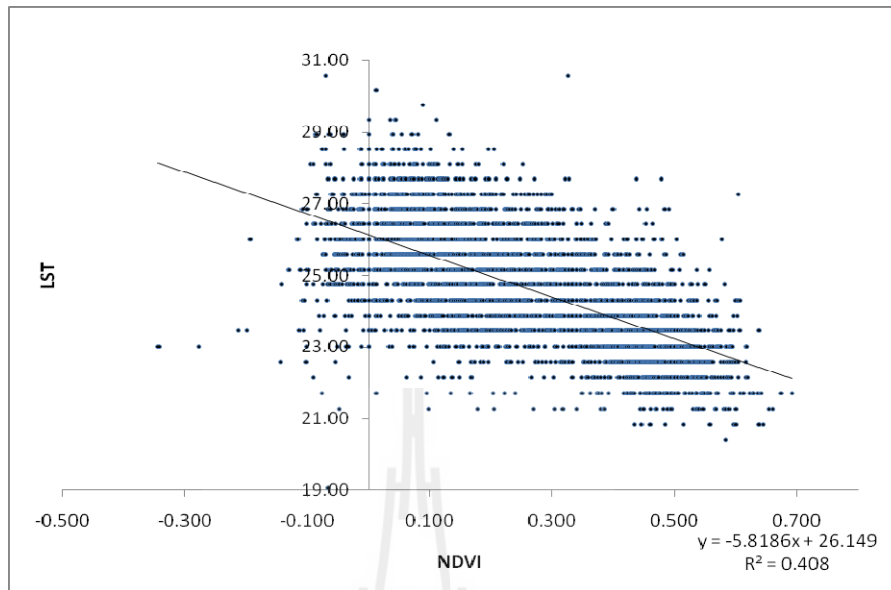
(a)   NDVI-LST (2008).
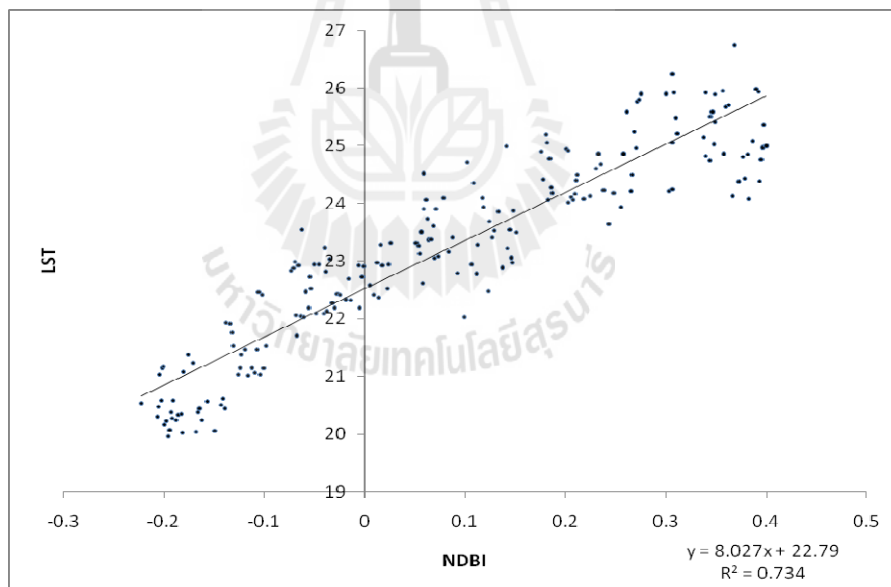
(b)   NDBI-LST (2008).

Figure 4.12   Relationships of the observed LST data with (a) NDVI, (b) NDBI, (c)
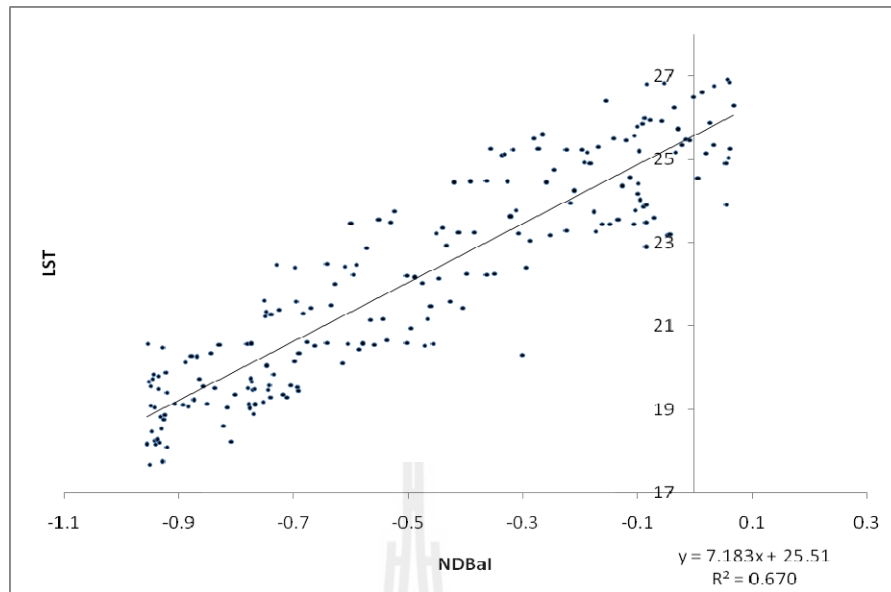
NDBaI, and (d) %ISC.

(c)   NDBaI-LST (2008).
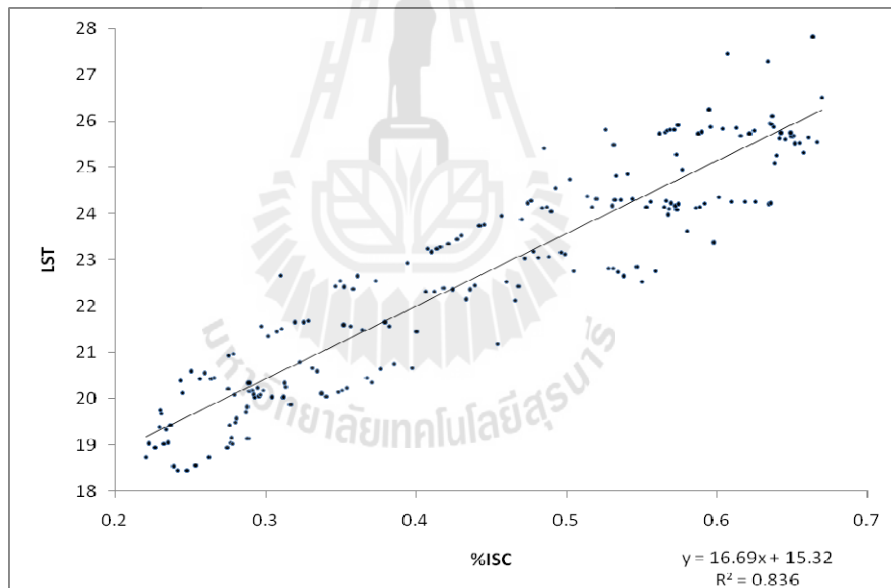
(d)   %ISC-LST (2008).

Figure 4.12   Relationships of the observed LST data with (a) NDVI, (b) NDBI, (c) NDBaI, and (d) %ISC (Continued).
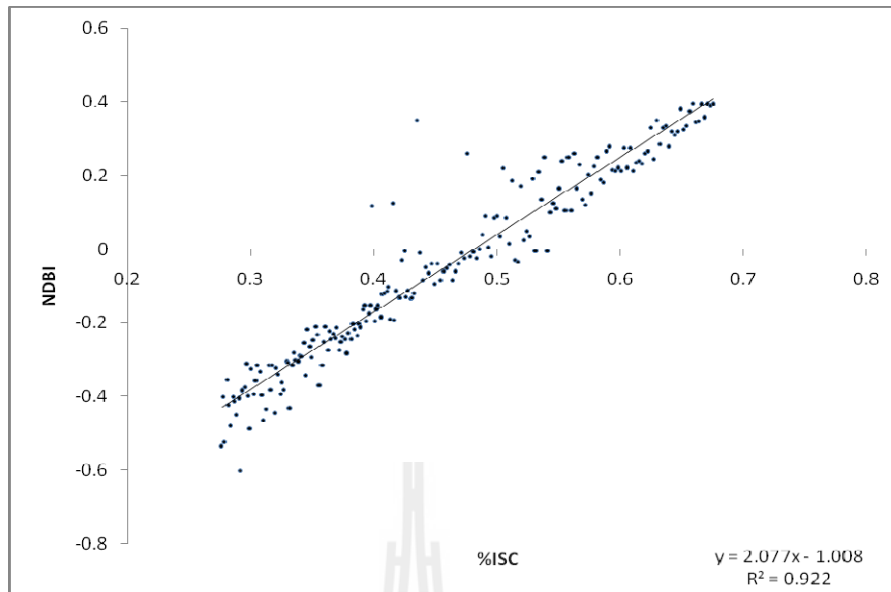
(a)   Relationship: %ISC-NDBI.
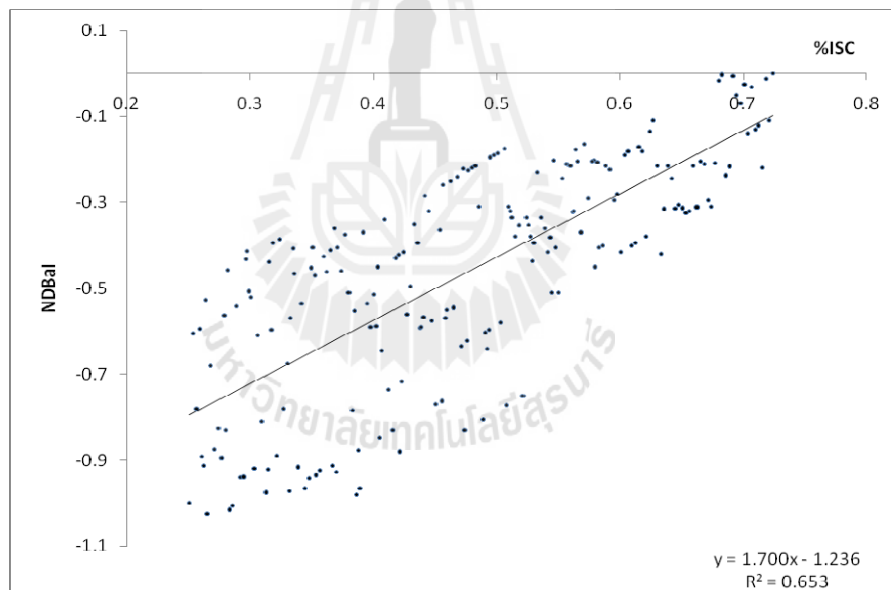
(b)   Relationship: %ISC-NDBaI.

Figure 4.13   Relationships between LULC indices for (a) %ISC-NDBI, (b) %ISC-NDBaI, (c) %ISC-NDVI, and (d) NDVI-NDBI.
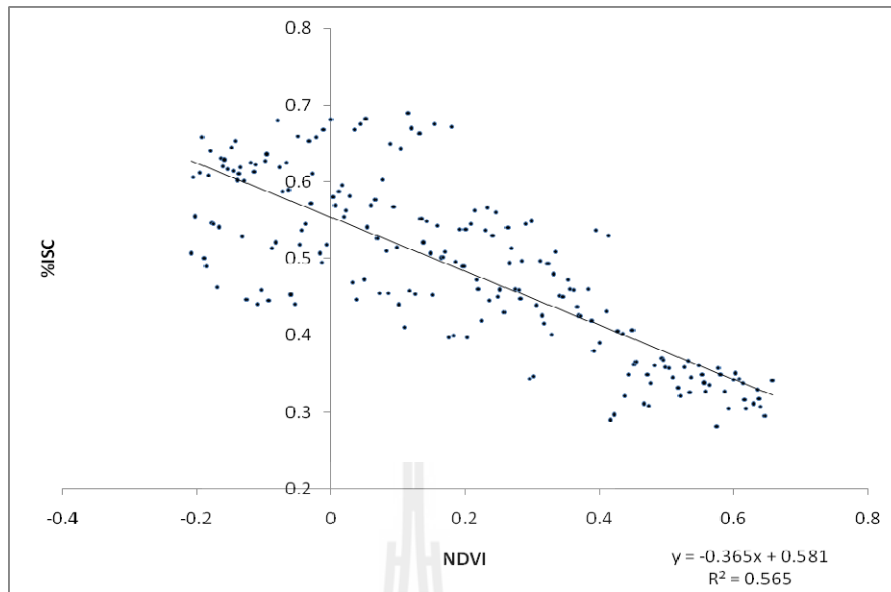
(c)   Relationship: NDVI-%ISC.
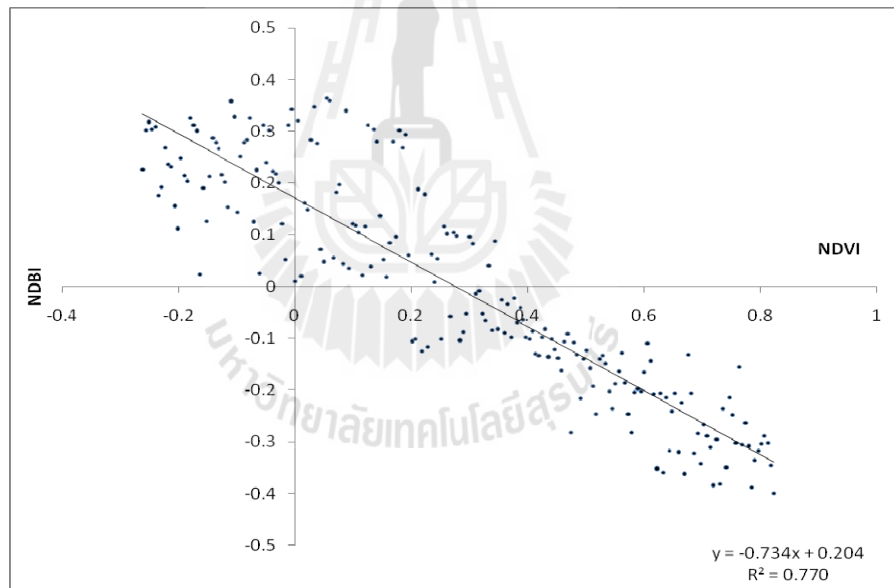
(d)   Relationship: NDVI-NDBI.

Figure 4.13   Relationships between LULC indices for (a) %ISC-NDBI, (b) %ISC-

NDBaI, (c) %ISC-NDVI, and (d) NDVI-NDBI (Continued).

4.4   Impact of Urban Green Areas on Ambient Air Temperature

Role of urban green areas in reducing observed ambient air temperature has been known for long time. In case of large green areas such as parks, vegetation affects the air above it and thus improve thermal environment of urban area. Cooling effect of urban park was investigated by many researchers with several values of temperature differences found, large. Usually, temperature reduction of about 0.5-5°C was reports for parks with dense trees. The influence distant of a park on the surrounding area was also investigated by various works which usually found that the lager parks have longer distance impact than the smaller ones (Wong and Yu, 2005).

To examine impact of urban parks in Bangkok on ambient temperature reduction, three locations of parks were chosen for further analysis according to their reported sizes: Santipap Park (small), Lumpini Park (medium), Chatuchak Park Complex (CPC) (large). The CPC comprises of Chatuchak Park, Queen Sirikit Park, and Wachirabenchathat Park which locate very close to each other in the Chatuchak District. General environmental settings in some of these parks are as illustrated in Figure 3.4.

Figure 4.14 presents NDVI maps and their corresponding LST maps of two main public parks included in the study: Lumpini Park and CPC. In both cases, the high NDVI portions usually represent the dense pact of trees while the relatively low NDVI portions generally signify large water bodies situated inside these parks. Both of these park's LULC components can noticeably reduce ambient air temperature within and around the parks as illustrated in the LST maps of Figure 4.14 (see Figure 4.15 for additional details).
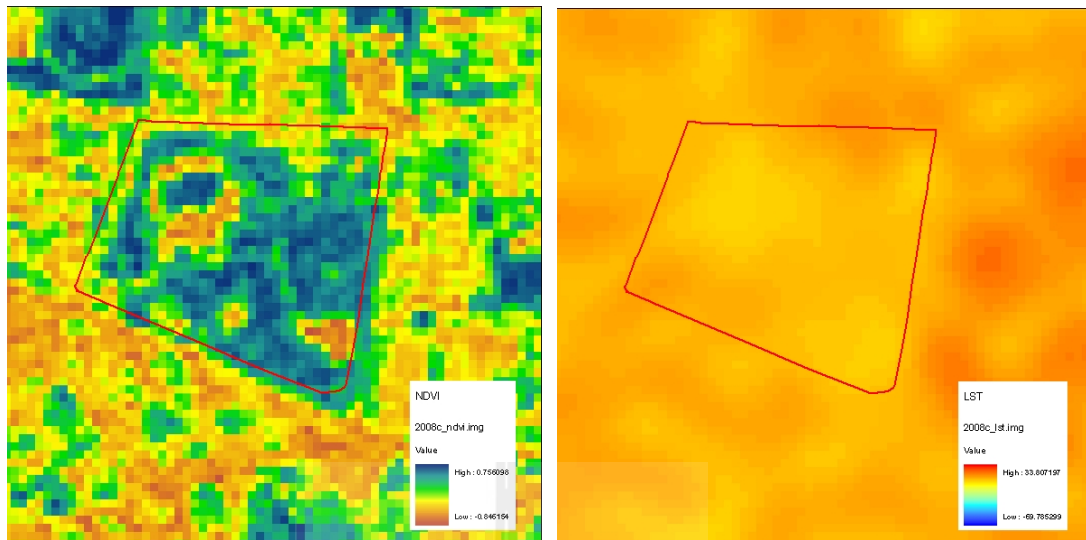
(a)   NDVI and LST maps (Lumpini Park).
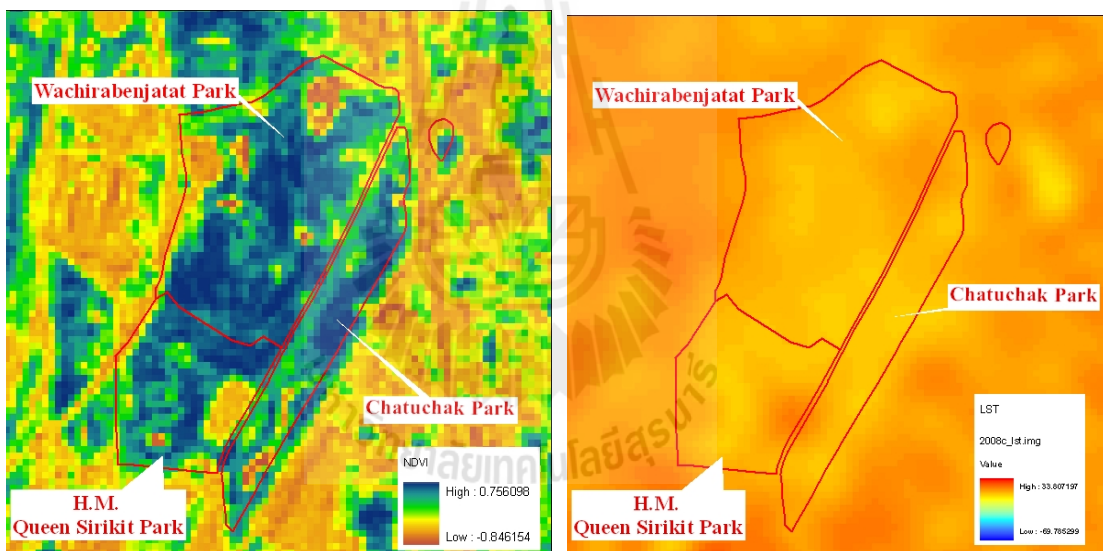
(b)   NDVI and LST maps (Chatuchak Park Complex).

Figure 4.14   NDVI and LST maps of (a) Lumpini Park and (b) Chatuchak Park
Complex.
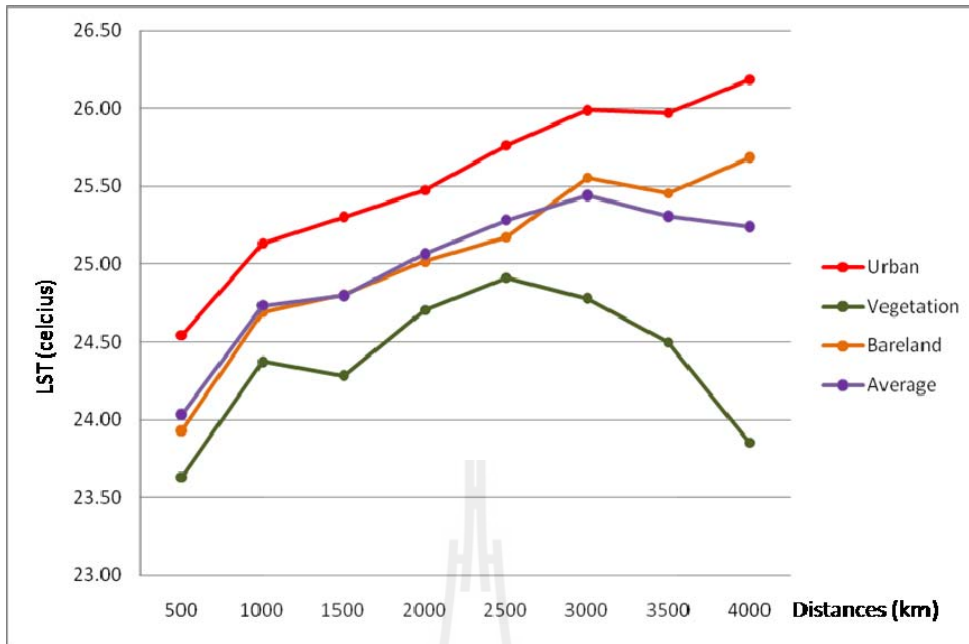
(a)   Lumpini Park.
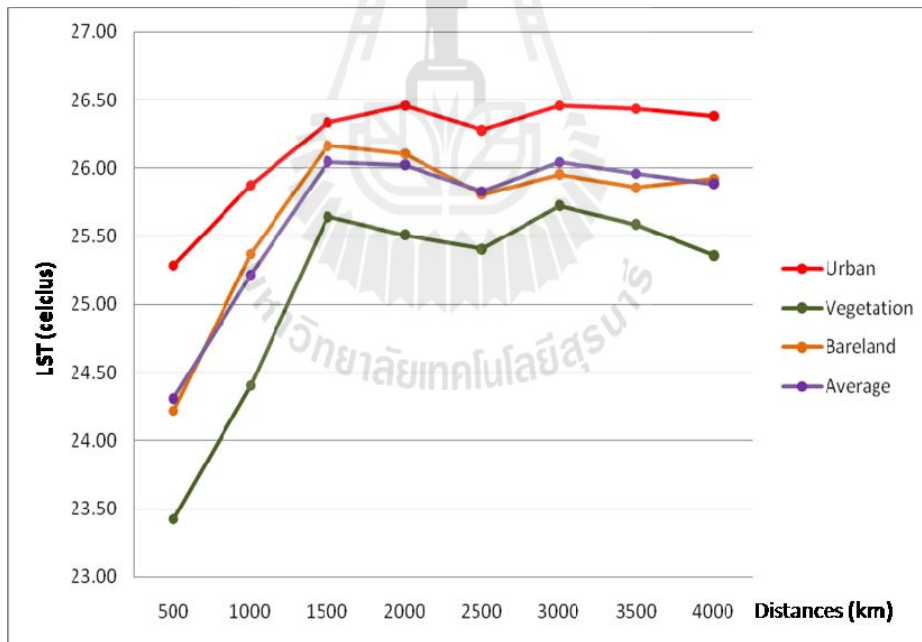
(b)   Chatuchak Park Complex.

Figure 4.15   Variations of temperatures with distance from park's center based on

the satellite-based LST data (Landsat TM on 02/12/2008).

4.4.1   Ground-based temperature mapping from field surveys

As mentioned in Section 3.4, field measurements of air temperature data inside and outside each chosen park were conducted during mid-daytime (within radius distance of about 3 km from park's center) on several bright and calm days during May-October 2009. The measurements were made just above the ground surface so that the recorded data can be confidentially resembled the actual LST data of the studied area. Group of the trained staffs (Figure 3.14) were organized the measurements using devices like GPS receivers, VelociCalc 9555, and QUESTemp 34 (Figure 3.15). The obtained data were used for the construction of air temperature maps presented in Chapter 4. Figure 4.16 illustrates the field measuring location maps for each park, in which the sampling points were mostly located along major roads and some accessible public spaces situated nearby. However, there were still several surrounding spaces that could not be accessed to measure temperature data inside. These exclusions can introduce large homogeneous portions on the interpolated temperature maps as seen in Figure 4.17.

In all cases of interest depicted in Figure 4.17, the interpolated LST map for each considered park indicates great variation of air temperature pattern within and around the park's occupying area. But all these parks exhibit tendency in having lower temperature inside when compared to those of the surrounding urban environment. As stated earlier, this notable reduction in air temperature within the park's area (and its vicinity) should be resulted from the existing of the two main components of its LULC: (1) pacts of the dense trees or other vegetations and (2) large water bodies.

Considering that radial variation of temperature data moves inwards to the chosen park's center, Santipap Park seems to have least distance of temperature decrease toward park's center (about 500 meters with about 1°C drop) while the Lumpini Park has longer temperature-dropping distance (about 700 meters with about 0.5°C drop). And the largest park of the interest, Chatuchak Park Complex (CPC), has dropping distance of about 1,600 meters with about 4°C decrease (Table 4.12 and Figure 4.18). These results clearly demonstrate strong influence of large urban green areas, like the CPC, in the introducing of notably cooler atmosphere within their territory and also over the vicinity surrounding.

However, influences of small or medium parks (like the Santipap Park or Lumpini Parks considered here) on the cooling of concerned ambient air temperature are not much pronounced in this research. This observed small impact might be due to the dense urban buildings existing rather close to both parks that can introduce substantial warming air to diminish cooling environment in the park. In addition, the production of LST maps using satellite TIR images (like Figure 4.15) seems to provided more accurate pattern of LST variation than those produced from field observations due to no problem of accessibility.

In addition, apparent influences of different LULC components on LST variation were also assessed by observing pattern of temperature data recorded by the mobile sensor along two selected routes (as seen in Figure 4.19). Their corresponding satellite-based LST data along the same routes were also displayed for a comparison. Results of this work indicate that higher temperature values seem to appear under strong urban environment whereas in rural area, recorded temperatures noticeably drop as expected.
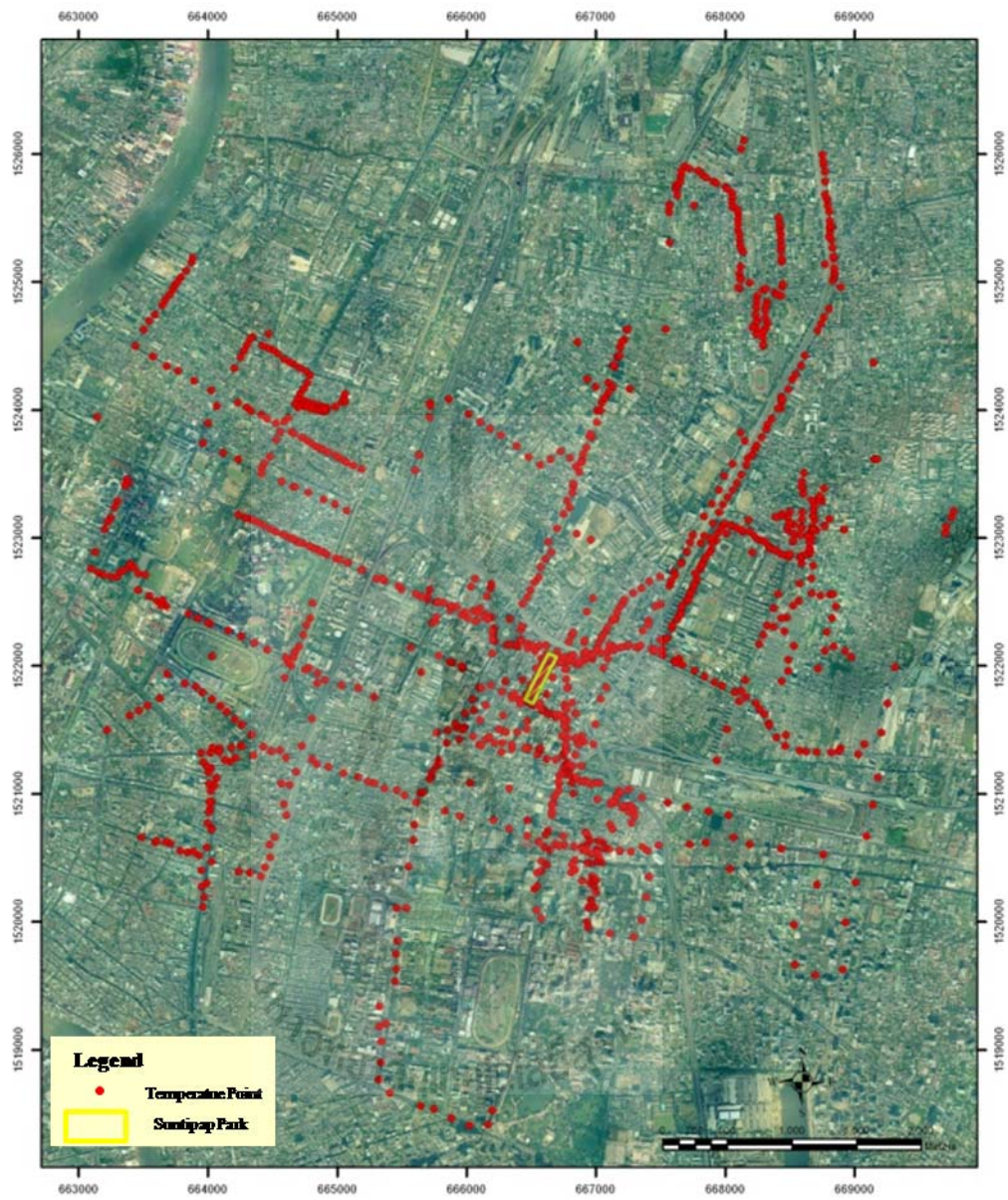
Figure 4.16a Field measuring location maps of the Suntipap Park (small size).
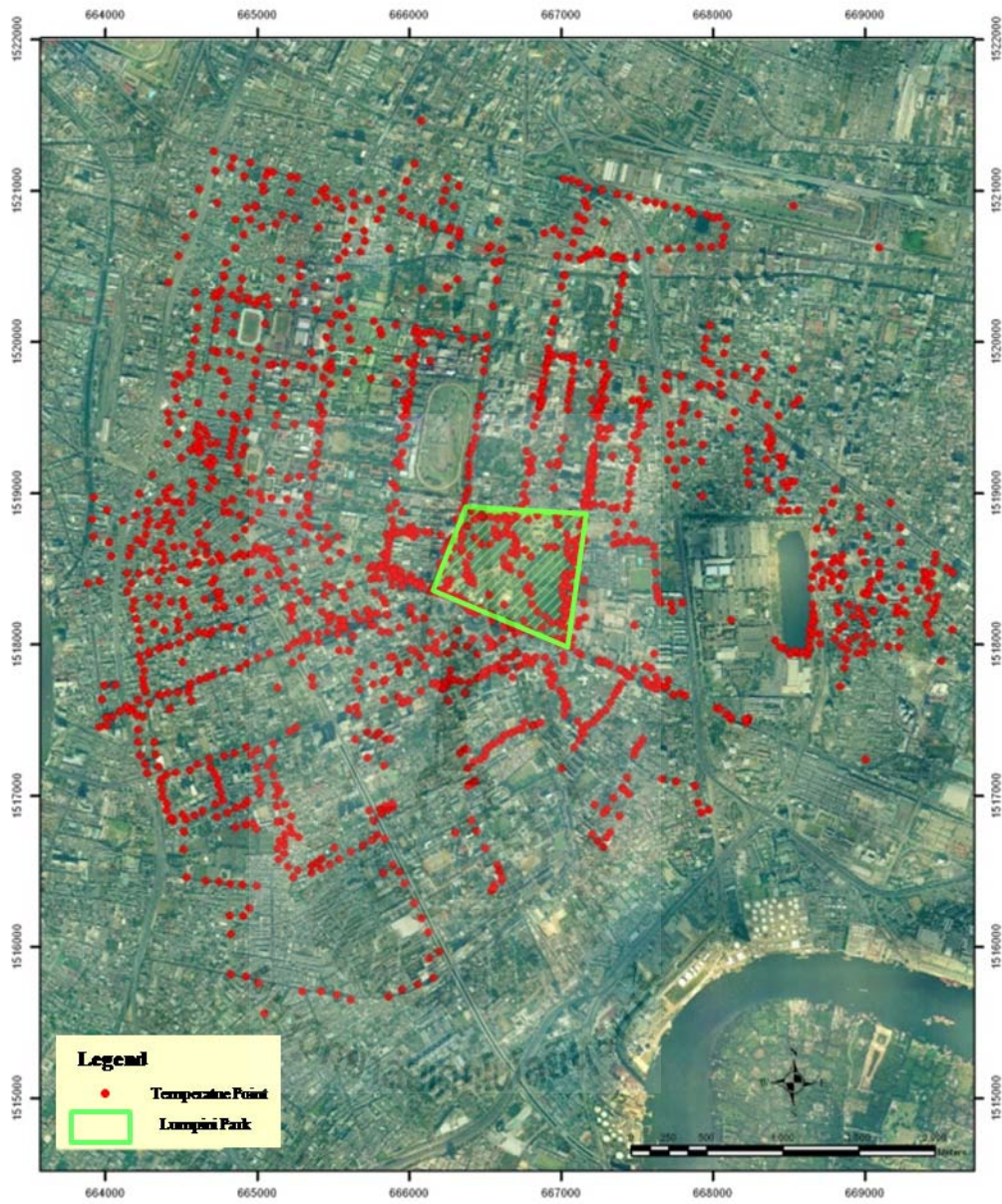
Figure 4.16b Field measuring location maps of the Lumpini Park (medium size).
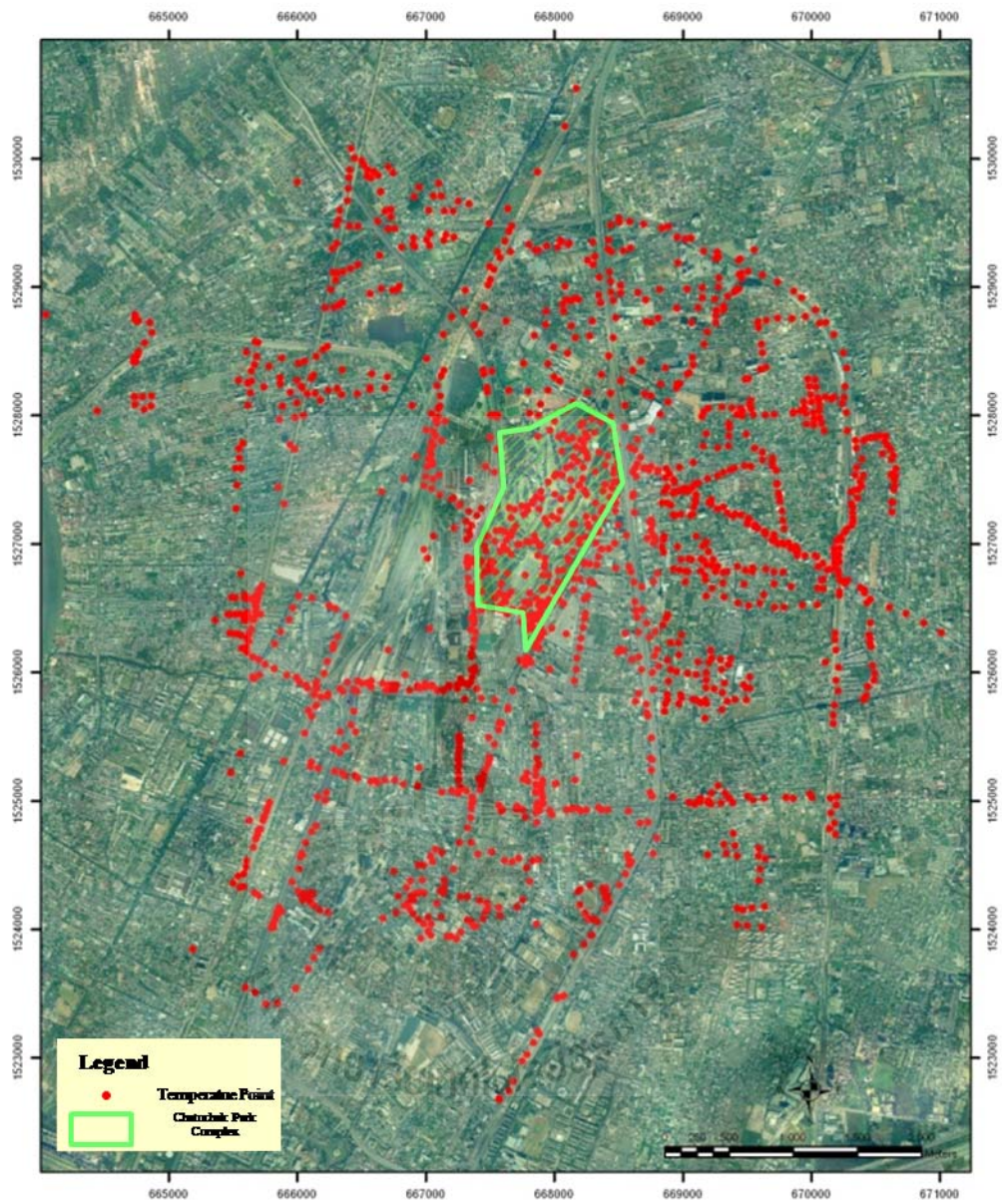
Figure 4.16c Field measuring location maps of the Chatuchak Park Complex (large size).
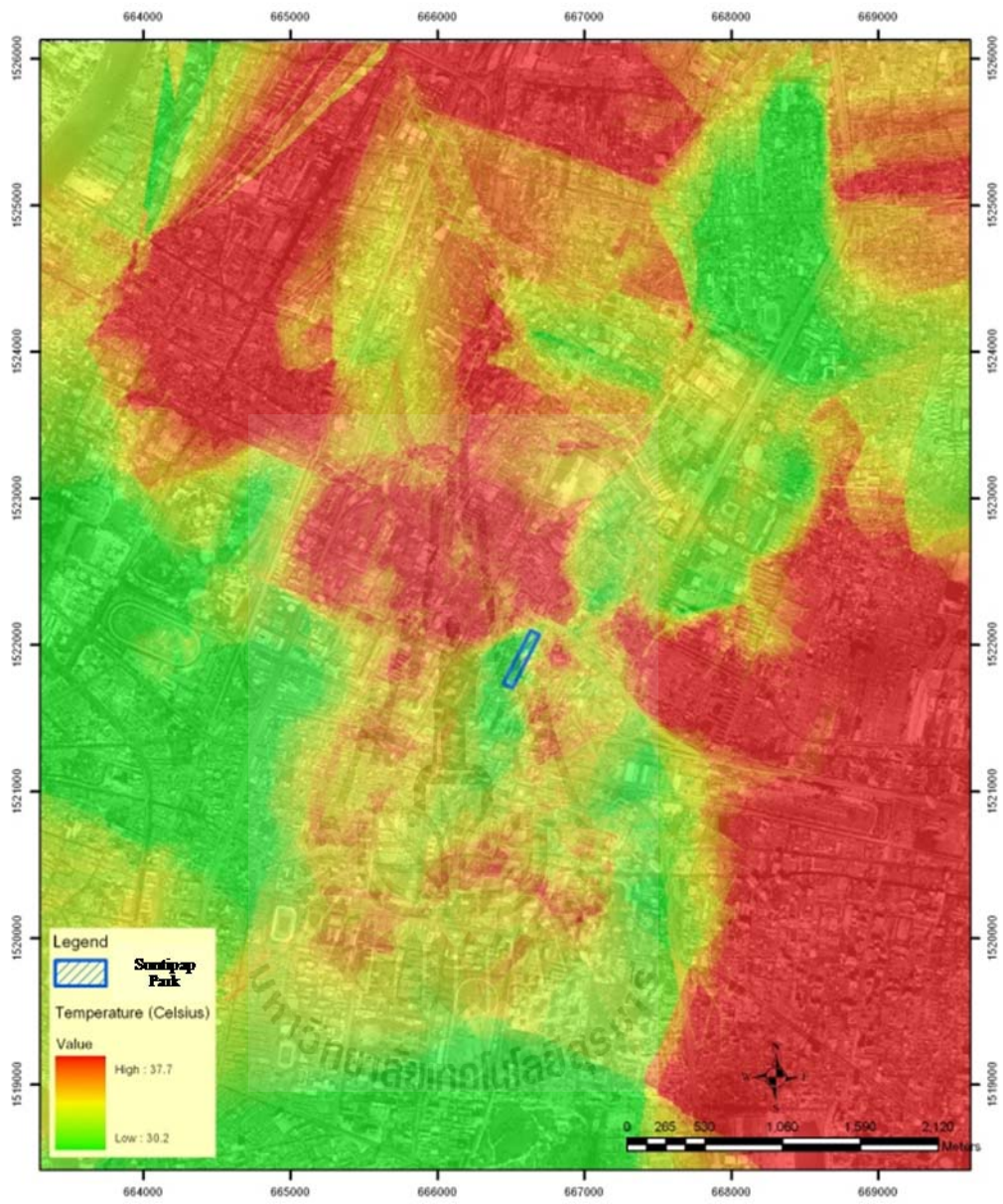
Figure 4.17a Interpolated temperature map of the Suntipap Park (small size).
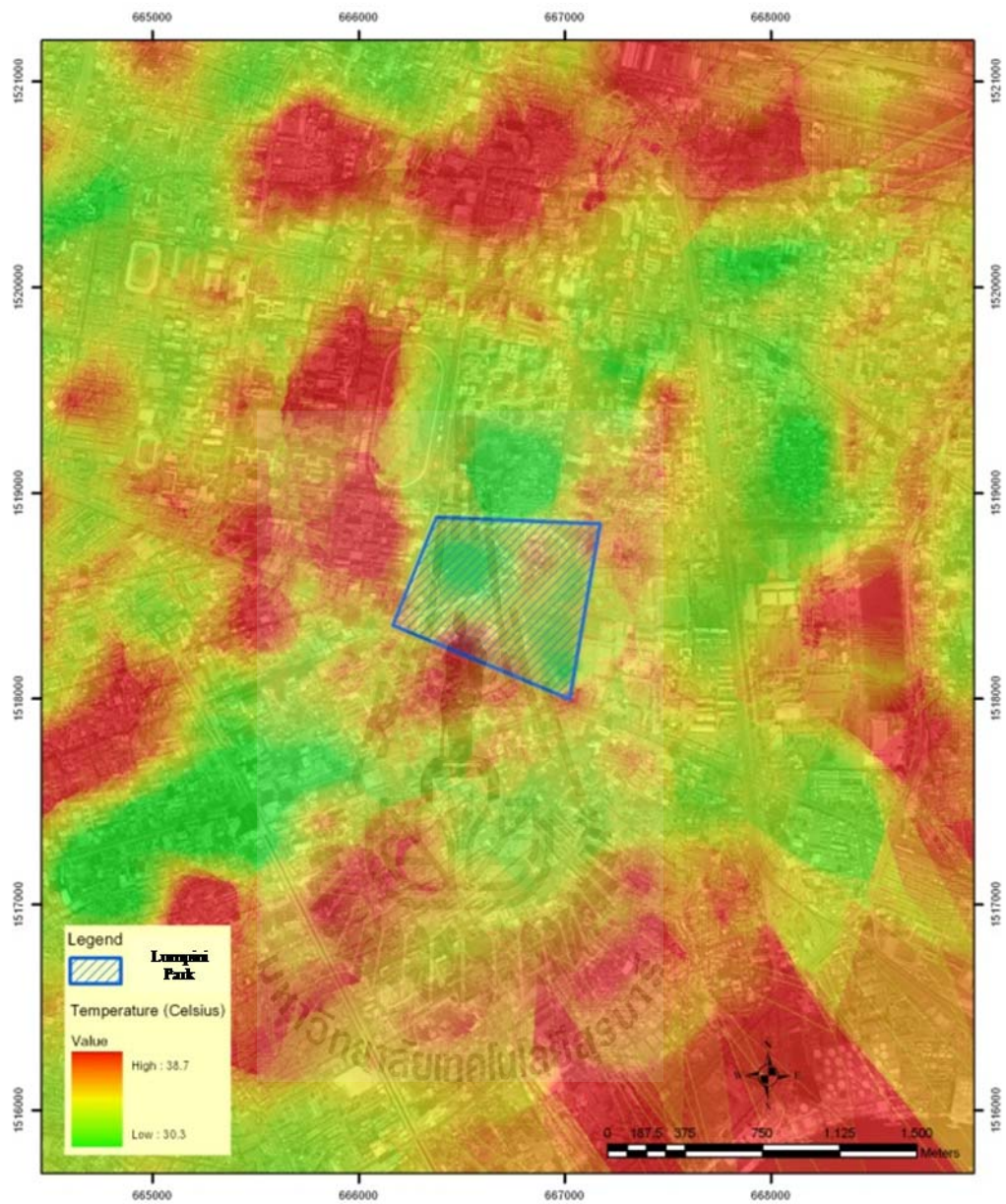
Figure 4.17b Interpolated temperature map of the Lumpini Park (medium size).
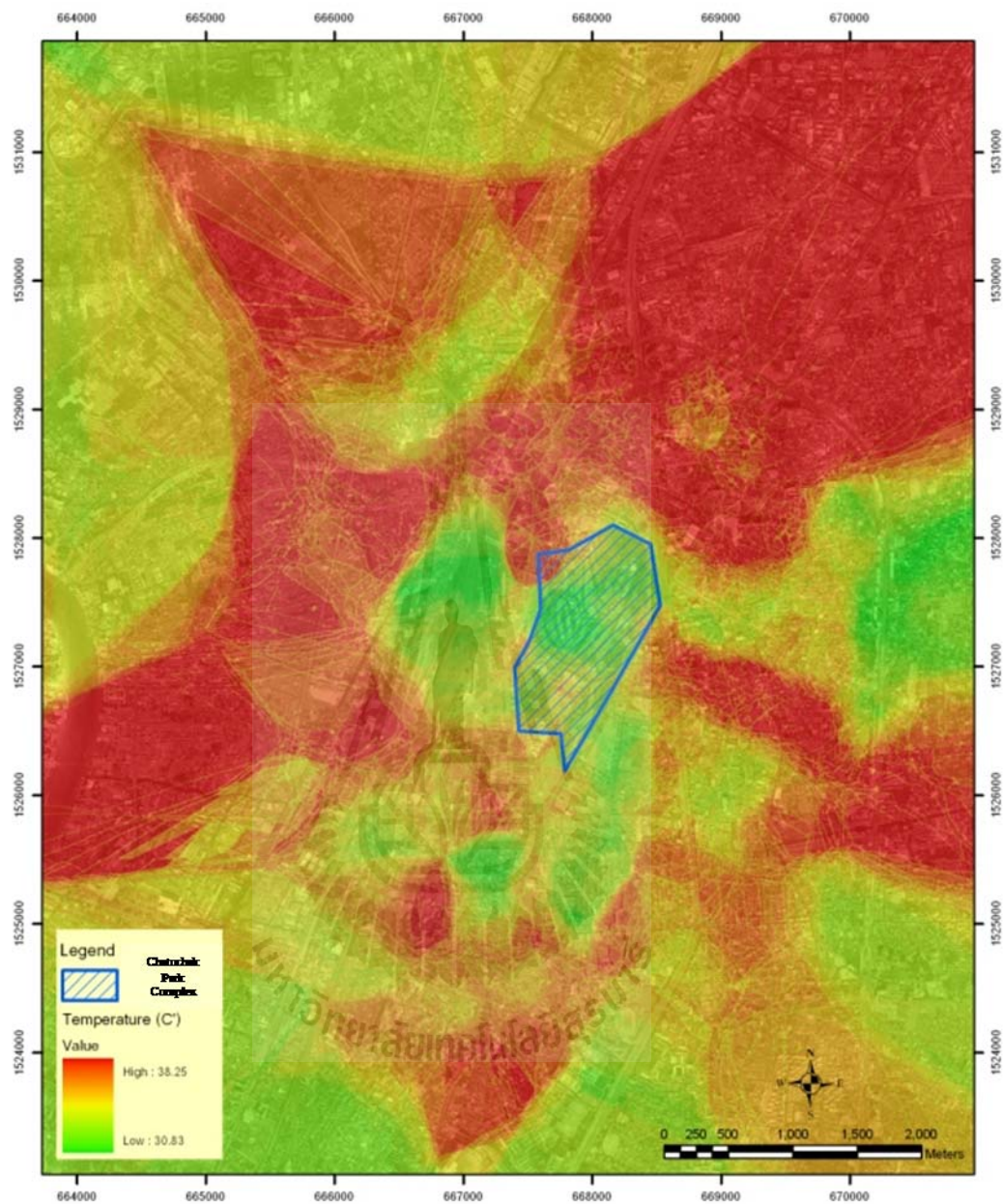
Figure 4.17c Interpolated temperature map of the Chatuchak Park Complex (large size).

Table 4.12 Variation of ground-based average surface temperature values (^{o}C) with the radial distances (in km) away from the park center.

Park	Distance from the park's center						
	0.0	0.5	1.0	1.5	2.0	2.5	3.0
Suntipap	34.02	35.02	35.10	34.96	34.86	35.20	34.98
Lumpini	33.29	33.59	33.72	33.57	34.26	33.91	33.94
CPC	32.21	34.20	34.47	35.30	35.35	35.38	35.43
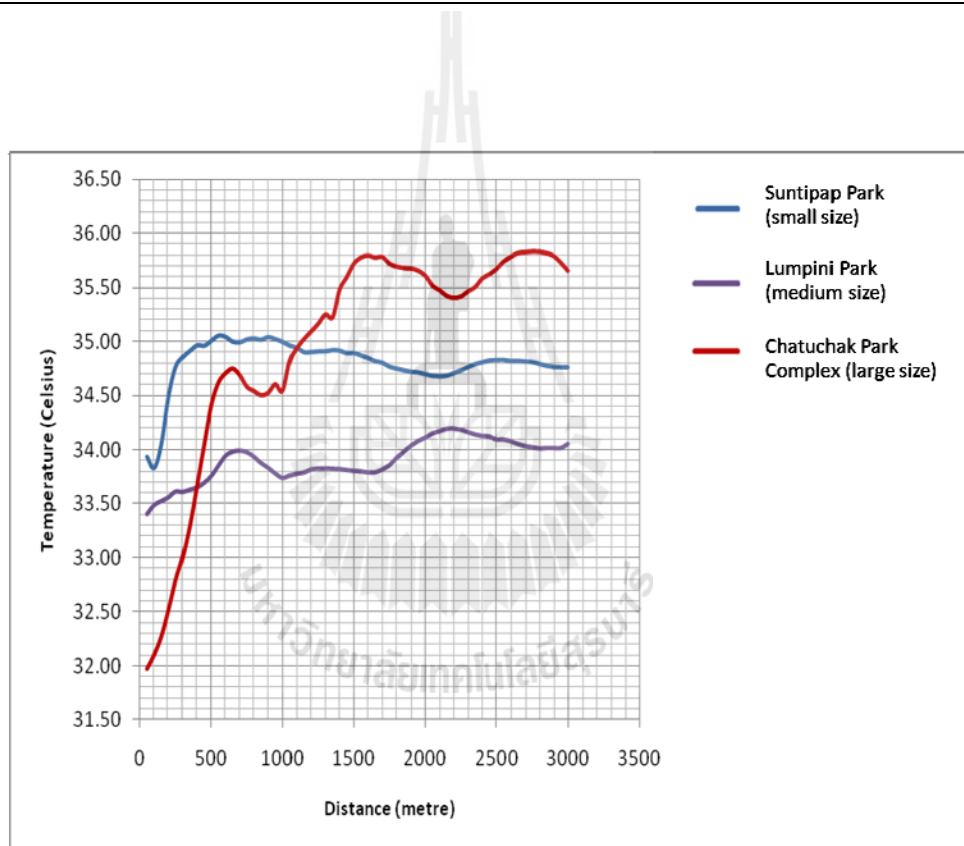
Figure 4.18 Variation of average air temperature with distance from park centers.
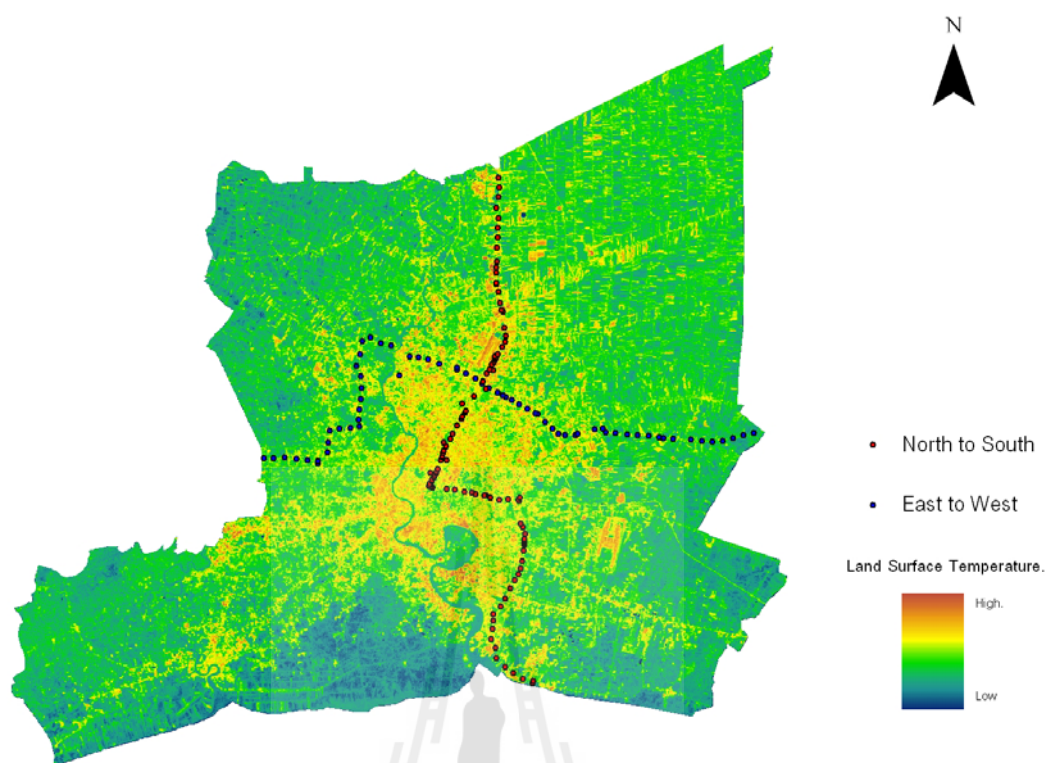
Figure 4.19a Two chosen routes for the construction of UHI profiles (along the route).
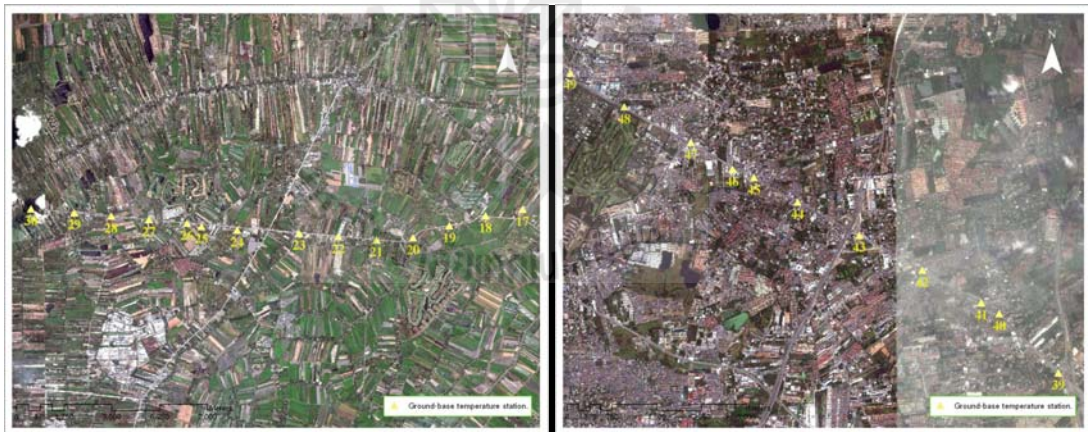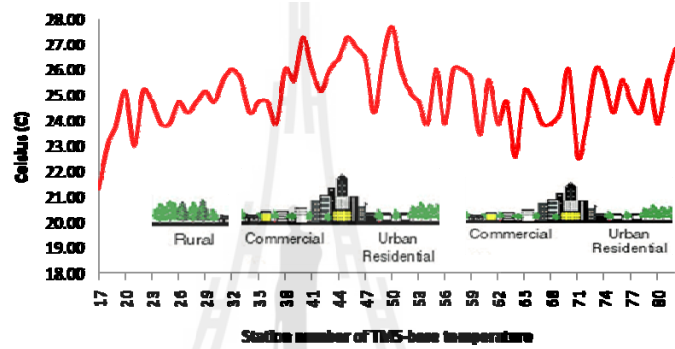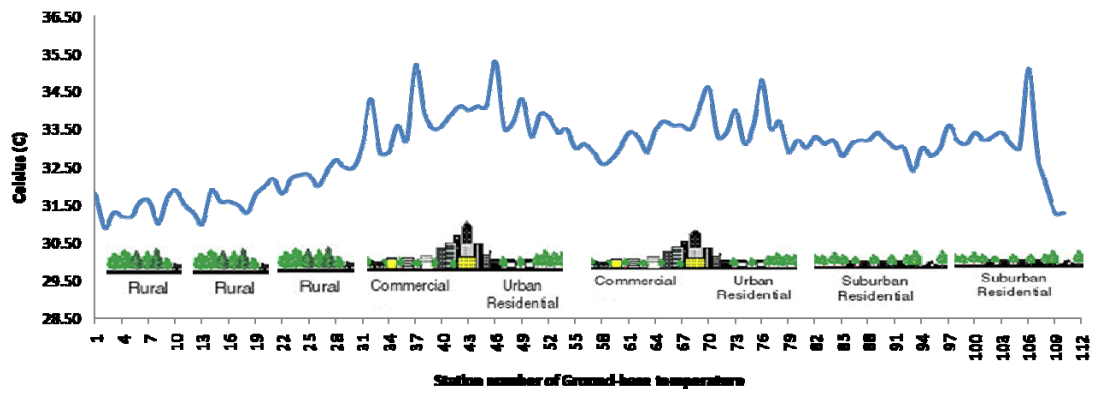
(a) Route 1 (East-West).

Figure 4.19b Ground-based/satellite-based temperature profiles along used routes.
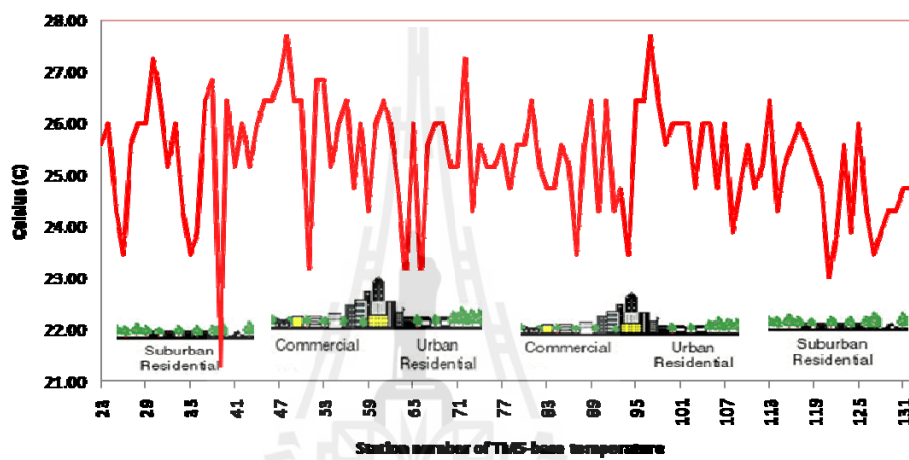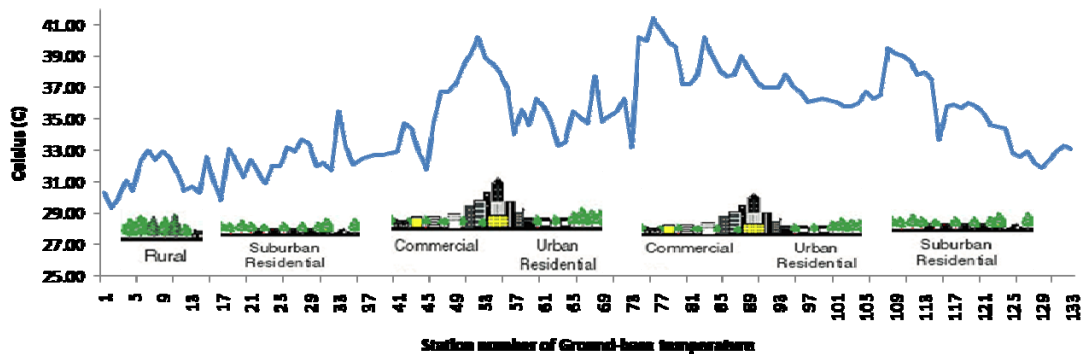
(b) Route 2 (North-South).

Figure 4.19b Ground-based/satellite-based temperature profiles along used routes

(Continued).

4.5 Impact of Temperature Variation on Electricity Consumption

Heat island phenomena can lead directly to visibly higher electrical energy consumption mostly due to heavier uses of cooling system appliances, especially air-conditioners. But they significantly reduce need for heating in the winter also. It is also well-acknowledged in Thailand that rising temperature can lead to substantial rise in electricity consuming, especially during the summer season. However, actual relationship between temperature variation and changing rate of the electricity consuming is still not explicitly explored by any known researches on this topic so far in Thailand. To attain more knowledge on this issue, the explicit relationship between electrical loading and recorded temperature data in the BMA area is evaluated in this thesis based on electrical consuming data provided by the MEA in 2008 and monthly-mean temperature derived from recorded temperature data of the responsible agencies (as detailed in Table 3.1)

The needed data of electricity consumption were acquired from internet resource where five broad groups of the MEA registered users were considered: (1) residential (RES), (2) small general service (SGS), (3) medium general service (MGS), (4) large general service (LGS), (5) governmental office (GOV)/non-profit organization (NPO). Relationship of the monthly mean temperature data in BMA and the associated electrical consumption was examined and results are shown in Figures 4.20 and 4.21. It was found that there is strong correlation between amount of electricity consumption in BMA and the monthly mean temperature with highest R^2 of 0.937 (for the RES group) and 0.843 (for the SGS group). The correlation levels are lower for LGS and MGS with $R^2 = 0.615$ and 0.518, respectively while lowest correlation is at GOV/NPO group with $R^2 = 0.308$.

Table 4.13 Data of monthly electricity consumption in 2008 as reported by the MEA.

Month	Load	RES	General Service (GS)			GOV	Others	Total
			SGS	MGS	LGS			
Jan	GW	707,482	491,415	646,940	1,273,014	94,513	166,700.76	3,380,064
	%	20.93	14.54	19.14	37.66	2.80	4.93	100.00
	CUS	2,197,909	474,352	19,902	1,602	10,813	2,261.00	2,706,839
	L/CUS	0.32	1.04	32.51	794.64	8.74	73.73	1.25
Feb	GW	715,968	493,137	629,545	1,229,916	94,583	158,032.89	3,321,181
	%	21.56	14.85	18.96	37.03	2.85	4.76	100.00
	CUS	2,194,119	474,124	19,892	1,608	10,831	2,267.00	2,702,841
	L/CUS	0.33	1.04	31.65	764.87	8.73	69.71	1.23
Mar	GW	805,008	535,022	713,668	1,374,665	102,678	180,978.08	3,712,018
	%	21.69	14.41	19.23	37.03	2.77	4.88	100.00
	CUS	2,210,113	475,493	19,898	1,615	10,870	2,280.00	2,720,269
	L/CUS	0.36	1.13	35.87	851.19	9.45	79.38	1.36
Apr	GW	900,305	546,700	630,623	1,257,126	93,811	177,376.35	3,605,939
	%	24.97	15.16	17.49	34.86	2.60	4.92	100.00
	CUS	2,216,847	476,202	19,877	1,620	10,878	2,278.00	2,727,702
	L/CUS	0.41	1.15	31.73	776.00	8.62	77.86	1.32
May	GW	845,239	548,115	706,871	1,364,611	105,438	179,770.28	3,750,044
	%	22.54	14.62	18.85	36.39	2.81	4.79	100.00
	CUS	2,222,518	477,189	19,872	1,625	10,878	2,283.00	2,734,365
	L/CUS	0.38	1.15	35.57	839.76	9.69	78.74	1.37
Jun	GW	815,896	540,286	691,308	1,342,363	116,716	174,840.46	3,681,410
	%	22.16	14.68	18.78	36.46	3.17	4.75	100.00
	CUS	2,225,810	477,813	19,819	1,628	10,889	2,282.00	2,738,241
	L/CUS	0.37	1.13	34.88	824.55	10.72	76.62	1.34
Jul	GW	810,090	537,390	686,996	1,344,627	112,960	177,923.62	3,669,988
	%	22.07	14.64	18.72	36.64	3.08	4.85	100.00
	CUS	2,233,409	478,551	19,838	1,624	10,920	2,297.00	2,746,639
	L/CUS	0.36	1.12	34.63	827.97	10.34	77.46	1.37
Aug	GW	829,347	551,106	692,399	1,366,035	119,926	181,029.74	3,739,843
	%	22.18	14.74	18.51	36.53	3.21	4.84	100.00
	CUS	2,238,801	480,128	19,842	1,645	11,931	2,320.00	2,754,667
	L/CUS	0.37	1.15	34.90	830.42	10.05	78.03	1.36
Sep	GW	807,658	536,809	661,228	1,270,945	110,279	167,010.32	3,553,930
	%	22.73	15.10	18.61	35.76	3.10	4.70	100.00
	CUS	2,247,875	479,119	19,886	1,655	11,973	2,331.00	2,762,839
	L/CUS	0.36	1.12	33.25	767.94	9.21	71.65	1.27

Table 4.13 Data of monthly electricity consumption in 2008 as reported by the MEA (Continued).

| Month | Load | RES | General Service (GS) | | | GOV | Others | Total |
			SGS	MGS	LGS			
Oct	GW	817,123	543,107	672,093	1,315,060	113,439	175,791.53	3,636,615
	%	22.47	14.93	18.48	36.16	3.12	4.83	100.00
	CUS	2,266,987	480,674	19,870	1,657	11,132	2,347.00	2,782,667
	L/CUS	0.36	1.13	33.82	793.64	10.19	74.90	1.31
Nov	GW	715,172	488,995	619,894	1,173,345	102,171	159,618.25	3,259,195
	%	21.94	15.00	19.02	36.00	3.13	4.90	100.00
	CUS	2,268,989	479,562	19,835	1,661	11,250	2,343.00	2,783,640
	L/CUS	0.32	1.02	31.25	706.41	9.08	68.13	1.17
Dec	GW	612,129	441,013	561,933	1,082,315	84,269	144,027.52	2,925,687
	%	20.92	15.07	19.21	36.99	2.88	4.92	100.00
	CUS	2,278,072	480,159	19,791	1,660	11,317	6,514.00	2,797,513
	L/CUS	0.27	0.92	28.39	652.00	7.45	22.11	1.05

Note: 1. RES ≡ Residential, SGS ≡ Small general service, MGS ≡ Medium general service,

   LGS ≡ Large general service, GOV ≡ Governmental and non-profit organizations.

  2. GW ≡ Gigawatt, CUS ≡ Customer, L/CUS ≡ Electrical loading per customer

Table 4.14 Monthly mean ground-base temperature for the BMA in 2008 (in $^{\circ}$C).

Month	Jan	Feb	Mar	Apr	May	Jun	Jul	Aug	Sep	Oct	Nov	Dec
Temp.	27.70	27.80	29.50	30.20	29.20	29.20	28.60	29.00	28.40	28.50	27.30	26.30
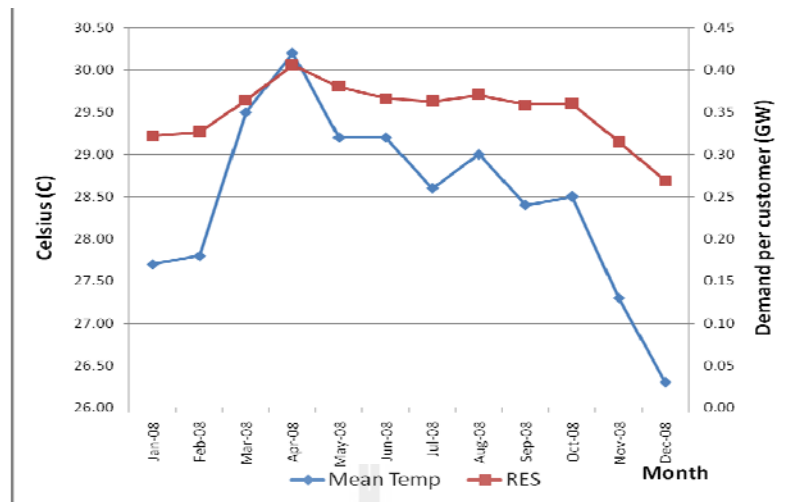
(a) Residential (RES).
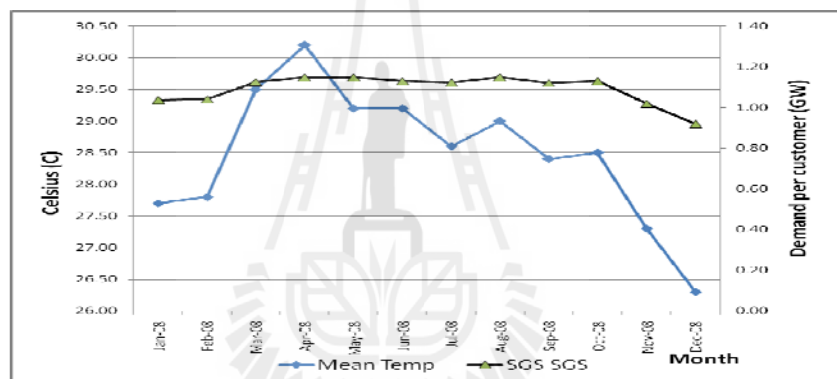
(b) Small general service (SGS).
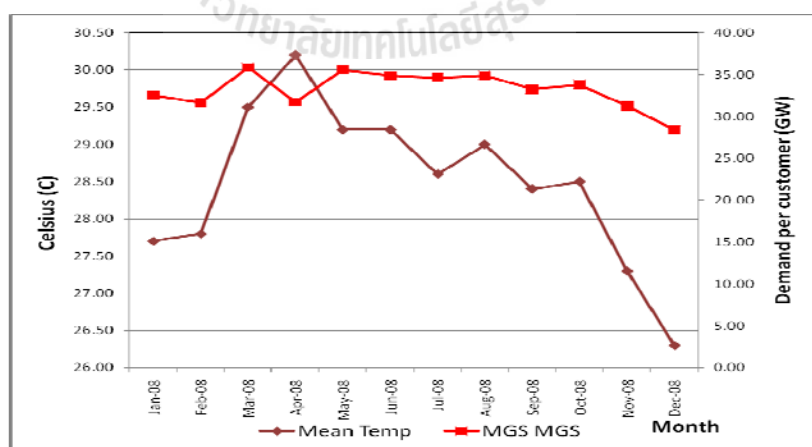
(c) Medium general service (MGS).

Figure 4.20 Variations of monthly L/CUS with average temperatures in 2008.
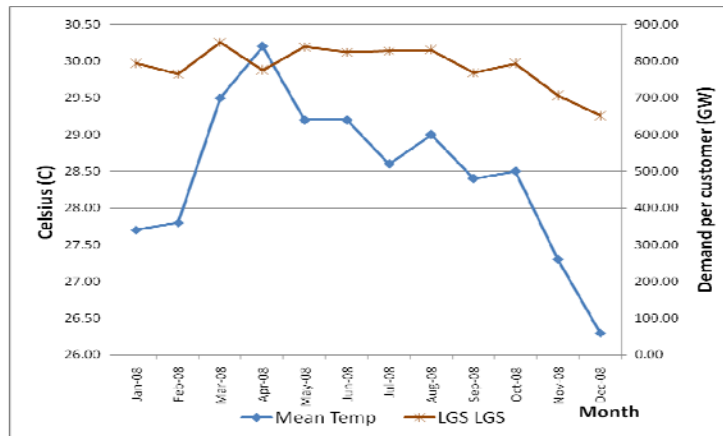
(d)   Large general service (LGS).
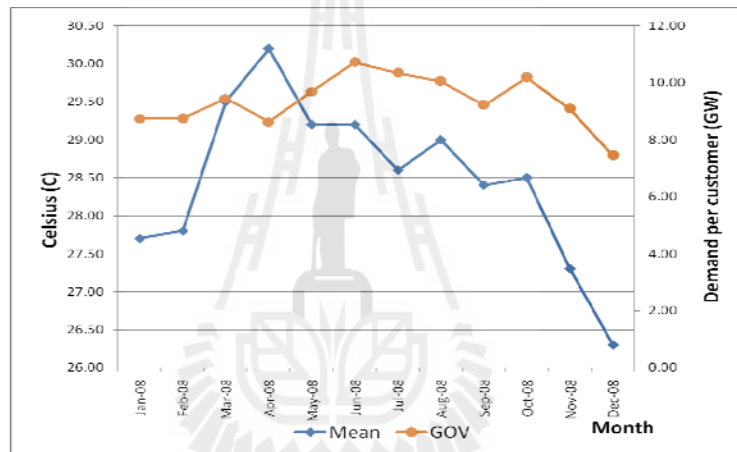
(e)   Governmental office (GOV).

Figure 4.20 Variations of the monthly L/CUS with average temperatures in 2008 (Continued).
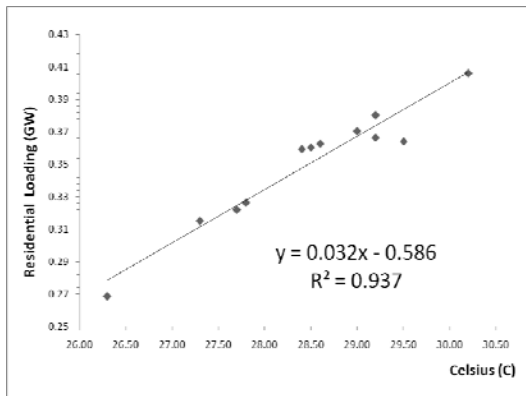
(a) Residential (RES).
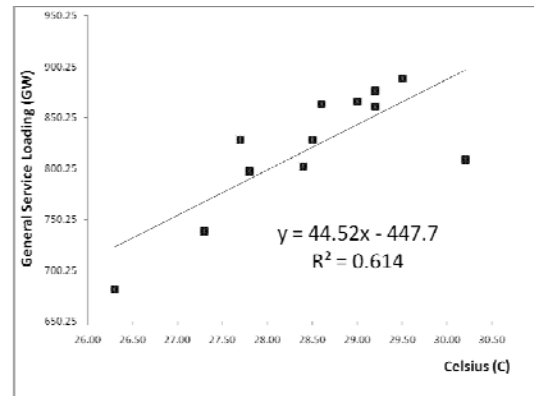
(b) General service (GS).
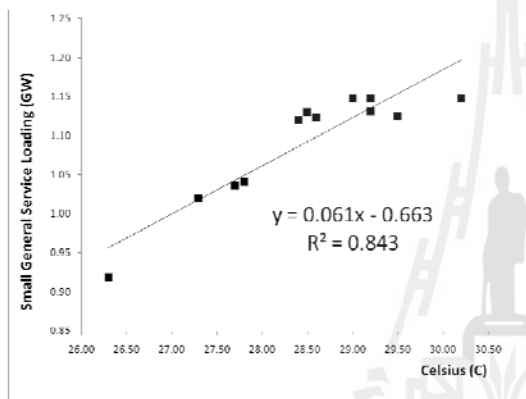
(c) Small general service (SGS).
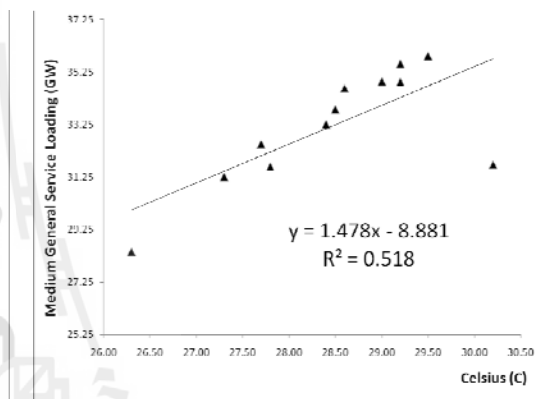
(d) Medium general service (MGS).
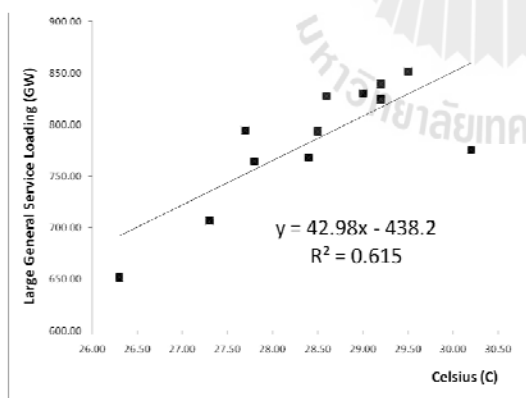
(e) Large general service (LGS).
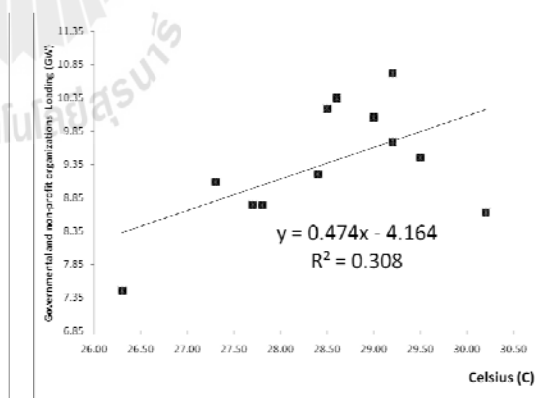
(f) Governmental office (GOV).

Figure 4.21 Relations of monthly L/CUS with average temperatures for (a) RES, (b) GS, (c) SGS, (d) MGS, (e) LGS (f) GOV (from Figure 4.20).

These obtained results emphasize impact of the rising air temperature in making higher electricity demand, especially in household and SGS activities. The strong linear relationship found here is very useful for the prediction of demand for electrical energy (especially for the household and SGS sections) if average temperature in BMA is known in advance. However, it appears that only consuming rate in April that is notably dropped for the MGS, LGS and GOV sections, while average temperature is rising. This dropping in loading demand results in the lower correlation level for both groups and reasonable explanation for this unexpected finding should be studied more.

The diurnal variations in electrical loading were also examined for summer days (in April) and winter days (in January) for three broad groups of the formal MEA users: residential, general services, and governmental and non-profit organization (Figure 4.22). It was found that, for the residential category, diurnal loading patterns look quite different between summer and winter. In summer, total electrical demand is relatively low during daytime but greatly rising during nighttime and reaching its peak around 21-23 o'clock. In winter, electrical loading is also high during mid-daytime as well as at nighttime but the overall demand is much lower than that in summer.

For the general services category, the loading patterns are pretty identical for both seasons where loading is constantly high during daytime (with some marked drop during lunchtime) and noticeably low in the evening and at nighttime. The lowest demands were seen on Sunday and holidays. For the governmental and non-profit organization category, loading is constantly high during daytime (with some marked drop during lunchtime) and relatively low demand was found at nighttime and also on weekend and holidays.
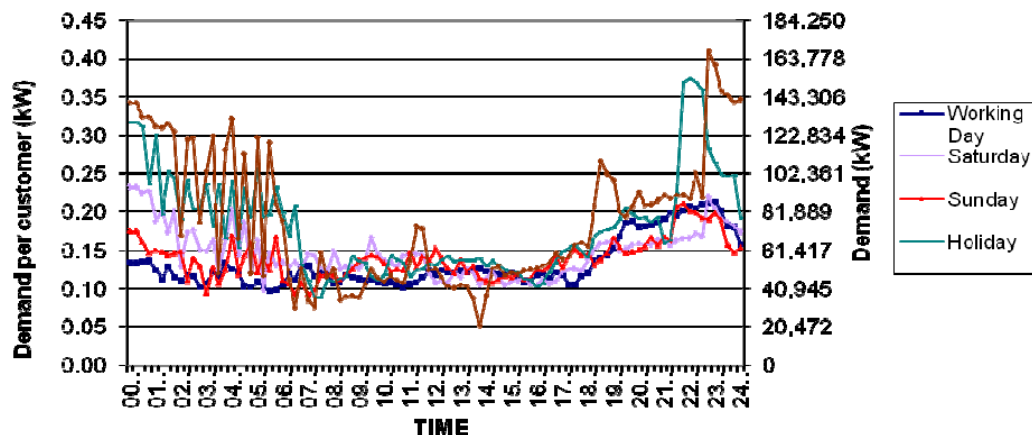
(a1)　　Summer (April 2008).
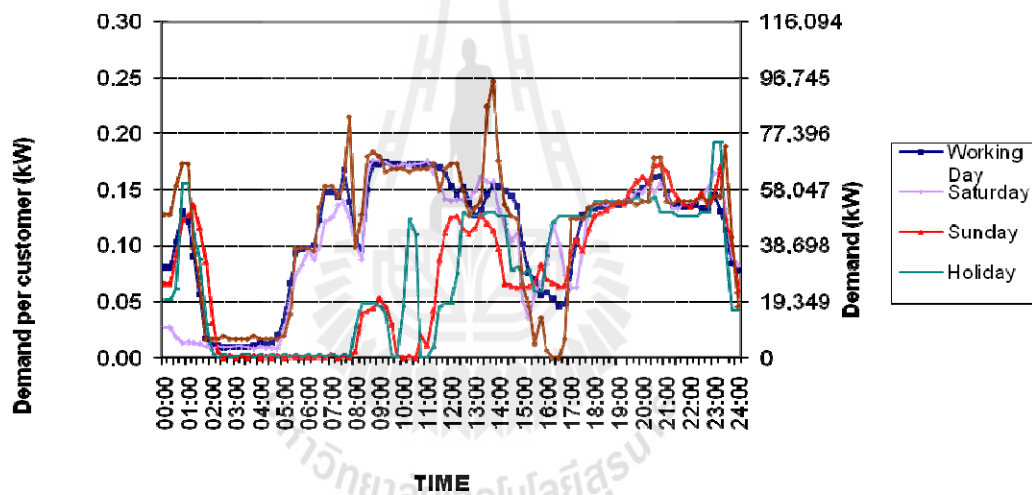
(a2)　　Winter (January 2008).

Figure 4.22 Diurnal variations of L/CUS in summer and winter days for (a) Residential, (b) General services, and (c) Governmental and non-profit organizations.
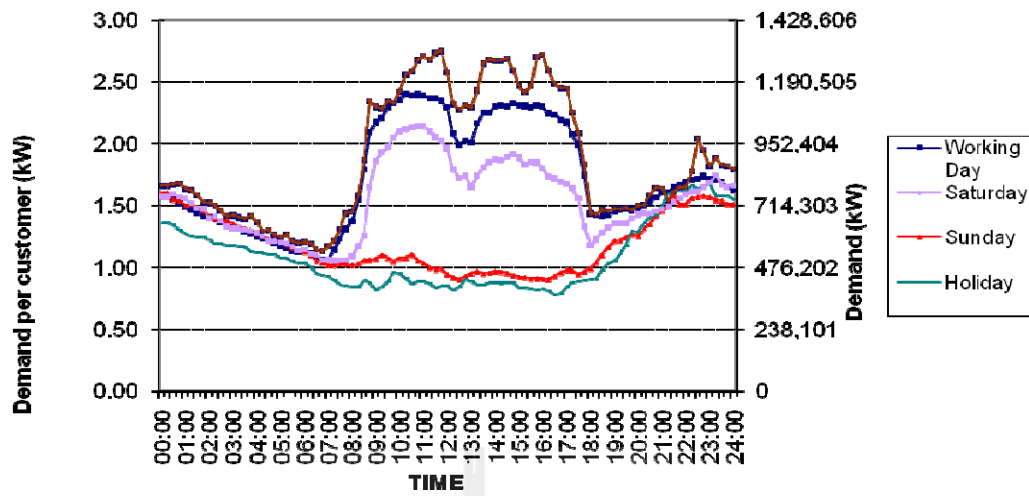
(b1)   Summer (April 2008).
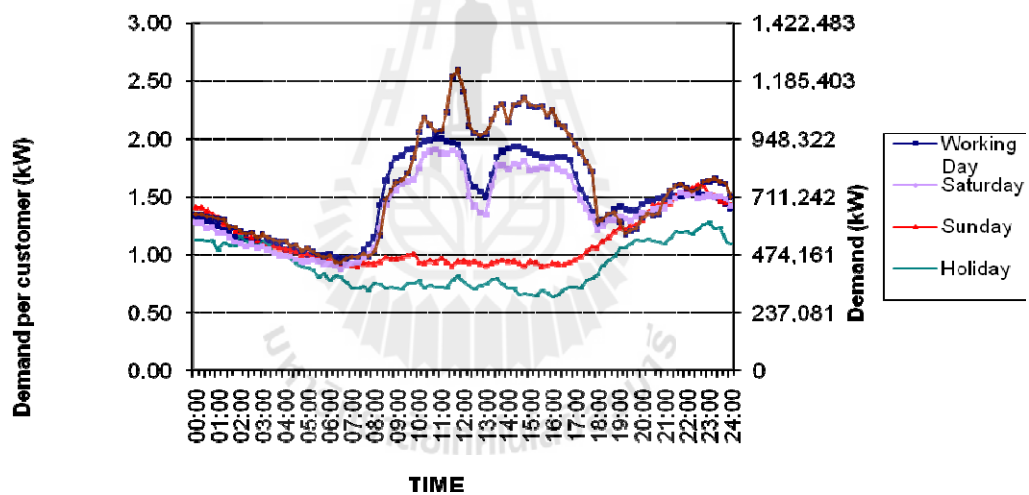
(b2)   Winter (January 2008).

Figure 4.22   Diurnal variations of L/CUS in summer and winter days for (a) Residential, (b) General services, and (c) Governmental and non-profit organizations (Continued).
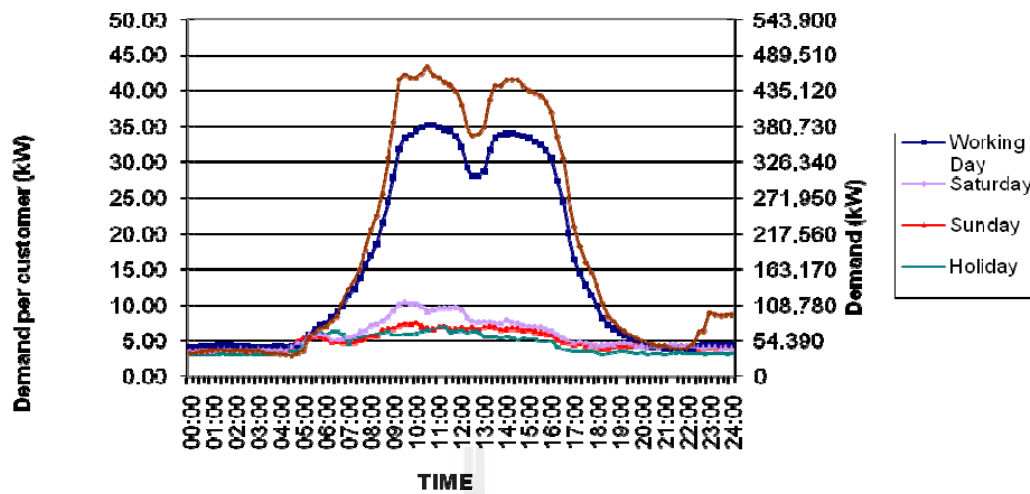
(c1)   Summer (April 2008).
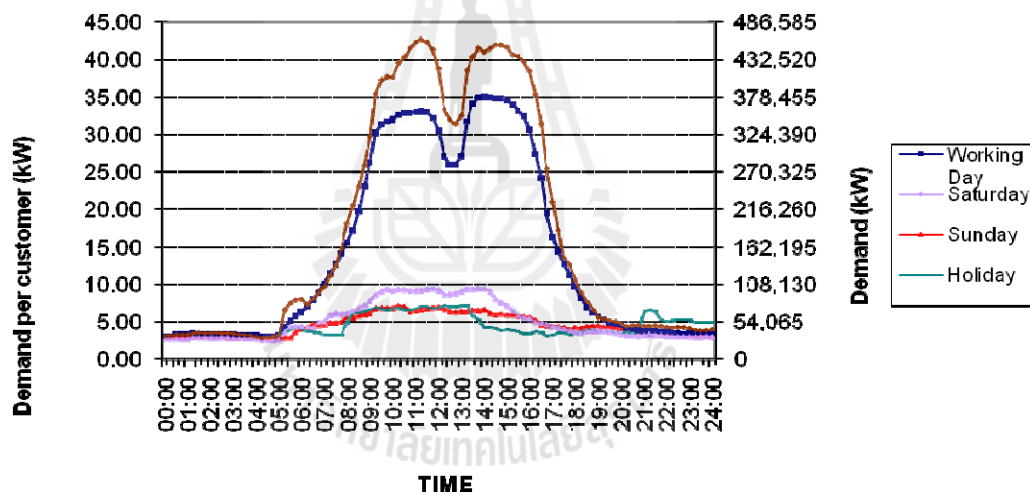
(c2)   Winter (January 2008).

Figure 4.22 Diurnal variations of L/CUS in summer and winter days for (a) Residential, (b) General services, and (c) Governmental and non-profit organizations. (Continued).

Relationships of electrical consumption and LULC characteristics

The final task in this research is to find relationships of the electrical consumption and LULC characteristics over BMA region. To achieve this intention, three districts with different LULC components were chosen for detailed analysis: Bang Khen (mixed urban and rural environment), Phaya Thai (urban environment), and Bang Khun Tian (coastal environment). Average air temperature data for each district were approximated from the daytime MODIS-TIR images on 25 selected days distributing all year round whereas the corresponding electrical load/customer data (for each district on those chosen days) were calculated from the original data acquired from the MEA (as detailed in Table 4.16).

It was found that the observed temperature data at each district were mostly found at the 27-30°C range. However, when compared these obtained temperature data with the corresponding L/C data acquired on the same day, no obvious pattern of the relationship was found for each district as evidenced in the relatively low correlation level, which are, 0.007 (Bang Khen), 0.014 (Phaya Thai), and 0.070 (Bang Khun Tian). The resulted low correlations for all districts might be due to the still lack of both temperature data and the electrical loading data to represent their actual relationship. This is because temperature can vary considerably all day round, but the used value obtained from the MODIS image (for each day) represents just only a moment of time (when the MODIS image was taken) and may not be suitable to represent the average air temperature for each specified day. Similarly, measuring locations for electrical loading data at each chosen district are still rather low (5-10 stations at most) compared to the whole district area, and their obtained data might not be suitable to represent the actual electrical load for a district as a whole.

Table 4.16 Daily electrical consumption and temperature data for selected districts.

Date	Bang Khen		Phaya Thai		Bang Khun Tian	
	Temp (^{o}C)	L/CUS (MW)	Temp (^{o}C)	L/CUS (MW)	Temp (^{o}C)	L/CUS (MW)
1 (09 Jan 08)	27.98	150.06	26.57	267.88	27.29	326.71
2 (11 Jan 08)	28.89	158.29	27.80	317.13	28.58	337.70
3 (14 Jan 08)	27.50	205.37	27.23	397.68	26.97	366.02
4 (18 Jan 08)	27.70	155.71	26.17	279.43	26.94	277.73
5 (20 Jan 08)	28.67	187.88	26.82	355.11	27.47	350.70
6 (27 Jan 08)	25.39	228.45	23.36	351.45	24.35	356.26
7 (01 Feb 08)	22.48	128.83	27.42	332.66	23.71	195.95
8 (21 Feb 08)	29.67	122.77	29.47	332.07	29.60	301.76
9 (23 Feb 08)	29.85	100.72	29.70	285.69	29.69	330.14
10 (11 Mar 08)	29.40	177.64	29.80	318.14	29.74	676.30
11 (10 Apr 08)	30.23	207.82	30.11	391.01	30.12	367.36
12 (16 Apr 08)	29.67	259.63	29.70	357.15	28.00	427.17
13 (07 Jun 08)	28.43	273.33	29.01	357.25	28.12	356.19
14 (23 Jun 08)	29.73	240.77	29.76	356.50	29.68	403.27
15 (24 Jun 08)	29.39	235.10	29.18	387.21	29.13	413.47
16 (15 Aug 08)	29.42	171.76	29.87	305.09	29.09	373.77
17 (23 Sep 08)	28.57	162.82	28.27	275.56	29.21	325.54
18 (28 Nov 08)	28.55	147.82	28.44	237.18	28.22	259.27
19 (01 Dec 08)	28.89	113.78	28.81	220.47	28.93	163.30
20 (05 Dec 08)	28.44	127.87	28.48	296.63	28.47	276.88
21 (12 Dec 08)	29.26	110.05	29.14	242.71	29.23	249.82
22 (13 Dec 08)	29.03	115.60	29.03	335.61	29.21	361.10
23 (14 Dec 08)	29.16	133.99	28.90	260.97	29.31	308.93
24 (28 Dec 08)	29.51	122.94	29.48	276.90	29.50	296.92
25 (30 Dec 08)	28.84	122.94	28.52	276.90	29.29	296.92

Note: Temp $\equiv$ Average MODIS-based temperature, L/CUS $\equiv$ Load/customer.
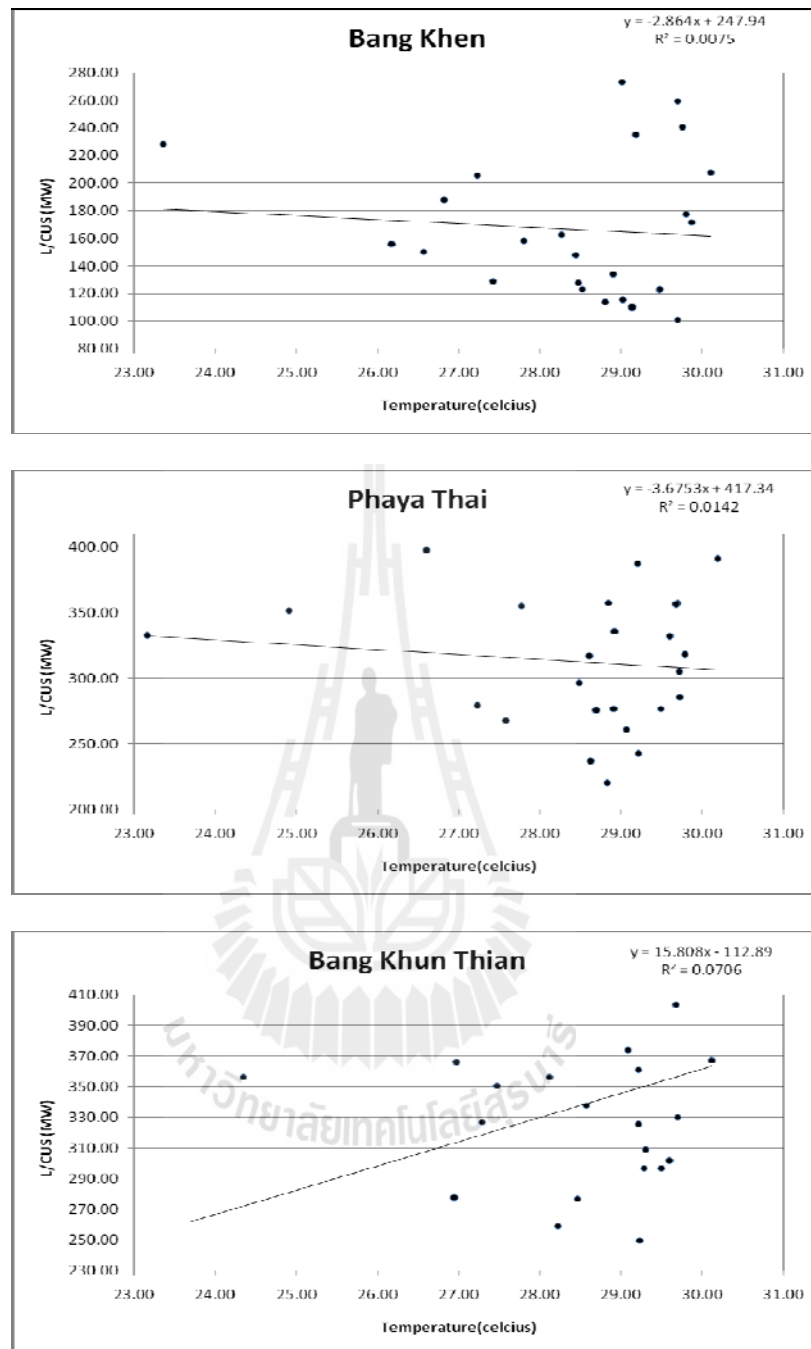
Figure 4.23 Relationships of the daily Loading/Customer data and MODIS-based LST data for some selected districts (from Table 4.16).

CHAPTER V

CONCLUSIONS AND SUGGESTIONS

This research has been divided into 4 principal parts. The first part focuses on the analysis of relationship between satellite-based observed land surface temperature (LST) maps (and the associated UHI maps) and urban growth pattern (or other LULC classes) in the BMA region during period 1992-2008. In the second part, influence of each LULC component on the observed LST data were determined quantitatively by using appropriate indices for each LULC type. These are (1) NDVI (for vegetation), (2) NDBI (for urban/built-up), (3) NDBaI (for bare land), (4) %ISC (for impervious surface). The linear relationship was primarily assumed based on extensive literature review on this issue. The third part presents an evaluation on effect of existing public parks in reduction of observed ambient air temperature. This analysis was conducted based on both field observation data and satellite-based temperature data. There were three parks of different sizes (small, medium, large) chosen for the detailed analysis on this topic. And, in the fourth part, relationships between observed temperature variation (from both ground-based and satellite-based measurements) and amount of electricity consumption in BMA region in 2008 were evaluated. The strong linear relationships were assumed to be evidenced from the study as well as distinct impacts of different LULC types on total amount of consumed electricity. To achieve these, different groups of the 2008 MEA customers were examined and reported separately. The conclusion for work in each part is as follows.

5.1 Urban growth and its impact on UHI phenomenon

From data of the derived LULC maps, it can be primarily concluded that, among all known LULC classes, the vegetation cover is the highest proportion of occupying area for all years of interest followed by bare land and water body, or urban/built-up, classes respectively. However, percentages of vegetation have dropped continuously, in general, from 42.27% in 1992 to 32.55% in 2008 (about 23% decrease from its original area in 1992). But, during the same period, urban/built-up area has substantially expanded from about 14.49% in 1992 to 27.88% in 2008 (about 92.5% increase from the original area in 1992). The highest increasing rate of urban and built-up was found during periods of 1996-2000 (31.62% increase) and 2004-2008 (32.38% increase). No obvious changing trends appear for water body and bare land classes during period of the study.

The expansion of urban/built-up area (at about 46.61 km^2 per year) occurs mostly along major roads traversing from central Bangkok to its satellite cities nearby and within Bangkok outskirt in most directions. Mixed classes of vegetation, bare-land, and inland water body usually signify agricultural zone (paddy fields in particular) surrounding the more developed urban/built-up space.

In term of the changing pattern between 1992-2008, out of about 1552.15 km^2 found of urban/built-up area in 2008, just only 518.19 km^2 existing in 1992 while the rest was converted from the other LULC classes, which are, vegetation (530.91 km^2), bare land (350.63 km^2) and water body (152.22 km^2). The transformations of original urban/built-up land to other LULC classes were also observed, especially to the vegetation (138.82 km^2) and bare land (115.94 km^2). These usually occur at remote areas far from city centers.

The gain LST maps during 1992-2008 indicate that, in 1992, the warmest zone were found mostly around central area of Bangkok but in 2008 the peak LST values have spread outward to occupy most areas in central Bangkok and across to the adjacent areas of its satellite provinces, especially Nonthaburi and Samut Prakarn also. The most intense UHI intensity occurs at core urban area of central Bangkok (like case of LST). Impact of UHI on LST variation is less visible at the rural area far from the central Bangkok as the dominant land classes there are vegetation and bare land, which are less vulnerable to the UHI phenomenon than the urban area.

In addition, low UHI intensity is clearly seen in coastal areas along the Thai Gulf in the south, that also have lowest average LST data. The LST data shown on these maps usually have peak values around 26-30°C and associated UHI of more than 2°C which are in broad agreement with the known ground-based data. However, peak values of the UHI intensity might vary considerably depending on dates or seasons of the year. It was most pronounced during wintertime (around November-January) and least pronounced during monsoon season (around July-September). Peak values of around 1.5-2.5°C were found at the ST4 station (Khlong Toei).

Proportions in area cover for the LST and UHI classes indicate dramatic increase in severity of UHI phenomenon during period 1992-2008. Most severity areas are still mostly visible in Bangkok territory but its neighboring provinces have also suffered more with UHI event in recent years due to great expansion of urban area crossing over from Bangkok border. In central Bangkok, only at Bang Krajao sub-district that is still not experienced much of the severe UHI.

5.2 Relationships of LULC Components and LST Data

It was found from obtained results that different LULC components have different impact on the UHI intensity. In general, the increase of urban/built-up area can enhance UHI intensity notably while the green vegetation tends to reduce UHI severity noticeably (like at the Bang Krajao sub-distict). Large water body also substantially helps to diminish the UHI intensity for the surrounding environment.

It was evidenced that relatively high temperature pixels tend to locate within the urban/built-up class (with average values of 25.11°C in 2008) while colder pixels were significantly found within the vegetation and water body classes (with average values of 22.96°C and 22.09°C in 2008). Influence of Thai Gulf on temperature variation was also clearly visible of up to 30km deep inland and less dense urban/built-up space away from Bangkok center was found to have lower UHI intensity.

Initial assessment indicates that the NDVI map can represent the vegetation class fairly well, especially at those areas with NDVI $\geq$ 0.4. The NDBI map also resembles the %ISC map and both can signify the urban/built-up class on the LULC map pretty well. The landmarks for urban green area, especially Bang Krajao sub-district and some parts of Nonthaburi Province are clearly visible on the gain NDVI map. Similarly, landmarks of the urban/built-up area, especially Bangkok inner zone and Suvarnbhumi Airport, were also readily detected on the gain NDBI map of the BMA area.

In addition, the negative values of NDVI were associated mostly to the water body class, especially those situate close to the border with Thai Gulf. The NDBaI map here does not exhibit any outstanding features on its content.

The comparison of the NDVI and NDBI maps with their corresponding LST map emphasizes the conventional believe that higher NDVI values are associated with lower LST values, but higher NDBI are associated with higher LST. It was found that, the correlation levels are rather moderate for LST and the NDVI (negative with R^2 = 0.408) but rather high (positive) for the other indices: R^2 = 0.734 (NDBI), 0.670 (NDBaI), and 0.836 (%ISC).The high positive correlation between %ISC and NDBI (with R^2 of 0.9221) was found and it might be useful for the determination of urban/built-up area in the urban growth study by using NDBI as a replacement for %ISC.

The strong negative correlations of NDVI with NDBI and %ISC, R^2 = 0.7703 and 0.5651 respectively, are as expected because they signify different groups of surfaces that are not generally coexistence. This means in dense urban area, healthy green vegetation (with high NDVI values) should be hard to find, and the opposite is true for dense green vegetation zone (e.g. mature crop fields).

5.3   Impact of Urban Green Areas on Ambient Air Temperature

The NDVI maps and their corresponding in situ LST maps of the two main public parks: Lumpini Park and CPC were generated. In both cases, the high NDVI portions usually represent the dense part of trees while the relatively low NDVI portions generally signify large water bodies situated inside the parks. Both of these main park's LULC components can noticeably reduce ambient air temperature within and around the parks. This finding was also supported by the ground-based observations.

The interpolated LST map for each considered park indicates great variation of the air temperature pattern within and around the park's occupying area. But all these parks exhibit tendency in having lower temperature inside. This notable reduction in air temperature within the park's area is resulted from the existing of two main components of its LULC: (1) pacts of the dense trees or other vegetations and (2) large water bodies.

If consider radial variation of temperature data inward to the chosen park's center, Santipap Park seems to have least distance of temperature decrease toward park's center (about 500 meters with about 1°C drop) while the Lumpini Park has longer temperature-dropping distance (about 700 meters with about 0.5°C drop). And the largest park of the interest, Chatuchak Park Complex (CPC), has dropping distance of about 1,600 meters with about 4°C decrease. The results clearly demonstrate strong influence of large urban green areas, like the CPC, in the introducing of notably cooler atmosphere within their territory and also over the vicinity surrounding.

In addition, influences of different LULC components on LST variation were also assessed by observing pattern of temperature data recorded by the mobile sensor along two selected routes. The corresponding satellite-based LST values also presented. Results indicate that the higher temperature data seem to appear under strong urban environment whereas in the rural area, the recorded temperatures noticeably drop as expected.

5.4   Impact of Temperature Variation on Electricity Consumption

There are five broad groups of the MEA registered users considered in the study area: (1) residential (RES), (2) small general service (SGS), (3) medium general service (MGS), (4) large general service (LGS), (5) governmental office (GOV)/non-profit organization (NPO). The strong correlation between electricity consumption in BMA and the monthly mean temperature was found with highest R^2 of 0.937 (for RES group) and 0.843 (for SGS group). The correlation levels for LGS and MGS are 0.615 and 0.518 respectively while lowest correlation of 0.308 is at GOV/NPO group.

These obtained results emphasize impact of the rising air temperature in making higher electricity demand, especially in household and SGS activities. The strong linear relationship found here is very useful for the prediction of demand for electrical energy (especially for the household and SGS sections) if average temperature in BMA is known in advance. However, it appears that only consuming rate in April that is notably dropped for the MGS, LGS and GOV sections, while average temperature is rising.

5.5   Suggestions

There are some interesting issues stemming from obtained results of the thesis that might be worth investigating in more details as follows.

(1)   Main influencing factors behind observed growth, or trend of future growth, or its critical impacts (e.g. on environment, socio-economy, or the fertile land resources) should be examined systematically using geoinformatics technology.

(2)   Details of the UHI intensity map over BMA region at different diurnal times (e.g. daytime and night), or at different seasons (e.g. winter and summer),

should be explored extensively as well as impact of strong UHI in general. The night-time LST data (e.g. from the MODIS image) are very valuable for this research.

The long-term knowledge of UHI severity (e.g. 50-year period) should also be assessed. The pattern and trend of UHI intensity due to urban/built-up expansion all over Thailand are also interesting topics to be pursued.

(3)   Modifications of the NDBI and NDBaI formulas to cover full range of their possible scales (-1 to 1) are recommended. The possibility of replacing %ISC by the NDBI for the analysis of urban growth within BMA region, or elsewhere, should also be assessed in more details, especially on its limitations for general use. The role of NDBaI on the study of urban LULC structure study should have more research as it still does not exhibit interesting outcome in the research.

(4)   The travelling time of about two hours for each chosen routes shown in Figure 4.19a can lead to some lag time between each consecutive measurement which ultimately makes the gained temperature profile along the route not synchronous in measuring time as it should be. To reduce impact of the time discrepancy issue, it might be useful to transform the originally-observed temperature data at each measuring location to be its expected values (of that location) at some reference time, e.g. at noon (12.00am), before plotting the temperature profile along each route.

This task can be done based on known diurnal changing pattern of the observed near-surface air temperature of BMA region on the chosen measuring days obtained from the ground measuring stations located within the area which can be used as a reference information to transform the original observed temperature data (at each location) to be its expected value at the preferred time.

(5) Influences of LULC components on the variation of LST (and UHI) data over

BMA region has been primarily assessed here based on only four board LULC classes (urban/built-up, vegetation, water body, and bare land) which might not be sufficient to provide a more subtle knowledge on impacts of some interested LULC components, like densely-populated residential or built-up zones, highly-congested traffic section, or small street-side park, on the increasing or decreasing of related LST (and UHI) intensity. To gain in-depth knowledge on this issue, more precise data of LULC structure over the area is needed, like ones derived from aerial photos or high spatial resolution satellite images.

(6)   It has been found in this research that the correlation level between NDVI and LST data for the BMA area is not high ($R^2 = 0.41$), therefore, conclusion about strong influences of the green vegetation on the reduction of LST (or UHI) intensity is still not solid in this case. However, more precise knowledge on the amount of the vegetation cover at pixel-scale (or %VEG) from the sub-pixel classification approach (like one being used to find %ISC) might be able to provide higher correlation level between the vegetation amount observed in the area and the associated LST at pixel-scale of the used satellite image (Landsat-TM in this case).

(7)   Variations in diurnal loading pattern (during daytime and nighttime) are worth considering. The validity of found relationship in this work between average temperature data and total electrical loading should be conducted based on other available data of both parameters in recent years. The plausible causes of unexpected drop in electrical loading in April for the MGS and LGS sections should also be further investigated.

Suggestions on mitigation methods

As detailed in this work, the average UHI intensity over BMA region has become more intense in recent years. This situation might be resulted in severe impacts on natural environment in the area and also on the human health as a whole. Therefore, effective plans to reduce this problem are really urgent to be implemented, for examples:

(1) Reduction overcrowded situation in the city center, or city inner area, that contribute most to the UHI problem, e.g. at Khlong Toei District,

(2) Using light-colored concrete for building pavements of solid structures more as it can reflect light better than popular asphalt. This practice can lead to more reducing in ambient temperature.

(3) Increase amount of well-watered vegetation both on ground and on top of available buildings (called green roofs). Green roofs are excellent insulators during warm weather months and the plants cool the surrounding environment.

(4) Producing more large/dense green areas, or large water body, like parks, canals, lakes, within city area. At present, BMA still needs a lot more green areas to cool the region down and to meet the UN-World Health Organization standard for megacity (Thaiutsa et al., 2008).

The city of New York determined that the cooling potential per area was highest for street trees, followed by living roofs, light covered surface, and open space planting. From the standpoint of cost effectiveness, light surfaces, light roofs, and curbside planting have lower costs per temperature reduction (New York State, 2006).

REFERENCES

REFERENCES

Adinna, E.N., Christion, E.I., and Okolie, T.N. (2009). Assessment of urban heat island and possible adaptations in Enugu urban using landsat-ETM. **Journal of Geography and Regional Planning**. 2(2): 30-36.

Akasaka, H., Nimiya, H., and Soga, K. (2002). Influence of heat island phenomenon on building heat load. **Building Services Engineering Research and Technology**. 23(4): 269-278.

Akbari, H. and Konopacki, S. (2005). Calculating energy-saving potentials of heat-island reduction strategies. **Energy Policy**. 33: 721-756.

Andrew. (2010). **Principles of Urban Meteorology (re atmospheric CO2)** [On-line]. Available: http://co2montreal.blogspot.com/2010/10/principles-of-urban-meteorology-re.html.

Aniello, C., Morgan, K. Busbey, A., Newland, and L. (1995). Mapping micro-urban heat islands using Landsat TM and a GIS. **Compuetr and Geosciences**. 21(8): 965-969.

Avissar, B. (1996). Potential effects of vegetation on the urban thermal environment. **Atmospheric Environment**. 30(3): 437-448.

Boonjawat, J., Niitsu, K., and Kubo, S. (2000). Urban Heat Island: Thermal pollution and climate change in Bangkok. **Journal of Health Science**. 9(1): 49-55.

Chen, X., Zhao, H., Li, P., and Yin, Z. (2006). Remote sensing image-based analysis of the Relationship between urban heat island and land use/cover changes. **Remote Sensing of Environment**. 104: 133-146.

Chen, Y., Wang, J., and Li, X. (2002). A study on urban thermal field in summer based on satellite remote sensing. **Remote Sensing for Land and Resources**. 4: 55-59.

Cutler Cleveland. (2010). **Heat island** [On-line]. Available: http://www.eoearth.

Dousset, B. and Gourmelon, F. (2003). Satellite multi-sensor data analysis of urban surface temperatures and land cover. **ISPRS Journal of Photogrammetry and Remote Sensing**. 58(1-2): 43-54.

EPA. (2011). **U.S. Environmental Protection Agency-Heat Island Impacts** [On-line]. Available: http://www.epa.gov/heatisld/impacts/index.htm.

Fisher, J.I., Mustard, J.F., and Vadeboncoeur, M.A. (2006). Green leaf phenology at Landsat resolution: Scaling from the field to the satellite. **Remote Sensing of Environment**. 100: 265-279.

Franco, G. and Sanstad, A.H. (2008). Climate change and electricity demand in California. **Climatic Change**. 87(Suppl 1): S139-S151.

Gallo, K.P. and Owen, T.W. (1999). Satellite-based adjustments for the urban heat island temperature bias. **Journal of Applied Meteorology**. 38: 806-813.

Gallo, K.P., McNab, A.L., Karl, T.R., Brown, J.F., Hood, J.J., and Tarpley, J.D. (1993). The use of NOAA AVHRR data for assessment of the urban heat island effect. **Journal of Applied Meteorology**. 32: 899-908.

Gallo, K.P., Tarpley, J.D., McNab, A.L., and Karl, T.R. (1995). Assessment of urban heat islands: A satellite perspective. **Atmospheric Research**. 37: 37-43.

Georgi, J. and Zafiriadis, K. (2006). The impact of park trees on microclimate in urban areas. **Urban Ecosystems**. 9: 195-209.

Gluch, R., Quattrochi, D.A., and Luvall, J.C. (2006). A multi-scale approach to urban thermal analysis. **Remote Sensing of Environment**. 104: 123-132.

Howard, L. (1818). **In: Climate of London Deduced from Meteorological Observations**. 1, W. Phillips, London.

Huang, S., Kwong, V.H.S., Gibbons, T.T., Fang, Z., Jiang, J., Knocke, H., Jiang, Y., Ruger, B., Braganza, E., Clark, W., and Gardner, L.D. (1990). Experimental apparatus for production, cooling, and storing multiply charged ions for charge-transfer measurements. **Journals Review of Scientific Instrument**. 61(7): 1931-1939.

Hung, T., Uchihama, D., Ochi, S., and Yasuoka, Y. (2006). Assessment with satellite data of the urban heat island effects in Asian mega cities. International. **Journal of Applied Earth Observation and Geoinformation**. 8: 34-48.

IAUC. (2011). **Teaching Resources-The Urban Canopy Layer Heat Island** [On-line]. Available:http://www.epa.gov/heatisland/resources/pdf/HeatIsland TeachingResource.pdf.

Jasuf, S.K., Wong, N.H., Hagen, E., Anggoro, R., and Hong, Y. (2007). The influence of land use on the urban heat island in Singapore. **Habitat International**. 31: 232-242.

Kataoka, K., Matsumoto, F., Ichinose, T., and Tanigushi, M. (2008). **Urban warming trends in several large Asian cities over the last years** [On-line]. Available: http://www.sciencedirect.com.

Kidder, S.Q. and Wu, H.T. (1987). A multispectral study of the St.Louise area under snow-covered conditions using NOAA-7 AVHRR data. **Remote Sensing of Environment**. 22: 159-172.

Kolokotroni, M., Zhang, Y., and Watkins, R. (2007). The London heat island building cooling design. **Solar Energy**. 81: 102-110.

Komolveeraket, K. (1998). **The effect of land use change on urban heat island phenomena in Bangkok**. Master Thesis, Chulalongkorn University, Thailand.

Lee, S. and Baik, J. (2010). Statistical and dynamical characteristics of the urban heat island intensity in Seoul. **Theoretical and Applied Climatology**. 100: 227-237.

Lee, S. and Baik, J. (2011). Evaluation of the Vegetated Urban Canopy Model (VUCM) and Its Impacts on Urban Boundary Layer Simulation. **Asia-Pacific Journal Atmosphere Science**. 47(2): 151-165.

Memon, R.A., Leung, D.Y.C., Liu, C., and Leung, M.K.H. (2011). Urban heat island and its effect on the cooling and heating demands in urban and suburban areas of Hong Kong. **Theoretical and Applied Climatology**. 103: 441-450.

Mills, G. (2010). **IAUC Teaching Resources The Urban Canopy Layer Heat Island** [On-line]. Available: http://www.epa.gov/heatisland/resources/pdf/ HeatIsland TeachingResource.pdf.

New York State. (2006). Mitigating New York City's Heat Island With Urban Forestry, Living Roofs, and Light Surfaces [On-line]. Available: http://www.nyserda.org/programs/environment/emep/project/6681_25/06-06 %20Complete%20report-web.pdf.

Park, P. (2011). **Map of Park in Bangkok** [On-line]. Available: http://www. parzapark.ob.tc/map.html?hl=th&tab=wl.

Rao, P.K. (1972). Remote sensing of urban "heat islands" from an environmental satellite. **Bulletin of the American Meteorological Society**. 53: 647-648.

Rong-bo, X., Ouyang, Z., Zheng, H., Li, W., Schienke, E.W., and Wang, X. (2007). Spatial pattern of impervious surfaces and their impacts on land surface temperature in Beijing, China. **Journal of Environmental Sciences**. 19: 250-256.

Santamouris, M., Papanikolaou, N., Livada, I., Koronakis, I., Georgakis, C., Argiriou, A., and Asimakopoulos, D. N. (2001). O the impact of urban climate on the energy consumption of buildings. **Solar Energy**. 70(3): 201-216.

Stathopoulou, M. and Cartalis, C. (2006). Daytime urban heat islands Landsat ETM+ and Corine land cover data: An application to major cities in Greece. **Solar Energy**. 81: 358-368.

Streutker, D.R. (2002). A remote sensing study of the urban heat island of Houstan, Texas. **International Journal of Remote Sensing**. 23(13): 2595-2608.

Thai Meteorological department. (2011). **Daily Weather Summary** [On-line]. Available: http://www.tmd.go.th/en/climate.php?FileID=1.

Thaiutsa, B., Puangchit, L., Kjelgren, R., and Arunpraparut, W. (2008). Urban green space, street tree and heritage large tree assessment in Bangkok, Thailand. **Elsevier Journals Urban Forestry & Urban Greening**. 7: 219-229.

Tonsuwonnont, P. (2006). **Heat island and electrical energy consumption in urban areas**. Master Thesis, Asian Institute of Technology, Thailand.

United States Environmental Protection Agency. (1992). **Cooling our communities: A guidebook on tree planting and light-colored surfacing**. US Government Printing Office, Pittsburgh, PA, USA.

Voogt, J.A. and Oke, T.R. (2003). Thermal remote sensing of urban climates. **Remote Sensing of Environment**. 86: 370-384.

Wan, Z. and Dozier, J. (1996). A generalized split-window algorithm for retrieving land-surface temperature from space. **IEEE Transactions on Geoscience and Remote Sensing**. 34(4): 892- 905.

Wan, Z., Zhang, Y., Zhang, Q., and Li, Z. (2002). Validation of the land-surface temperature products retrieved from Terra Moderate Resolution Imaging Spectroradiometer data. **Remote Sensing of Environment**. 83(1-2): 163-180.

Weng, Q. (2001). A remote sensing-GIS evaluation of urban expansion and its impact on surface temperature in Zhujiang Delta, China. **International Journal of Remote Sensing**. 22(10): 1999-2014.

Weng, Q., Lu, D., and Schubring, J. (2004). Estimation of land surface temperature-vegetation abundance relationship for urban heat island studies. **Remote Sensing of Environment**. 89: 467-483.

Wong, N.H. and Yu, C. (2005). Study of green areas and urban heat island in a tropical city. **Habitat International**. 29: 547-558.

Wu, C. (2004). Normalized spectral mixture analysis for monitoring urban composition using ETM+ imagery. **Remote Sensing of Environment**. 93(4): 480-492.

Yongnian, Z., Wet, H., Benjamin, Z., Honghui, Z., and Huimin, Z. (2010). Study on the urban heat island effects and its relationship with surface biophysical characteristics using MODIS imageries. **Geo-spatial Information Science**. 13(1): 1-7.

Yuan, F. and Bauer, M. (2007). Comparison of impervious surface area and normalized difference vegetation index as indicators of surface urban heat island effects in Landsat imagery. **Remote sensing of Environment**. 106: 375-386.

Zha, Y., Gao, J., and Ni, S. (2003). Use of normalized difference built-up index in automatically mapping urban areas from TM imagery. **International Journal of Remote Sensing**. 24(3): 583-594.

Zhang, X., Fridel, M.A., Schaaf, C.B., and Strahler, A.H. (2004). The footprint of urban climates on vegetation phenology. **Geophysical Research Letters**. 31: L12209.

Zhang, X., Friedl, M.A., Schaaf, C.B., Strahler, A.H., Hodges, J.C.F, Gao, F., Reed, B.C., and Huete, A. (2002). Monitoring vegetation phenology using MODIS. **Remote Sensing of Environment**. 84: 471-475.

Zhang, Y., Inakwu, O.A.O., and Han, C. (2009). Bi-temporal characterization of land surface temperature in relation to impervious surface area, NDVI and NDBI, using a sub-pixel image analysis. **International Journal of Applied Earth Observation and Geoinformation**. 11: 256-264.

Zhangyan, J., Yunhao, C., and Jing, L. (2006). On urban heat island of Beijing on Landsat TM data. **Geo-spatial Information Science (Quarterly)**. 9(4): 293-297.

CURRICULUM VITAE

Col. Parinya Chayapong was born in Bangkok Metropolis, Thailand on July 28, 1966. He received Bachelor of Education degree in General Science from Pranakorn Teachers' College in 1987, degree of Bachelor of Laws from Sukhothai Thammathirat Open University in 1997, and Master Degree in Computer Science and Information Technology from the King Mongkut's Institute of Technology Ladkrabang in 1999. He also graduated from Army Aviation School in 1989. During 1989-2002, he worked as an army pilot and captained the O-1 aircraft, in reconnaissance missions over the Thai-Combodian border, as well as the transport aircrafts: Short-330 and CASA-212. After graduation from the Command General Staff College (in 2003), he had worked as a programmer and chief of the Department of Information Warfare at the Military Technology Center (during 2003-2008). At present, he is a lecturer at the Department of Research and Development and Administration¸ Royal Thai Army War College.

His main research interest is on urban heat island (UHI) using remote sensing and GIS technologies being inspired from works achieved in his Ph.D. thesis.